Production and Optimisation of Biodiesel using Heterogeneous Catalyst

by

Vishen Papa

B.Sc.Eng (Chemical) – *UKZN*

Submitted in Fulfilment of the Academic Requirements for
Master of Science in Engineering

Discipline of Chemical Engineering
School of Engineering
College of Agriculture, Engineering and Science
University of KwaZulu-Natal
Howard College Campus
Durban, South Africa

March 2020

Supervisor: Prof. Amir H. Mohammadi

DECLARATION 1 - PLAGIARISM

I, …Vishen Papa (214546849)……., declare that

1. The research reported in this thesis, except where otherwise indicated, is my original research.

2. This thesis has not been submitted for any degree or examination at any other university.

3. This thesis does not contain other persons' data, pictures, graphs or other information, unless specifically acknowledged as being sourced from other persons.

4. This thesis does not contain other persons' writing, unless specifically acknowledged as being sourced from other researchers. Where other written sources have been quoted, then:

a. Their words have been re-written but the general information attributed to them has been referenced

b. Where their exact words have been used, then their writing has been placed in italics and inside quotation marks, and referenced.

5. This thesis does not contain text, graphics or tables copied and pasted from the Internet, unless specifically acknowledged, and the source being detailed in the thesis and in the References sections.

Vishen Papa

As the candidate's Supervisor I agree to the submission of this thesis:

…….

Prof. Amir H. Mohammadi

Acknowledgements

The Author would like to acknowledge the following people:

- Firstly, I would like to thank Prof. Amir H. Mohammadi for providing such an interesting topic. His guidance and has been most helpful during difficult times during this research project.

- Secondly, I would like to thank my friend, Muhammad Shezaad Adam, for his continuous support and help during this project.

- Finally, I would like to thank my family for their support and motivation throughout my academic career.

Abstract

In this work, it is required to investigate the production and optimisation of biodiesel using heterogeneous catalyst to determine whether the resulting biodiesel may be utilised in an existing diesel engine without modification. Castor oil and sunflower oils were chosen in the present study and conventional methods of biodiesel production, in the form of transesterification, were employed. The type of alcohol and catalyst chosen was methanol and calcium oxide, respectively, due to their relatively low cost and wide availability.

The Box-Behnken Design was used to design the experiments and conduct statistical analysis in *Minitab*™ on each oil. The factors tested were temperature, catalyst loading, reaction time and alcohol/oil molar ratio. The experimental methodology followed was the conventional method which comprised the heating of oil and alcohol in the presence of a catalyst under continuous stirring, followed by separation using a separation funnel. However, due to the high acid value of castor oil, esterification was performed using sulphuric acid as a catalyst in the presence of methanol. The process of esterification meant that three types of oils were now considered in the design, viz, base castor oil, esterified castor oil and sunflower oil.

The optimisation study conducted on castor oil esterification revealed that alcohol/oil molar ratio had the largest effect on the reduction of free fatty acids, resulting in a value of 0.715 % from a value of 12 % free fatty acids. Calcium oxide catalyst required calcination at 600℃ for $3\ hrs$ for activation. Castor oil transesterification was conducted by first producing a large amount of esterified castor oil; at the optimal conditions; in the presence of calcium oxide and methanol where temperature proved to have the largest effect on the yield of biodiesel produced and a maximum yield of 97.2 % was achieved which was in accordance with the optimal conditions predicted by the regression full quadratic model. Similar to esterification, sunflower oil transesterification was largely affected by alcohol/oil molar ratio and an optimal yield of 98 % was achieved.

The physical properties of the resulting fuels were tested, and biodiesel produced from sunflower oil is recommended, whereas biodiesel produced from castor oil does not meet ASTM D6751 fuel standards. The resulting fuels were blended with kerosene to form bio-jet fuel in fractions of 10 % and 20 %. The resulting blends are recommended for fuel testing to determine if further refinements are necessary according to ASTM standards. Biodiesel derived from sunflower oil could potentially reduce the strain on depleting fossil fuel reserves, lower overall greenhouse gas emissions, as well as promote job creation and further academic advancement within the alternative fuel environment.

Table of Contents

List of Figures

List of Tables

Chapter 1 – Introduction

1.1. Background

Biodiesel is a fuel derived from renewable feedstocks with the potential to provide an alternative to conventional petro-diesel. These feedstocks can be categorized as edible or non-edible and provide the basis for biodiesel production all around the world. Biodiesel is commonly produced via a transesterification reaction with alcohol in the presence of a catalyst. This process converts fats and oils (triglycerides) into mono-alkyl esters. Oils such as palm, sunflower, soybean and olive are among the most common edible feedstocks utilised. Biodiesel production can be decentralised, thus promoting economic development in rural areas as well as limit toxicity to residential areas (Gebremariam & Marchetti, 2017). In comparison to petro-diesel, biodiesel offers zero sulphur and reduced carbon monoxide and dioxide emissions.

Typical catalysts used in the transesterification reaction include sodium hydroxide (NaOH), potassium hydroxide (KOH) and calcium oxide (CaO). Generally, methanol is preferred to ethanol due to increased biodiesel yield. Other methods of biodiesel production include direct blending of oils, microemulsions and combustion of oils and fats in the absence of oxygen (pyrolysis) (Gebremariam & Marchetti, 2017). Less common methods of biodiesel production using nano-catalysts and ionic liquids offer greater efficiency in the conversion of fatty acids into biodiesel but suffer from high capital and production costs (Lin, et al., 2017).

1.2. Problem Statement

Petro-diesel contributes significantly to global warming and increased green-house gas emissions. Biodiesel derived from non-edible feedstocks such as castor and neem oil serve as a renewable means to reduce the increased demand for petro-diesel, thus reducing strain on fossil fuel reserves. Heterogenous catalysts such a CaO provide high reaction rates and yields as well as ease of separation thus promoting recycling and reusability of the catalyst.

1.3. Motivation and Research Aim

The main aim of this work is to investigate whether biodiesel produced via heterogeneous catalysis using esterification and transesterification reactions, with optimised parameters; temperature, alcohol/oil ratio, catalyst concentration and reaction time; can serve as a suitable alternative to petro-diesel and be used in a normal diesel engine without modification. These parameters can easily be scaled-up to accommodate large scale biodiesel production and aid in energy and economic saving.

The objectives of this work include:

- Literature review prior to experimental design necessary to determine the optimal conditions

- Experimental work in the form of esterification and transesterification reactions according to the experimental design to investigate the factors that influence the yield of biodiesel produced and data, statistical and gas chromatography (GC) analysis
- Optimisation and model validation at the optimal conditions
- Physical property analysis of biodiesel produced in accordance with ASTM standards to confirm/reject if biodiesel produced can serve as a replacement for petro-diesel
- Blending of biodiesel with kerosene to produce blended bio-jet fuel

1.4. Thesis Statement

The hypothesis of this work is that the biodiesel produced via heterogeneous catalyst in the presence of methanol can serve as a suitable alternative to petro-diesel and can be used in a normal diesel engine without modification.

1.5. Research Contributions

This work involves the use of castor and sunflower oils as renewable non-edible and edible feedstocks, respectively, in the presence of methanol. Calcium oxide catalyst (CaO) facilitates the increase in reaction rate and yield of biodiesel produced. The optimal conditions determined can aid in existing biodiesel production plants currently using the feedstocks mentioned to further optimise their process and increase the purity of biodiesel produced. This work can also help to realise the potential of bio-jet fuel and reduce strain on depleting fossil fuels.

1.6. Overview of Thesis

Chapter 1 highlights the necessary information about the materials used as well as the need for such an investigation. Additionally, an overview of the research objectives and motivations are mentioned so that the reader has a comprehensive understanding of why the investigation was conducted.

Chapter 2 focuses mainly on the literature behind biodiesel production and aims to give a comprehensive understanding of the process of biodiesel production and concerns arising from the different production methods. The different and common feedstocks and alcohols are highlighted as well as difficulties associated with the use of the materials mentioned. Common processes of biodiesel and petro-diesel production are also mentioned and discussed. Typical catalysts and operating conditions are discussed as well as other production factors such as, separation time and stirrer speed.

Chapter 3 describes the methods and materials used in the conduction of the esterification and transesterification reactions as well as the equipment used. A schematic of the equipment setup is also presented to provide a visual representation of the experimental procedure and aid in further understanding of the experimental design.

Chapter 4 focuses on the chosen experimental design and method and provides an in-depth view into the experimental design. This step is crucial in determining the optimal conditions from response surface plots conducted via data analysis in *Minitab*™ software.

Chapter 5 focuses mainly on the esterification of castor oil using sulphuric acid as a catalyst and methanol and the results and discussion therein. The focus of the esterification reaction was aimed at the reduction in acid value of castor oil and not the biodiesel yield produced.

Chapter 6 highlights the transesterification of the esterified castor oil, at the optimal conditions, and optimization procedure and results obtained in determining the optimal conditions in the presence of calcium oxide catalyst and methanol.

Chapter 7 highlights the transesterification of sunflower oil and optimization procedure and results obtained in determining the optimal conditions. The individual effects of the reaction conditions investigated are discussed as well as differences in yield obtained.

Chapter 8 deals mainly with the physical property comparison of biodiesel produced. Physical properties such a density, pour point and kinematic viscosity are investigated and discussed. The effect of catalyst reusability on reaction rate and biodiesel yield is also discussed. Potential strategies to alleviate deposition of material into the catalyst pores is discussed. The blending of biodiesel with kerosene is investigated and the resulting physical properties are discussed.

Chapter 9 provides the main conclusions that can be drawn from this work and recommendations necessary for future work. Conclusions between the two different oils and catalyst used will be discussed.

Chapter 2 – Literature Review

2.1. Introduction

In recent years biodiesel production has become more attractive owing to depleting fossil fuel reserves, global warming and climate change as well as energy production. Biodiesel can be derived from various edible and non-edible feedstocks, making it a renewable, non-toxic, environmentally friendly and biodegradable fuel source. In order to be an effective replacement for petro-diesel, biodiesel has to conform to ASTM (American Society for Testing and Materials) D6751 and EN (European Standard) 14214 standards. These standards regulate the quality of fuel that may be used in an engine without modification. Kinematic viscosity, density and cetane number are among the more important properties. There are various methods for the production of biodiesel, however, transesterification using a base catalyst is regarded as the most common.

2.2. Properties of Raw Materials

Biodiesel is produced primarily by four different methods, viz., transesterification, pyrolysis, direct use and blending and microemulsions of which transesterification is the most common. Generally, edible or non-edible oil, animal fat and microalgae and fungi oil are used for the production of biodiesel in the presence of an alcohol (Marwaha, et al., 2018).

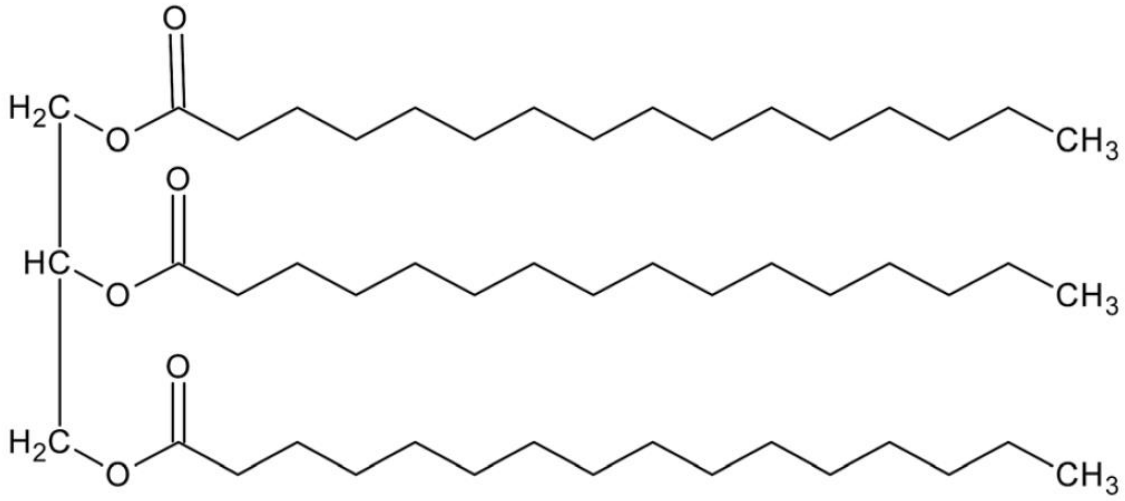

Figure 1 – Molecular Structure of Triglyceride (Vegetable oil) (Ruhul, et al., 2015)

A typical selection of oils used for biodiesel production can be seen in Table 1 below:

Table 1 – Physiochemical Properties of Different Oils (Marwaha, et al., 2018)

Feedstock (Oil)	Heating Value (MJ/kg)	Density (kg/m^3)	Kinematic Viscosity at (38 ℃) (mm^2/s)	Flash Point	Pour Point (℃)	Cetane Number	References
Corn	39.5	909.5	34.9	277	-40.0	37.6	(Barnwal & Sharma, 2005)
Cottonseed	–	915	33.7 (40 ℃)	234	-15.0	33.7	(Canakci & Sanli, 2008)
Linseed	39.3	923.6	27.2	241	-15.0	34.6	(Srivastava & Prasad, 2000)
Peanut	–	903	40 (40 ℃)	271	-6.7	34.6	(Canakci & Sanli, 2008)
Rapeseed	39.7	–	37.0	246	-31.7	37.6	(Jain & Sharma, 2010)
Safflower	39.5	914.4	31.3	260	-6.7	41.3	(Barnwal & Sharma, 2005)
Sesame	39.3	–	35.5	260	-9.4	40.2	(Jain & Sharma, 2010)
Soya bean	39.6	913.8	32.6	254	-12.2	37.9	(Srivastava & Prasad, 2000)
Sunflower	39.6	916.1	33.9	274	-15.0	37.1	(Jain & Sharma, 2010)
Palm	–	918.8	39.6	267	–	42.0	(Barnwal & Sharma, 2005)
Babassu	–	946.0	30.3	150	–	38.0	(Srivastava & Prasad, 2000)
Jatropha	39-40	912	55 (30 ℃)	240	–	40-45	(Jain & Sharma, 2010)
Karanja	–	936.5	43.6 (40 ℃)	–	–	–	(Karmakar, et al., 2010)
Neem	–	918.5	50.3 (40 ℃)	–	–	–	(Karmakar, et al., 2010)
Castor	37.4	955.0	251 (40 ℃)	–	–	42.3	(Karmakar, et al., 2010)
Mahua	36.0	960	24.5 (40 ℃)	232	–	–	(Karmakar, et al., 2010)
Tallow	–	903	51.2 (40 ℃)	201	–	40.2	(Canakci & Sanli, 2008)

With reference to Table 1, the extremely high kinematic viscosity of castor oil can be regarded as an outlier. This may be attributed to the high percentage of Ricinoleic acid ($\sim 90\ wt\%$) present in castor oil. However, the physiochemical properties of castor oil vary depending on the extraction method. For instance, castor oil extracted from cold pressing method (mechanical) has low acid content, low iodine content with a lighter colour but high saponification value in comparison to castor oil extracted by solvent extraction method (Omari, et al., 2015).

Table 2 – Feedstocks (Mujeeb, et al., 2016)

Group	Source of Oil
Non-edible oils	Babassu tree, copaiba, jatropha, jojoba, mahua, milk bush, nagchampa, neem, petroleum nut, rubber seed tree, silk cotton tree and castor
Major oils	Coconut (copra), corn (maize), cottonseed, canola (a variety of rapeseed), olive, peanut (groundnut), safflower, sesame, soybean and sunflower
Nut oils	Almond, cashew, hazelnut, macadamia, pecan, pistachio and walnut
Other edible oils	Amaranth, apricot, artichoke, avocado, babassu, bay laurel, beech nut, ben, Borneo tallow nut, carob pod, cohune, coriander seed, false flax, grape seed, hemp, kapok seed, lemon seed, meadowfoam seed, mustard, okra seed (hibiscus seed), perilla seed, pine nut, poppy seed, prune kernel, quinoa, rice bran, tallow, tea (camellia), thistle and wheat germ

Table 3 – Physical Properties of Different Oils (Ambat, et al., 2018)

Oil	Saponification value	Iodine value	Acid value ($mgKOH/g\ oil$)	References
Canola	188-193	109-126	0.6-0.8	(Thanh, et al., 2012)
Olive	184-196	75-94	0.9-2.2	(Dorado, et al., 2004)
Corn	187-198	103-140	0.1-5.7	(Thanh, et al., 2012)
Jatropha Curcas	177-189	92-112	15.6-43	(Thanh, et al., 2012)
Palm	186-209	35-61	6.9-50.8	(Thanh, et al., 2012)
Rapeseed	168-187	94-120	0.2	(Gryglewicz, 1999)
Soybean	189-195	117-143	0.1-0.2	(Thanh, et al., 2012)
Sunflower	186-194	110-143	0.2-0.5	(Thanh, et al., 2012)

Table 4 – Composition of Fatty Acid ($wt\%$) in Different Feedstocks (Ambat, et al., 2018)

Oil	Myristic $C_{14:0}$	Palmitic $C_{16:0}$	Stearic $C_{18:0}$	Oleic $C_{18:1}$	Linoleic $C_{18:2}$	Linolenic $C_{18:3}$	References
Edible							
Sunflower		5-8	2-6	15-40	30-70	3-5	(Li & Khanal, 2016)
Rapeseed		1-3	0-1	10-15	12-15	8-12	(Li & Khanal, 2016)
Soybean		6-10	2-5	20-30	50-60	5-11	(Li & Khanal, 2016)
Peanut		8-9	2-3	50-65	20-30		(Li & Khanal, 2016)
Olive		9-10	2-3	72-85	10-12	0-1	(Li & Khanal, 2016)
Palm	0.5-2	39-48	3-6	36-44	9-12		(Li & Khanal, 2016)
Mustard			1-2	8-23	10-24	8-18	(Li & Khanal, 2016)
Coconut	16-21	7-10	2-4	5-10	1-2.5		(Li & Khanal, 2016)
Almond		6.5	1.4	70.7	20	0.9	(Singh & Singh, 2010)
Walnut		7.2	1.9	18.5	56	16.2	(Singh & Singh, 2010)
Sesame		13	4	53	30		(Singh & Singh, 2010)
Non-edible							
Linseed		4-7	2-4	25-40	35-40	25-60	(Li & Khanal, 2016)
Neem		13-16		49.1-61.9			(Li & Khanal, 2016)
Jatropha	14-15	0-13		34.3-45.8	14-15	0-0.3	(Li & Khanal, 2016)
Cotton seed		23-28	0.8-0.9	13.3-18.3		0.2	(Li & Khanal, 2016)
Rubber	2.2	10.2	8.7	24.6	39.6	16.3	(Ghazali, et al., 2015)
Karanja		3.7-7.9	2.4-8.6	44.5-71.3	10-18		(Ghazali, et al., 2015)
Pongamia	11.6			51.5	11.6		(Ambat, et al., 2018)
Stillingia	0.1	7.5	2.3	16.7	31.5	41.5	(Ghazali, et al., 2015)
Other							
Chicken fat	3.1	19.8	3.1	37.62			(Ambat, et al., 2018)
Waste cooking		8.5	3.1	21.2	55.2	5.9	(Ambat, et al., 2018)
Tallow	23.3	19.3	42.4	2.9	0.9	2.9	(Singh & Singh, 2010)
Brown grease	1.6	22.8	12.5	42.3	12.1	0.8	(Ghazali, et al., 2015)
Microalgal	12-15	10-20					(Ambat, et al., 2018)
Yellow grease	2.4	23.2	12.9	44.3	6.9	0.	(Ghazali, et al., 2015)

2.3. Properties of Biodiesel

The properties of biodiesel present an inherent issue that may prove difficult to overcome in the pursuit of meeting American, European and South African fuel standards. These properties stem from the base oils used in the production of biodiesel. For instance, if waste cooking oil and castor oil are used as the base oil in a single stage transesterification reaction then biodiesel with high acid content and high kinematic viscosity will be produced, respectively. There are various factors that influence the properties of biodiesel and these factors are discussed below.

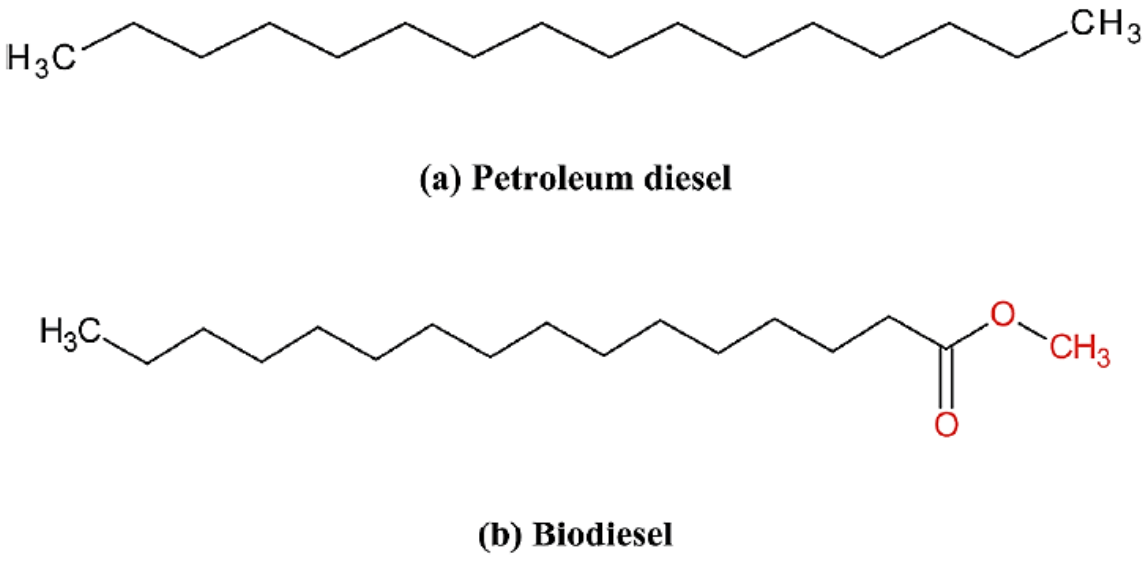

Figure 2 – Molecular Structure of (a) Petroleum diesel and (b) Biodiesel (Ruhul, et al., 2015)

2.3.1. Kinematic Viscosity

Kinematic viscosity represents the resistance to flow occurring between adjacent layers within a fluid. According to Goering et al. (1982), kinematic viscosity increases with increasing chain length and decreases with an increase in the number of unsaturated bonds present in the fuel. Therefore, biodiesel with a high kinematic viscosity may not be suitable for engine use as this may cause fuel filter and pump clogging, lower engine performance and higher greenhouse gas emissions (Ayetor, et al., 2015). Biodiesel with high kinematic viscosity may result in reduced fuel atomization and insufficient fuel to air ratios within the engine. As a result, the mean diameter of the fuel particles increases which leads to increased penetration within the combustion chamber (Choi & Reitz, 1999). This is because of inhibited fuel injector processes due to the high kinematic viscosity. Moreover, with an increase in kinematic viscosity comes an increase in fuel line pressure leading to the injectors. This may cause early injection and result in incomplete and ineffective combustion of the fuel (Lee, et al., 2002).

A two-step transesterification process using 1 $wt\%$ H_2SO_4 highlighted by Ayetor et al. (2015) was found to significantly reduce the kinematic viscosity of the biodiesel produced from Coconut oil,

Jatropha oil and Palm kernel oil by 38.5 %, 35.1 % and 24 %, respectively. Najafi et al. (2018) reported a kinematic viscosity of 6.482 (mm^2/s) when waste cooking oil was used in the production of biodiesel in the presence of methanol and sodium hydroxide (NaOH). Additionally, when waste cooking oil in used in the presence of ethanol and an acid-catalyst, a two-step process may be employed as seen in the work of Tchameni et al. (2015) whereby the acid-esterification is followed by ethanolic de-acidification to reduce the Free Fatty Acid (FFA) content. This process resulted in biodiesel with a kinematic viscosity of 4 (mm^2/s), which is significantly better than the work by Najafi et al. (2018).

2.3.2. Density

The density of biodiesel generally differs according to the feedstock used. This is evident by the work of Azocar et al. (2007) who used rapeseed oil and waste cooking oil with densities of 930 and 940 (kg/m^3), respectively, to produce biodiesel with lower densities of 880 and 890 (kg/m^3), respectively. Biodiesel which has a low density will result in better engine performance as the diameter and inertia of the fuel droplet will be smaller in comparison with biodiesel having a higher density (Choi & Reitz, 1999; Canakci & Sanli, 2008). The density is also a function of viscosity and heating value. Hoekman et al. (2012) reported that biodiesel comprising longer chain lengths have lower density.

2.3.3. Cetane Number

The cetane number of a fuel represents its quality during ignition and combustion (Giakoumis & Sarakatsanis, 2019). This number is usually between 55-60 for biodiesel and 35-60 for petro-diesel. The high cetane number for biodiesel can be attributed to the methyl esters present in biodiesel which result in straight-chained bonds that improve the auto-ignition of biodiesel. This process, however, is hindered by the unsaturated bonds present in biodiesel which may result in poor combustion, depending on the feedstock and purity of biodiesel used (Giakoumis & Sarakatsanis, 2019).

2.3.4. Cloud and Pour Point

The cloud point refers to the temperature at which crystals begin to form and the pour point refers to the temperature at which biodiesel can be poured during refrigerated conditions (Muhammad, et al., 2019). The process for determination of the cloud point is (1) refrigerate a small sample of biodiesel and remove it from the freezer every minute to check for any visible changes, (2) record the temperature at which crystals begin to form using a thermometer. Similarly, for pour point, the frozen biodiesel is removed from the freezer and the temperature is recorded when the mixture is able to be poured.

2.3.5. Flash Point

The flash point is the defined as the minimum temperature needed for the fuel to form a combustible mixture with air. Muhammad et al. (2019) observed a reduction of 35 ± 1℃ in flash point temperatures between crude and refined castor oil biodiesel. This serves as an indication of increased volatility between crude and refined castor oil biodiesel.

2.3.6. Acid Value

The acid value of biodiesel is defined simply as the amount of base, measured in $mg\ KOH$, necessary to neutralise the free fatty acids in $1\ g$ of biodiesel (Tubino & Aricetti, 2011). Azocar et al. (2007) reported the acid values of waste cooking oil collected from restaurants and residential areas to be $1.62\ mg\ KOH/g$ and $0.17\ mg\ KOH/g$, respectively. Typically, waste cooking oil has a high acid value and must undergo acid-esterification to lower the acid value. However, in the case of Azocar et al. (2007), the low acid values can be attributed to the original oils (soybean and sunflower) having low acid values. The acid value greatly effects the amount of refining necessary to obtain biodiesel within ASTM D6751 standards. This is evident in the work of Tchameni et al. (2015) who used a two-step process (acid esterification and ethanolic de-acidification) to lower the acid value of waste cooking oil from 83.07 to 3.36 and finally to $0.56\ mg\ KOH/g$.

2.3.7. Measuring of Biodiesel Properties

Table 5 – Measuring of Biodiesel Properties

Property	Typical Apparatus	Limits	Units	Standard	References
Kinematic viscosity	Ostwald viscometer Red wood viscometer	1.9 – 6.0	mm^2/s	ASTM D445	(Gabriel, et al., 2018) (Sivaramakrishnan & Ravikumar, 2012)
Density	Anton Paar digital densimeter Hydrometer	$820 - 900$	kg/m^3	ASTM D4052 ASTM D941	(Pratas, et al., 2011) (Sivaramakrishnan & Ravikumar, 2012)
Iodine content	Method of Wijs	120 max	–	EN14214	(Zahan & Kano, 2018)
Acid value	Burette	0.8 max	$mg\ KOH/g$	ASTM D974	(Zahan & Kano, 2018)
Cetane number	Ignition quality tester	47 min	–	ASTM D613 ASTM D976	(Sivaramakrishnan & Ravikumar, 2012)
Flash point (closed cup)	Penksy Martins apparatus	93 min	℃	ASTM D93	(Sivaramakrishnan & Ravikumar, 2012)
Pour point	Dry ice	-15	℃	ASTM D6751	(Zahan & Kano, 2018)

2.3.8. Characterisation of Biodiesel by Analytical Methods

Whilst the other methods focus on testing of physiochemical properties of biodiesel, there exists a need to determine the composition and hence characterise the biodiesel produced. This is usually achieved by gas chromatography mass spectroscopy (GC-MS) analysis. The main purpose of this process is to determine the composition of biodiesel produced in an attempt to characterise the quality of biodiesel produced. The gas chromatography unit is a device which vaporises a small amount of liquid sample

injected into the unit. The detector in the unit then detects the various components within the vapour sample. Therefore, adequate temperature control needs to be maintained within the unit and this is achieved by means of a temperature-controlled program. The temperature-controlled program needs to effectively and carefully exploit the difference in the boiling points of the different compounds present in the biodiesel, such that the sample containing various compounds may vaporise gradually over time as to not overwhelm the detector and produce incorrect chromatograms (Ambat, et al., 2018).

Table 6 – Analytical Methods for the Characterisation of Biodiesel (Ambat, et al., 2018)

Feedstock (oil)	Analytical technique	Analysis conditions	References
Stillingia	GC	Column with thermal profiling or ramp; temperature from 190℃ to 280℃; flow rate of nitrogen, hydrogen and air at 25 ml/min, 40 ml/min, 400 ml/min, respectively	(Wen, et al., 2010)
Karanja	NMR	Esters are analysed at 400 MHz with $CDCl_3$ as solvent	(Kaur & Ali, 2011)
Jatropha	NMR	Esters are analysed at 400 MHz with $CDCl_3$ as solvent	(Kaur & Ali, 2011)
Sunflower	GC	DB wax column with thermal profiling or ramp; temperatures from 100℃ to 240℃; detector and injector temperatures 280℃and 260℃, respectively	(Bet-Moushoul, et al., 2016)
Oleic acid	GC	Clarus 580 GC, Perkin Elmer, USA used	(Mahdavi, et al., 2015)
Soybean	GC	HP − 5 capillary column with thermal profiling or ramp; temperature from 135℃ to 250℃; detector and injector temperatures 300℃ and 280℃, respectively	(Qiu, et al., 2011)
Jatropha	GC-MS	Samples diluted using chloroform; esters determined based on comparison of standards, sample retention time and peak area	(Hashmi, et al., 2016)
Soybean	HPLC	C18 Kromasil column with methanol as mobile phase and a flow rate of 1 ml/min; samples are detected at 250 nm	(Liu, et al., 2012)
Soybean	GC-MS	Helium as carrier gas; DB − 1 column	(Istadi, et al., 2015)
Waste cooking	GC	Alltech EC − 5 column with deactivated straight liner with thermal profiling, or ramp the temperature from 35℃ to 300℃ at the rate of 20℃/min	(Gurunathan & Ravi, 2015)
Madhuca indica	GC-MS, NMR	HP − 5 capillary column with thermal profiling, or ramp the temperature from 50℃ to 290℃, carrier gas (helium) flow rate of 1 ml/min In NMR analysis at 300 MHz with $CDCl_3$ as solvent, with an internal standard, tetramethylsilane	(Thangaraj & Piraman, 2016)
Vegetable	GC-MS with FID	HP − 5 capillary column with thermal profiling, or ramp the temperature from 50℃ to 280℃	(Feyzi & Shahbazi, 2015)
Algae lipids	GC-MS, GC-FID	HP − 5 capillary column with a constant oven temperature of 320℃; detector and injector temperature 280℃	(Teo, et al., 2016)

Chicken fat	NMR	In NMR analysis, esters were analysed at 300 MHz with $CDCl_3$ for sample preparation	(Shi, et al., 2013)

2.3.9. Prediction Models for Biodiesel Properties

Recently the use of prediction models using Least Squares Support Vector Machine (LSSVM) offer great accuracy in the prediction of properties for biodiesel. In a recent study by Razavi et al. (2019) comprising 56, 59, 44 and 25 experimental and literature data points; obtained from a variety of sources in literature (Razavi et al. (2019)); for Iodine content, kinematic viscosity, cloud point and pour point, respectively, was used in conjunction with the LSSVM model and particle swarm optimization (PSO). The LSSVM-PSO model resulted in coefficients of 0.99995, 0.99981, 0.99848 and 0.99930 for pour point, cloud point, iodine value and kinematic viscosity, respectively, which clearly indicates that the model can accurately describe the physical properties associated with the experimental and literature data.

2.4. Biodiesel Production Methods

As with any fuel production process, there are many different methods to produce the same fuel with moderate variations. The methods discussed below comprise different ways to produce biodiesel from a variety of feedstocks and techniques.

2.4.1. Direct Use and Blending

This method involves the direct use of vegetable oil in diesel engines without further processing and modifications to the engine. According to Mujeeb et al. (2016), vegetable oil has been successfully blended with petro-diesel in a ratio of 20 % vegetable oil and 80 % petro-diesel. However, blending ratios of greater than 20 % may led to fuel injector blockages, gelling of engine oil lubricant and increased carbon deposition on pistons due to increased reactivity of unsaturated bonds and higher viscosity presented by vegetable oil (Demirbas, 2008). Prolonged direct use of vegetable oil may raise the issue of food vs fuel as well as result in incomplete combustion owing to lower volatility of the blended fuel mixture. Ma & Hanna (1999) emphasized the issue of oil deterioration during storage of blended fuel. The issues associated with direct use of vegetable oil can be mitigated by the addition of 4 $wt\%$ ethanol to the blend to improve brake thermal efficiency (Bilgin, et al., 2002). Additionally, pure ethanol may be used to reduce the kinematic viscosity of the oil as seen in the work of Ma & Hanna (1999), who used canola oil and 10 $wt\%$ ethanol to reduce the kinematic viscosity of the oil from 37.82 to 21.15 (mm^2/s) at 37℃.

According to a study conducted by Ziejewski et al. (1986), the blending of 25 % sunflower oil with 75 % petro-diesel resulted in a kinematic viscosity of 4.88 (mm^2/s), which is within the range of $1.9 - 6$ (mm^2/s) according to ASTM D6751 standards. Generally, the use of direct and blended oils

is regarded as impractical due to poor engine performance, high kinematic viscosity, high free fatty acid content, gum formation and oxidation and polymerization during storage and combustion, respectively (Ma & Hanna, 1999).

Table 7 – Problem, Probable Cause and Potential Solutions for Direct Use and Blending of Oils (Harwood, 1984)

Problem	Probable Cause	Potential Solution
Short-term		
Cold weather starting	High viscosity, low cetane and low flash point of vegetable oils	Preheat fuel prior to injection. Chemically alter fuel to an ester
Plugging and gumming of filters, lines and injectors	Natural gums (phosphatides) in vegetable oil. Other ash	Partially refine the oil to remove gums. Filter to 4-microns
Engine knocking	Very low cetane number of some oils. Improper injection timing	Adjust injection timing. Use higher compression engines. Preheat fuel prior to injection. Chemically alter fuel to an ester
Long-term		
Coking of injectors on piston and head of engine	High viscosity of vegetable oil, incomplete combustion of fuel. Poor combustion at part load with vegetable oils	Heat fuel prior to injection. Switch engine to diesel fuel when operation at part load. Chemically alter the vegetable oil to an ester
Carbon deposits in piston and head of engine	High viscosity of vegetable oil, incomplete combustion of fuel. Poor combustion at part load with vegetable oils	Heat fuel prior to injection. Switch engine to diesel fuel when operation at part load. Chemically alter the vegetable oil to an ester
Excessive engine wear	High viscosity of vegetable oil, incomplete combustion of fuel. Poor combustion at part load with vegetable oils. Possible free fatty acids in vegetable oil. Dilution of engine lubrication oil due to blow-by of vegetable oil	Heat fuel prior to injection. Switch engine to diesel fuel when operation at part load. Chemically alter the vegetable oil to an ester. Increase motor oil changes. Motor oil additives to inhibit oxidation
Failure of engine lubricating oil due to polymerization	Collection of polyunsaturated vegetable oil blow-by in crankcase to the point where polymerization occurs	Heat fuel prior to injection. Switch engine to diesel fuel when operation at part load. Chemically alter the vegetable oil to an ester. Increase motor oil changes. Motor oil additives to inhibit oxidation

2.4.2. Microemulsion

Microemulsion can be regarded as a thermodynamically stable state between two immiscible liquids and an amphiphile in which there exists a stable liquid solution which is visibly isotropic (Ma & Hanna, 1999). Generally, a microemulsion of biodiesel comprises diesel fuel, alcohol, cetane improver and surfactant. The purpose of alcohol serves to lower the viscosity of the fuel whereas long-chain alcohols act as surfactants and the cetane number is adjusted by the use of alkyl nitrates (Chiaramonti, et al., 2003).

This process involves the addition of a solvent to biodiesel and petro-diesel in the presence of a surfactant in an attempt to lower the viscosity of the blended biodiesel blend. The surfactant serves to lower the surface tension between the two immiscible solvent and fuel phases and typically has a hydrophilic-lipophilic balance (HLB) value in the range of $8 - 18$ for oil-to-water emulsions (Maawa, et al., 2019). Ziejewski et al. (1984) prepared a microemulsion of 53 % akali-refined sunflower oil, 13.3 % ethanol and 33.4 % butan-1-ol with a viscosity of 6.31 (mm^2/s) at 40℃ and concluded that viscosity decreased and an improvement in spray pattern from fuel injectors could be noticed when the volume percentage of butan-1-ol increased. The study also conducted a 200-hour endurance performance test and observed fuel injector sticking, significant carbon deposits and incomplete combustion. Furthermore, ternary phase equilibrium diagrams and plots of viscosity versus solvent fraction may be used to determine the ratios necessary for successful emulsion (Schwab, et al., 1987).

2.4.3. Conventional Transesterification

2.4.3.1 Homogeneous Acid-Catalysed Transesterification

This method employs an acid catalyst such as HCl or H_2SO_4 to convert the triglycerides present in various edible and non-edible oils into biodiesel and glycerol. Typically, this method is employed and economically viable when feedstocks with high acid values are used for the production of biodiesel (Gebremariam & Marchetti, 2017). The presence of water can reduce the yield by competitive formation of carboxylic acids (Park, et al., 2010). The high reaction time corresponding to a slow reaction rate when acid catalysts are utilized presences a disadvantage as the resulting process conditions may not be feasible. This method, however, is extremely useful for the conversion of high acid value feedstocks into biodiesel which meet ASTM standards.

A yield of $99 \pm 1\%$ can be achieved using acid catalysts when methanol is used in excess which drives the forward reaction to equilibrium at 70℃ for 4 h (Zheng, et al., 2006). Generally, for acid catalysed transesterification, a large excess of methanol is used which is evident by the works of Soriano Jr et al. (2009) and Miao et al. (2009) who reported optimal methanol to oil molar ratios of 24:1 for 18 h at 100℃ in the presence of 5 $wt\%$ $AlCl_3$ and 20:1 at 120℃ in the presence of 2.0 Molar (M) trifluoroacetic, respectively.

2.4.3.2 Homogeneous Base-Catalysed Transesterification

Typical base catalysts include NaOH, KOH and carbonates (Ma & Hanna, 1999). This method of transesterification offers reduced reaction time corresponding to high reaction rates; in comparison to acid catalysts; which may reduce the overall operating cost of the process. Alkaline catalysts are more commonly used commercially due to the non-corrosive nature of the catalyst (Ranganathan, et al., 2008). In addition, only low acid content feedstocks may be used with base catalysts as the presence of

high acid content and water results in saponification which lowers the yield as well as introduces a degree of difficulty during separation of biodiesel and glycerol (Parawira, 2010).

Typically, sodium hydroxide is preferred over potassium hydroxide and sodium methoxide owing to its lower cost and moderate catalytic activity. According to a study by Leung & Guo (2006), sodium hydroxide resulted in a higher purity of biodiesel whilst still maintaining a relatively high biodiesel yield, in comparison to potassium hydroxide and sodium methoxide, under the same reaction conditions. However, potassium hydroxide proved to result in less emulsion and easier separation than sodium hydroxide (Hossain & Boyce, 2009).

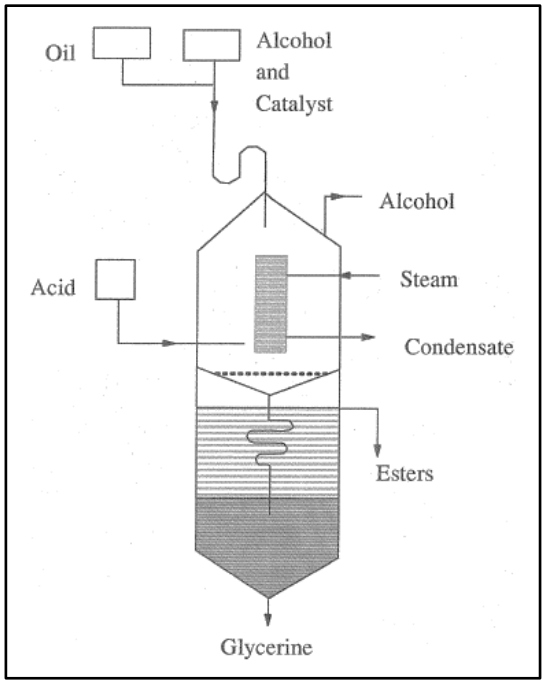

Figure 3 – Continuous Transesterification Reactor (Ma & Hanna, 1999)

Table 8 – Comparison between Different Separation and Purification Techniques (Atadashi, et al., 2010)

Type of catalyst	Separation method	Purification method	Advantages	Disadvantages
Solid oxide	Gravitational settling	Evaporation	Removal of methanol	Less energy consumption
Sodium hydroxide	Microwave irradiation	Water washing	Removal of excess methanol and catalyst	Large amount of waste wash water and energy consumption
Sodium methoxide	Centrifugation	Distillation, neutralization, water washing	Methanol recovery, removal of excess methanol and catalyst	Energy and water waste
Sodium hydroxide	Gravitational settling	Neutralization with acid, warm water washing	Removal of methanol, residual catalyst and soap	High energy and water consumption

Acid/potassium hydroxide	Centrifugation	Hot water washing	Removal of residual methanol and other contaminants	High energy and water consumption
Sodium hydroxide	Membrane filtration	Neutralization, membrane, water washing	Removal of excess methanol, residual catalyst and soap	Less water, time and energy waste
Enzyme/acid	Gravitational settling	Evaporation	Removal of excess methanol	Less water waste
Sodium hydroxide	Membrane reactor	Washing with reverse osmosis water	Removal of unreacted oil and soap traces	Less water requirement
Potassium hydroxide	Separative membrane	Separative membrane	Removal of excess methanol and soap	No waste water
Sodium hydroxide	Membrane separator	Membrane separator	Removal of unreacted tri- and mono-glycerides and glycerol	No water requirement
Sodium methoxide	Membrane separator	Neutralization, distilled water washing, distillation	Removal of contaminants	High water waste and energy consumption

2.4.3.3 Heterogeneous Catalysed Transesterification

Unlike homogeneous catalysts, heterogeneous catalysts can be easily separated after the reaction but prior to decantation (Ma & Hanna, 1999). This type of catalyst is usually solid, in the form of powder and offers more economic reaction conditions in comparison to their homogeneous counterparts. Generally, acid heterogeneous catalysts may be used for an esterification reaction because the acid catalyst can catalyse the free fatty acids present in the reaction mixture and base catalysts are used in transesterification reactions to facilitate the conversion of triglycerides into fatty acid methyl esters and glycerol (Ma & Hanna, 1999). In addition, heterogeneous catalysts are highly selective and may be reused once recovered. The potential for separation by filtration or centrifugation eliminates the need for waste water treatment and reduces product contamination by catalyst.

Furthermore, as mentioned by Refaat (2011), heterogeneous catalysts such as calcium oxide can produce biodiesel with exceptional high yield and purity that are close to the theoretical value as well as produce glycerol as a by-product with at least a purity of 98 % without salt contaminants. However, the major drawback of heterogeneous catalysts is deactivation, which occurs over time either due to poisoning, coking, leaching and sintering.

Malani et al. (2019) used wet impregnation method to synthesis KI impregnated ZnO catalyst for ultrasound assisted biodiesel production. To determine the role of sonication, transesterification was used as a base case. They reported that esterification using concentrated H_2SO_4 was necessary when high acid value non-edible oils are used. The heterogeneous catalyst was able to be recovered by high

speed centrifugation at $6000g$ for 15 min at room temperature. The catalyst surface was washed with *n*-hexane to remove impurities such as oil, methanol, glycerol, biodiesel as well as impurities present in the oil. In order to reuse the catalyst, an oven drying time of $1\ h$ and temperature of 110℃ was necessary which is followed by calcination at 500℃ for $3\ h$.

da Silva Castro et al. (2019) synthesized CaO from eggshells by first washing all organic matter followed by drying, crushing, separation by sieves and finally calcination at different temperatures. After transesterification, they reported a directly proportional relationship between calcination temperature and yield, however, as calcination temperature increased to the maximum tested value of 1000℃, the kinematic viscosity of the biodiesel produced using the catalyst that was calcinated at 1000℃ did not meet the required specification.

2.4.3.3.1 Reaction Mechanism of Heterogenous Catalysts (CaO)

Biodiesel production via heterogenous catalysis follows similar reaction mechanism principles to homogenous catalysis. The main mechanism in homogeneous catalysis is the formation of nucleophilic alcoxides that attack the electrophilic sites on the triglycerides, whilst protonation occurs in the carbonyl functional group of the triglycerides which is attacked by the alcohol to generate an intermediate tetrahedral complex in acid catalysis (Endalew, et al., 2011).

Biodiesel production from vegetable oils (triglycerides) is typically achieved via three steps, (1) generation of a tetrahedral intermediate complex, (2) chemical breakdown of the tetrahedral intermediate to a diacylglycerol (DAG) ion and fatty acid ester, (3) catalyst recovery by proton transfer. This process is repeated three times to yield three fatty acid esters and one glycerol molecule, as seen in Figure 4 which represents the stoichiometric equation of the reaction system.

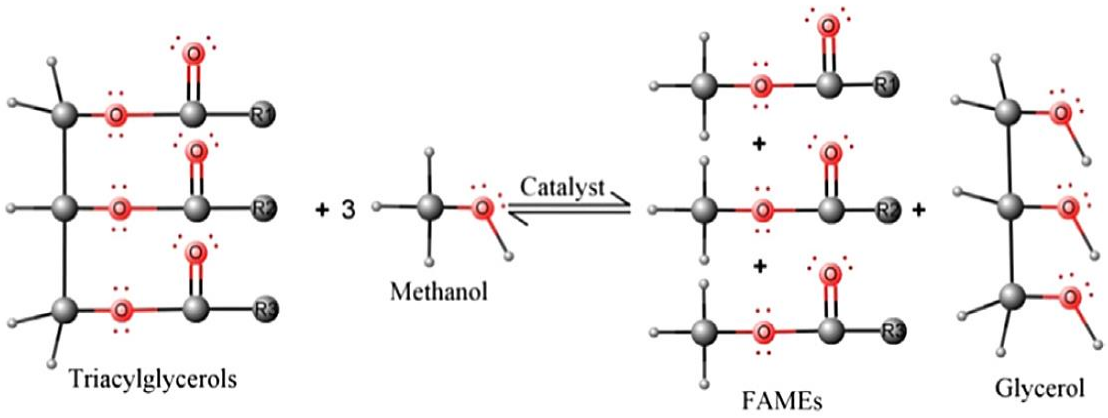

Figure 4 – Stoichiometric Equation of Biodiesel Production (Marinković, et al., 2016)

However, calcium oxide powder is solid in nature and does not dissolve in methanol. Therefore, for heterogenous catalysis, the reaction occurs on the catalyst surface which is understood by two basic

mechanisms, viz. Eley-Rideal (ER) and Langmuir-Hinshelwood-Hougen-Watson (LHHW). The ER mechanism works on the assumption that the reaction occurs by the direct pickup of reactants from the surface by the liquid phase and the LHHW mechanisms works by assuming that reactants are first adsorbed onto the catalyst surface, and then the reaction occurs on the catalyst surface, and finally the products is desorbed from the catalyst surface (Marinković, et al., 2016).

2.4.3.3.2 Properties and Reaction Kinetics of Heterogenous Catalysts (CaO)

The production of biodiesel usually occurs when triglycerides and methanol react in the presence of a catalyst. The catalyst chosen for this work is heterogeneous in nature which means, it is not soluble in the oil or methanol. Instead, the catalyst mixes with the reactants, promotes the production of biodiesel and at the end, is able to be recovered as solid powder. Calcium oxide powder was chosen for this work due to its wide availability and cost.

Calcium oxide catalyst is usually derived from organic matter containing calcium, such as limestone, calcite and eggshells containing calcium carbonate ($CaCO_3$). The process of thermal decomposition or calcination results in a release of a molecule of carbon dioxide from $CaCO_3$, which then reduces to quicklime (CaO). The calcination temperature is highly dependent on the base material used and often affects the yield and quality of biodiesel produced.

Table 9 – Temperature of Formation of CaO depending on Precursor (Marinković, et al., 2016)

Precursor	Calcination conditions (heating rate, atmosphere)	Formation temperature (K)
Calcium hydroxide	1.5 K/min, N_2	693-923
Calcium hydroxide	10 K/min, 20 $vol\%$ O_2/Ar	705-725
Calcium nitrate	1.5 K/min, N_2	873
Calcium nitrate	10 K/min, 20 $vol\%$ O_2/Ar	906
Limestone	–	990
Calcium carbonate	10 K/min, N_2	914 or 1144
Calcium carbonate	Vacuum	934
Calcium carbonate	1.5 K/min, N_2	~973
Calcium carbonate	10 K/min, 20 $vol\%$ O_2/Ar	1058
Calcium acetate	< 20 K/min, Air	973
Calcium acetate	20 K/min, Air	1038
Calcium oxalate	10 K/min, 20 $vol\%$ O_2/Ar	1000-1040
Calcite (Iceland spar)	2 K/min, Air	1073-1123

Table 10 – Physiochemical Properties of CaO (Marinković, et al., 2016)

Characteristic	Description
Chemical name	Calcium oxide
Chemical formula	CaO
Common name	Lime, quicklime, caustic lime, calx, fluxing lime
Molar mass (g/mol)	56.0774

Density (kg/m^3)	3340
Odour	Odourless
Melting point (K)	2886
Boiling point (K)	3123
Heat of formation (kJ/mol)	635.55
Heat of hydration (kJ/mol)	63.18
Solubility	
Water $(mg\ CaO/ml)$	1.19 $(298\ K)$, 0.57 $(373\ K)$, exothermic reaction
Methanol $(mg\ CaO/ml)$	0.1-0.2 $(298\ K)$, 0.03-0.04 $(333\ K)$, exothermic reaction
Glycerol $(mg\ CaO/ml)$	1.6 $(0.5\ h, 298\ K)$, 5.7 $(2\ h, 298\ K)$
Glycerol and methanol $(mg\ CaO/ml)$	~1 $(333\ K)$
Biodiesel, glycerol and methanol $(mg\ CaO/ml\ alcohol)$	0.4 $(298\ K)$, 0.6 $(373\ K)$,

In a recent study by da Silva Castro et al. (2019), they report a directly proportional relationship between calcination temperature and kinematic viscosity of the biodiesel produced. They conclude that once the calcination temperature is in excess, the biodiesel produced via heterogeneous catalysis does not meet fuel specifications, because the kinematic viscosity increased with an increase in calcination temperature.

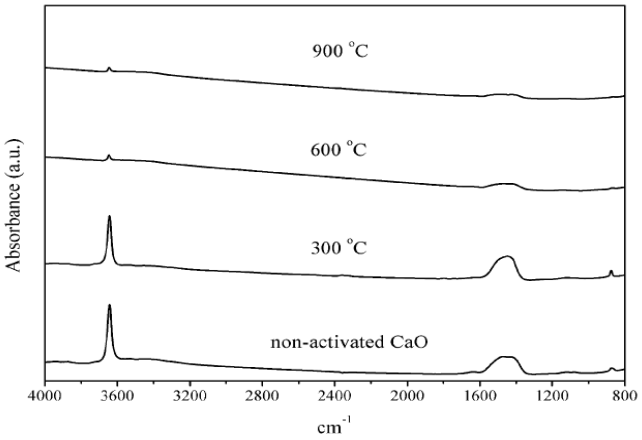

Figure 5 – IR Spectrum of CaO Calcinated at different Temperatures (Esipovich, et al., 2014)

As seen by the IR spectrum in Figure 5, the absorbance peaks decrease with an increase in temperature, with little or no effect observed between the calcination temperatures of 600℃ and 900℃. Therefore, a suitable calcination temperature of 600℃ may be employed regarding calcium oxide catalyst. This is due to the thermal decomposition of hydroxides and carbonates at 600℃. In addition, the amount of basic centers; as shown in Table 11; is the highest for the calcination temperature of 600℃.

Table 11 – Basic strength distribution of CaO catalyst (Esipovich, et al., 2014)

Catalyst	Basicity $(mmol/g)$
Commercial CaO (un-calcinated)	0.03
CaO calcinated at 300℃	0.01

CaO calcinated at 600℃	0.08
CaO calcinated at 900℃	0.04

Furthermore, calcinated calcium oxide is a chemically unstable compound as it readily reacts with carbon dioxide and water in the air to quickly form calcium carbonate again, thus partially undoing the calcination process by covering the outermost surface of the catalyst with a layer of calcium carbonate, hence deactivating the catalyst.

However, Liu et al. (2008) showed that despite water having negative effects directly after calcination, the addition of 0.2 $wt\%$ $(of\ oil)$ of water into the reaction system resulted in an increase in yield. This is illustrated in Figure 6 which represents the influence of water on a reaction system comprising soybean oil and methanol in a molar ratio of 9:1, calcinated calcium oxide catalyst with a loading of 1.3 $wt\%$ $(of\ oil)$ and reaction temperature of 60℃.

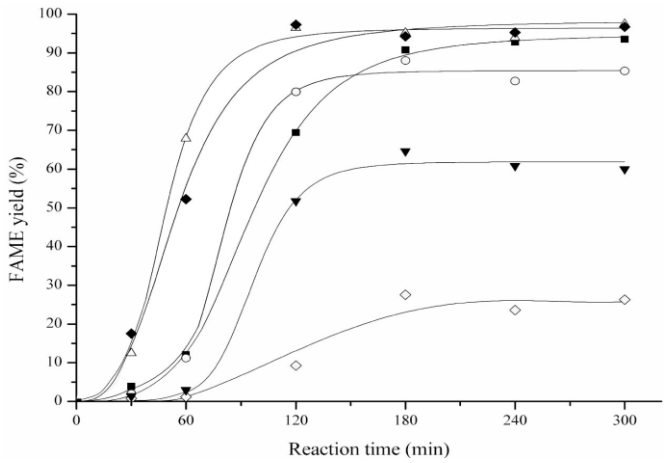

Figure 6 – Influence of Water Addition (Esipovich, et al., 2014)

CaO calcined at 600 °C; 0.2 wt.% water; 0.8 wt.% water; 2 wt.% water; 5 wt.% water; 10 wt.% water.

As seen in Figure 6, there is an increase in catalytic activity by the addition of water into the reaction system, however, the largest yield can be observed by the addition of the smallest amount of water added which is 0.2 $wt\%$ $(of\ oil)$ water. Esipovich et al. (2014) suggested the formation of active hydroxide sites (OH^-) on the catalyst surface as a result of the interaction between the catalyst active centers and water. This facilitates an increase in methoxide anions formation and resulted in a higher yield. According to Kouzu et al. (2009), the addition of water improves the solubility of the catalyst medium in the reaction system, thus promoting a higher reaction rate because the reaction is catalysed by diluted active calcium oxide rather than active calcium oxide. However, excess water may result in partial hydrolysis of fatty acid methyl esters (FAME), which significantly lowers the reaction rate as well as the yield produced by deactivating the catalyst surface, as seen in Figure 6. The reaction mechanism for the effect of water on the catalyst surface is seen in Figure 7.

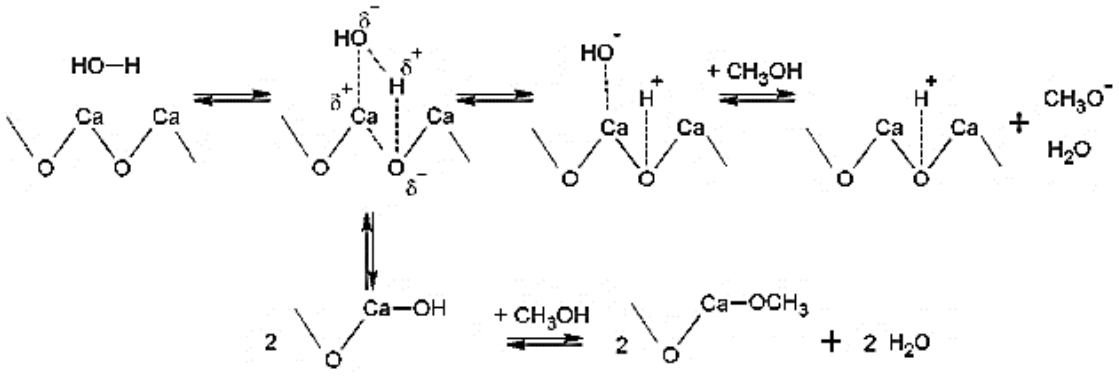

Figure 7 – Reaction Mechanism of Water on CaO Surface (Esipovich, et al., 2014)

Table 12 – Reaction Kinetics of CaO-based Catalysts (Marinković, et al., 2016)

Oil	Reaction conditions			Kinetic model	R^2
	Catalyst/ loading (%)	Methanol/ Oil molar ratio	Temperature (K)		
Cameline sativa	CaO/0.5	15:1	373	$\frac{dx_A}{dt} = k(\theta_B - 3x_A)$	0.332
Soybean	CaO/0.5	–	488	$-\frac{dC_A}{dt} = 3.9579x10^{-3}C_A{C_B}^{-0.5}$	0.490
Soybean	CaO/2	12:1	313-338	$-\frac{dC_A}{dt} = k_{app}C_A$	–
Waste frying soybean	CaO/2	6:1	333	–	–
Soybean	CaO/1.2	12:1	–	–	–
Soybean, virgin	K-CaO/7.5	12:1	308-338	–	–
Sunflower	CaO/ 1-10	6:1	333	$\frac{dx_A}{dt} = \frac{k_{mt,A}k_2}{k_{mt,A}+k_2}(1-x_A)$	0.920-0.981
Sunflower	Quicklime/ 1-10	6:1-18:1	333	$\frac{dx_A}{dt} = k_m\frac{(1-x_A)(C_{RO}+3C_{Ao}x_A)}{K+C_{Ao}(1-x_A)}$	0.968-0.998
Sunflower (refined, used)	CaO·ZnO/2	10:1	333-369	$\frac{dx_A}{dt} = \frac{k(k_{mt,A})_o[1+\alpha{x_A}^\beta]}{k+(k_{mt,A})_o[1+\alpha{x_A}^\beta]}(1-x_A)$	0.960-0.994
Sunflower	CaO·ZnO/ 0.5-2	6:1, 10:1	333	–	–
Jojoba	Mussel shell CaO/6-10	6:1-12:1	318-338	–	–

2.4.3.4 Lipase Catalysed Transesterification

This method utilises enzymes instead of acid and base catalysts to facilitate the conversion of triglycerides into biodiesel. Enzyme catalysts do not result in saponification and can be used with feedstocks that have a high free fatty acid percentage. In addition, enzyme catalysts are capable of converting more of the oil into biodiesel but suffer from high costs associated with increased reaction

times (Gebremariam & Marchetti, 2017). Pairiawi (2010) mentioned that generally enzyme, whole cells or lipase catalysts are immobilised during biodiesel production to enable mild operating temperatures of 50℃ and enzyme reusability without separation. Gebremariam & Marchetti (2017) reported that methanol and glycerol serve to inhibit immobilised enzyme catalyst activity. They reported that tert-butyl and continuous glycerol removal as well as stepwise addition of methanol into the reaction mixture serve to prevent the reduction in catalyst activity and decrease the overall cost (Ranganathan, et al., 2008).

Table 13 – Advantages and Disadvantages of Lipase Catalysed Transesterification (Parawira, 2010)

Advantages	Disadvantages
Biocompatible, biodegradable and environmental acceptability	Loss of some initial activity due to volume of the oil molecule
Possibility of regeneration and reuse of the immobilized residue, because it can be left in the reactor if one keep the reactive flow	Number of support enzyme is not uniform
Use of enzymes in reactors allows use of high concentration of them and that makes for a longer activation of the lipases	More expensive
Immobilization of lipase could protect it from the solvent that could be used in the reaction and that will prevent all enzyme particles getting together	
Separation of product will be easier using this catalyst, producing product of very high purity with less or no downstream operations	

2.4.3.5 Nano-Catalysed Transesterification

Nano catalysts are very small particles with high surface area. This large surface area serves to reduces side reactions and mass transfer resistance associated with conventional catalysts. Seffati et al. (2019) used $CaO/CuFe_2O_4$ nano catalyst for the production of biodiesel from chicken fat. They report that the distinct advantage of this catalyst was its magnetic characteristics which enabled easy separation by the use of a magnet. Their work shows that when catalyst content increases, biodiesel yield also increases with a maximum yield of 94.69 % noted when 3 % (W/v) catalyst is used. Borah et al. (2019) prepared Zinc (Zn) doped CaO nanocatalyst derived from waste egg shells by wet impregnation method. They reported a decrease in catalytic activity when the catalyst is reused due to leaching of Zn or blockage of reaction sites on the catalyst by products. Hu et al. (2011) report that calcination temperature should be taken into account as a parameter for biodiesel optimization as this influenced the yield of biodiesel produced when $KF/CaO-Fe_3O_4$, $KF/SrO-Fe_3O_4$ and $KF/MgO-Fe_3O_4$ nano-catalysts are used.

In a recent study, Saxena et al. (2019) produced biodiesel rich in C_{18} methyl esters from soybean oil and methanol in a ratio of 1:10 in the presence of bimetallic Fe(III) doped ZnO nano-particles with average particle size and surface area of $76.24 \pm 17\ nm$ and $12.39\ m^2 g^{-1}$, respectively. They reported

a reaction time of $3\ h$, temperature of $65℃$ and stirrer speed of $900\ rpm$. Additionally, recovery by magnetic current was used to recover $90 \pm 2\%$ of the nano-catalyst which was easily reused by first washing with anhydrous methanol then drying at $80℃$ overnight to obtain efficient transesterification under reuse at the same conditions. Similarly, Salimi & Hosseini (2019) observed a biodiesel yield of $92.08\ \%$ after subjecting their $ZnO/BiFeO_3$ nano-catalyst to a reusability test for five consecutive experiments which was attributed to the high catalytic activity of the nano-catalyst.

2.4.3.6 Ionic Liquids Transesterification

Ionic liquids are liquids comprising organic or inorganic anions and organic cations (Gebremariam & Marchetti, 2017; Reddy, 2015). Roman et al. (2019) recently showed that ionic liquids can serve as a viable alternative to conventional catalysts with reference to esterification reactions for the production of biodiesel. In their work with 1-methylimidazolium hydrogen sulfate, $[HMIM]HSO_4$, they showed that their ionic liquid can convert oils with high acid content into biodiesel. They however report a high catalyst dosage of $13.5\ wt\ \%$ which is necessary to facilitate the optimal conversion of oleic acid into fatty acid methyl esters. The optimal reaction temperature of $110℃$, which seems high with regards to conventional esterification reactions, was negated by the low activation energy of $6.8\ kJ/mol$ determined by a kinetic study.

In addition, Gebremariam & Marchetti (2017) report that ionic liquids are not soluble in the organic phase of biodiesel, therefore, biodiesel with high purity may be filtered from the reaction mixture. Similarly, pure glycerol may be easily separated by conventional distillation leaving pure ionic liquid which may be reused without any further purification steps. With reference to transesterification, 1-n-butyl-3-methylimidazolium cation is the most widely studied ionic liquid (Andreani & Rocha, 2012).

The optimal conditions for biodiesel production using ionic liquids is not widely done in literature. This may be due to the relative complexity regarding ionic liquids or high costs associated with the production process. However, Guo et al. (2014) conducted a study to investigate the optimum conditions for biodiesel production when soybean oil is reacted in the presence of methanol and an ionic liquid via ultrasonic irradiation ($24\ kHz, 80\ W$). A yield of $96\ \%$ was achieved with a reaction time of $20\ min$ using an optimal temperature and an oil to alcohol molar ratio of $60℃$ and 1:14, respectively. Furthermore, they concluded that ionic liquid was effective in the conversion of soybean oil to biodiesel and that the ionic liquid could be separated by simple decantation.

Table 14 – Optimum Conditions for Biodiesel Production via Ionic Liquid Transesterification (Gebremariam & Marchetti, 2017)

Feedstock	Methanol/Oil molar ratio	Ionic liquid catalyst	Catalyst loading $(wt\%)$	Temperature (℃)	Reaction time (h)	Yield (%)
Soybean	8:1	Basic Ionic Liquids $[Hnmm]OH$	4	70	1.5	97
Cottonseed	12:1	1-(4-Sulfonic acid) butylpyridinium hydrogen sulfate	0.057	170	5	92
Rapeseed	10:1	1-propyl-3-methyl imidazolium hydrogen sulfate ($[PrMIM][HSO_4]$)	10	140	5	19.74
Rapeseed	10:1	1-propyl-3-methyl imidazolium hydrogen sulfate ($[PrMIM][HSO_4]$)	10	130	5	94.91
Rapeseed	10:1	1-butyl-3-methylimidazolium hydrogen sulfate ($[BMIM][HSO_4]$)	10	110	5	8.89
Rapeseed	10:1	1-butylsulfonate-3-methyl imidazolium hydrogen sulfate ($[BSO3HMIM][HSO_4]$)	10	130	5	100

2.4.3.7 Supercritical Transesterification

Supercritical method refers to the operation of a process beyond the critical points of the reactants such that liquid and vapour phases do not exist, instead a single supercritical phase exists. This method involves operation under extreme temperatures and pressures which seem unfeasible in comparison to convention transesterification methods. However, due to the existence of a single supercritical phase between the alcohol and oil, mass transfer limitations are negated resulting in significant reduction of reaction time (Leung, et al., 2010). This is due to the sharp reduction in dielectric constant of methanol; making it non-polar; above the critical points of methanol. Furthermore, at or above the critical points of methanol, there is a drastic change in solubility between methanol and oil, generating a homogeneous phase (Gebremariam & Marchetti, 2017).

Kusdiana & Saka (2004) reported that supercritical methanol transesterification is less energy intensive in comparison to commercial processes due to the drastic reduction in reaction time from 4 h to 4 min (Shahid & Jamal, 2011). This was proved by the work of Marulanda (2012) who conducted pilot plant supercritical methanol transesterification experiments at an oil/alcohol molar ratio and temperature of 9:1 and 400℃, respectively. They concluded that should the pilot plant be scaled up to produce 10000 $tons/yr$, the energy requirement would be 573 kW/yr. This is significantly lower than the energy requirement (2407 kW/yr) of a similar process operating at an oil/alcohol molar ratio and temperature of 1:42 and 300℃, respectively, and lower than the energy requirement (2326 kW/yr) of a conventional transesterification process.

However, the sensitive nature of the process may be costly due to the high energy requirement to achieve such extreme temperatures and pressures. In addition, the process may be non-catalytic in nature which simplifies purification and product recovery. Moreover, the utilization of co-solvents may reduce overall cost by improving conversion efficiency (Gebremariam & Marchetti, 2017). The use of a co-solvent to reduce cost is evident in the work of Van Kasteren & Nisworo (2007) who used propane as a co-solvent in a single-stage supercritical methanol transesterification reaction.

Table 15 – Optimum Conditions for Biodiesel Production via Supercritical Transesterification (Gebremariam & Marchetti, 2017)

Feedstock	Alcohol	Process variables				Yield (%)
		Alcohol/Oil	Temperature (℃)	Time (min)	Pressure (MPa)	
Refined lard	Methanol	45:1	335	15	20	89.9
Rapeseed oil	Methanol	45:1	350	4	14	95
Coconut oil	Methanol	42:1	350	7	19	95
Palm oil	Methanol	42:1	350	7	19	96
Rapeseed oil	Methanol	42:1	350	15	12	93
Rapeseed oil	Ethanol	42:1	350	20	12	91.9
Rapeseed oil	Propan-1-ol	42:1	350	25	12	91.1
Jatropha oil	Methanol	43:1	320	4	8.4	100
Sunflower oil	Methanol	41:1	252	20	24	95
Sunflower oil	Methanol with 0.3 % CaO	41:1	252	17	24	95
Sunflower oil	Methanol with 0.5 % CaO	41:1	252	13	24	100
Palm oil	Methanol	45:1	350	5	40	95
Vegetable oil	Ethanol with C_2O co-solvent	25:1	200	6	20	80

Numerous studies have been conducted in literature regarding the optimum conditions for supercritical transesterification. In general, temperature is regarded as the main parameter which has the most influence over yield and is followed by reaction time and lastly by pressure. In the work by Kiss et al. (2014), experiments regarding the effect of temperature, pressure and time was investigated. They reported that decreasing reaction pressure resulted in a decrease in yield whilst a decrease in temperature may be mitigated by an increase in reaction time.

Recently, in the work of Lamba et al. (2019), the combination of supercritical methanol method and catalytic transesterification was studied. This involved operation at a temperature and pressure of $250℃$ and $10\,MPa$, respectively, and oil to alcohol ratio of $1:40$. They concluded that $1\,wt\%$ of heterogeneous catalyst is sufficient to overcome the pathway limitations associated with supercritical methanol method and heterogeneous catalytic method.

2.4.3.8 Non-Catalytic Transesterification

Transesterification may be achieved via the BIOX cosolvent process, which is a non-catalytic process. According to Mujeeb et al. (2016), the BIOX process is a relatively new Canadian process and originates from Professor David Boocock of the University of Toronto. This process involves the use of inert cosolvents to produce a single oil-rich phase. The function of the cosolvent is to increase the solubility of the alcohol in the triglyceride phase, thus making inert cosolvent selection very important to the efficiency of the process. The resulting single oil-rich phase achieves transesterification under standard temperatures and pressures. The BIOX process offers the lowest reaction time among the aforementioned transesterification processes, with a reported reaction time of greater than 99 % complete within seconds (Mujeeb, et al., 2016).

In addition to the low reaction time and economical process conditions, the BIOX process can be adjusted to a two-step esterification and transesterification process to accommodate high acid value feedstocks of up to 10 % FFA. The robust nature of the process can be seen by the variety of feedstocks that may be processed. Typical feedstocks include, grain-based oils, waste cooking oils and greases and animal fats (Van Gerpen, et al., 2004). The inert nature of the cosolvent; Tetrahydrofuran; allows the single stage or dual stage BIOX process to be continuous by recycling of the cosolvent, which may be reused as many times as necessary. Cosolvents may also be designed for specific alcohols and feedstocks to maximize efficiency. Mujeeb et al. (2016) reported that complete transesterification occurs after $5 - 10\ mins$.

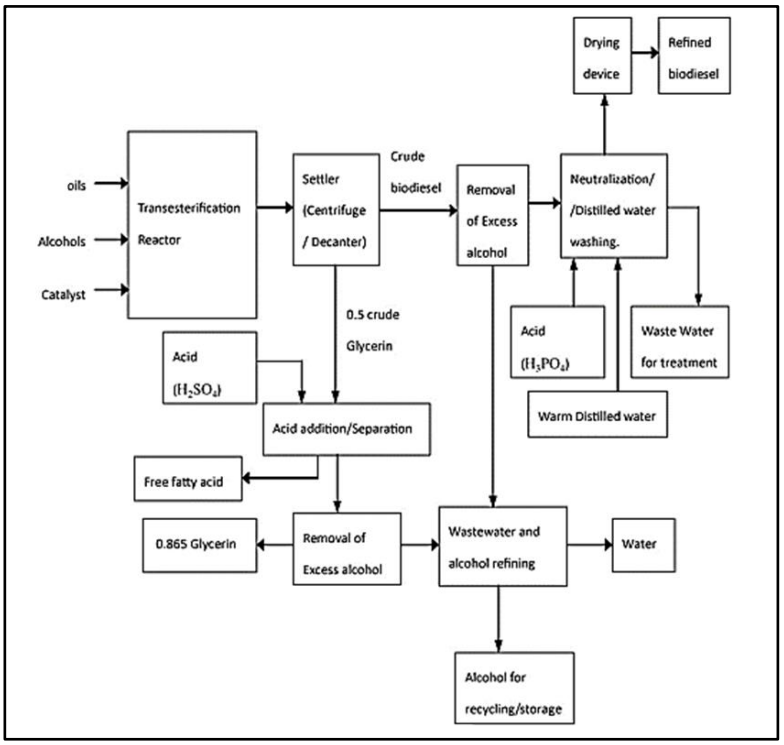

Figure 8 – Convention Biodiesel Production & Purification (Atadashi, et al., 2010)

2.4.4. Microwave Technology

This involves the production of biodiesel by electromagnetic waves with frequencies ranging from 0.3 GHz to 300 GHz (Nayak, et al., 2019). A conventional microwave functions by dielectric heating in which energy is not used to break and form new bonds, instead it is absorbed by water present in food, sugar and fats. According to Kapilan & Baykov (2014), thermal analysis of the dielectric properties of the microwave depend significantly on the temperature, frequency and catalyst which may facilitate industrial design and production of biodiesel by microwave assisted technology. In comparison to convention biodiesel production, microwave technology is less energy and time intensive with reaction times of 2 min, 3 min and 4 min reported for jatropha oil, waste cooking oil and palm oil, respectively (El Sherbiny, et al., 2010; Chen, et al., 2012; Khemthong & Faungnawakij, 2012).

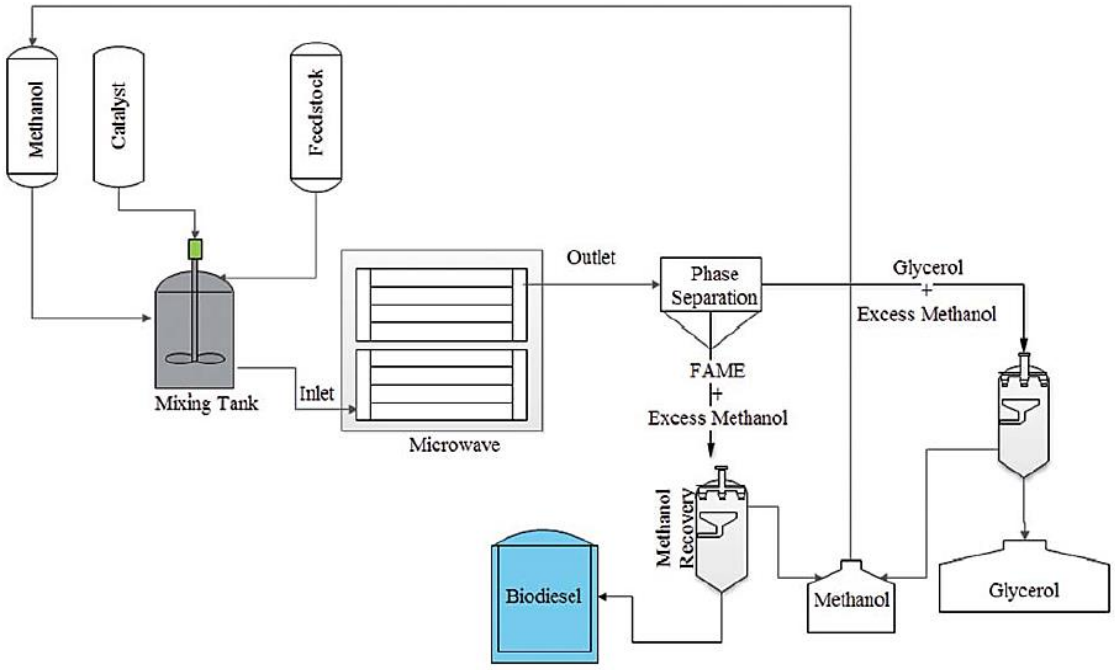

Figure 9 – Biodiesel Production via Microwave Technology (Ruhul, et al., 2015)

The procedure for microwave irradiation; highlighted by Kapilan & Baykov (2014); is as follows, (1) provide suitable agitation to the mixture of oil, alcohol and catalyst prior to microwave irradiation, (2) conduct transesterification via microwave irradiation for a suitable reaction time, generally under 10 $mins$ according to literature, (3) proceed with gravity separation in a separation funnel and hot water-washing to remove glycerol and other impurities, respectively, (4) proceed with product drying to reduce the moisture content generated by the reaction and residuals of water washing. The optimum conditions for biodiesel production with a variety of oils via microwave irradiation are seen in Table 16 below:

Table 16 – Optimum Conditions for Biodiesel Production via Microwave Irradiation Technology (Kapilan & Baykov, 2014)

Type of Oil	Optimum Conditions	References
Jatropha	Methanol/Oil molar ratio of 7.5:1, 1.5 $wt\%$ KOH, reaction temperature of 65℃, reaction time of 2 min	(El Sherbiny, et al., 2010)
Pongamia pinnata seed	Alcohol/Oil molar ratio of 6:1, reaction temperature of 60℃, 0.5 $wt\%$ NaOH and 1.0 $wt\%$ KOH	(Kumar, et al., 2011)
Waste cooking	Methanol/Oil molar ratio of 6:1, 0.75 $wt\%$ CH_3ONa or NaOH, reaction time of 3 min, microwave power of $750W$	(Chen, et al., 2012)
Yellow horn oil	Methanol/Oil molar ratio of 12:1, temperature of 60℃, reaction time of 10 min, 1 $wt\%$ heteropoly acid catalyst ($Cs_{2.5}H_{0.5}PW_{12}O_{40}$)	(Zhang, et al., 2010)
Palm	Methanol/Oil ratio of 18:1, reaction time of 4 min, 900 W microwave power, 15 $wt\%$ CaO catalysts derived from eggshells	(Khemthong, et al., 2012)
Waste frying palm	Ethanol/Oil molar ratio of 12:1, 3 $wt\%$ NaOH, reaction time of 30 sec	(Lertsathapornsuk, et al., 2008)

Microwave technology may also be applied to the production of biodiesel from wet microalgae. Cheng et al. (2013) conducted a novel approach in which wet microalgae was subject to microwave irradiation in a single step reaction. They concluded that, both the yield and conversion rate were higher than the corresponding two-step conventional reactions necessary for the production of biodiesel. Furthermore, they report that the microwave irradiation effects serve to increase the biocatalytic activity, rather than inhibit the catalyst activity by enzyme deactivation. As with any system, there exists a need for system wide control, however, very few researchers have employed the use of controllers to regulate the microwave power as well as automatic controllers to provide real-time adjustments to the process (Wali, et al., 2013).

Lertsathapornsuk et al. (2008) produced biodiesel via microwave irradiation from waste palm oil. The resultant biodiesel was then tested against conventional petro-diesel in a $100\,kW$ diesel generator, however, this comparison did not feature pure biodiesel in the test. They concluded that for B50 (50% petro-diesel/50% biodiesel) at all engine loads, engine thermal efficiency was reduced, however, lower emissions compared to petro-diesel were observed. Furthermore, they report that at the engine load of $75\,kW$, the emissions of CO, NO_X and HC were higher than that of petro-diesel.

2.4.5. Ultrasonic Technology

This type of biodiesel production employs the phenomenon of emulsification to induce cavitation of the liquid-liquid phase of the reactants. The cavitation causes radial motion of the system which in turn causes microturbulence within the reacting phase (Ji, et al., 2006). In a study conducted by Chen et al. (2011), tung oil and blends of tung oil of 20, 30 and $50\,wt\%$ was subject to ultrasonic irradiation in the presence of methanol and KOH. They concluded that blends of tung oil resulted in higher yields

with shorter reaction time and the resultant fuel was in accordance with biodiesel standards. Table 17 illustrates the optimum conditions for biodiesel production in accordance with ASTM standards using ultrasonic technology.

Table 17 – Optimum Conditions for Biodiesel Production via Ultrasonic Technology (Kapilan & Baykov, 2014)

Type of Oil	Optimum Conditions	References
Waste cooking oil	Methanol/Oil ratio of 6:1, 1 $wt\%$ KOH, temperature of 45℃, ultrasound power of 200 W, irradiation time of 40 min	(Hingu, et al., 2010)
Coconut oil	Ethanol/Oil ratio 1:6, 0.75 $wt\%$ KOH, 7 min reaction time	(Kumar, et al., 2010)
Canola oil	Methanol/Oil molar ratio of 5:1, 0.7 $wt\%$ KOH, reaction time 50 min, ultrasonic irradiation of 20 kHz with an input capacity of 1 kW	(Okitsu, et al., 2010)
Jatropha oil	Methanol/Oil ratio 1:4, catalyst of 5 $wt\%$ of oil, reaction time 30 min, ultrasonic amplitude 50 % ($100\ W/m^3$) and cycle 0.7 s	(Kumar, et al., 2011)
Crude cottonseed oil	Methanol/Oil ratio of 6.2:1, 1 $wt\%$ NaOH, reaction time of 8 min	(Fan, et al., 2010)

2.4.6. Microwave & Ultrasonic Technology

The combination of these two methods seem to result in an economical approach to biodiesel production, however, using ultrasound alone resulted in a reaction time of 60 min for esterification and 20 min for transesterification when high acid content nagchampa oil is used whilst the combination of the aforementioned methods resulted in reaction times of 15 and 6 minutes (Gole & Gogate, 2013). In an attempt to determine the most economical approach, Yin et al. (2012) conducted a study using four different methods, viz. mechanical agitation (MS), flat plate ultrasonic irradiation (FPUI), flat plate ultrasonic irradiation in conjunction with mechanical agitation (UIMS) and probe ultrasonic irradiation (PUI) with sunflower oil. They concluded that UIMS and PUI were among the better methods which resulted in lower catalyst dosage, reduced energy consumption, reduced reaction time and lower alcohol/oil ratio under the same reaction conditions.

2.4.7. Pyrolysis & Catalytic Cracking

Pyrolysis by definition is the thermal conversion or combustion of a substance by the addition of heat in the absence of oxygen or air to facilitate the cleavage of bonds to yield smaller molecules (Ma & Hanna, 1999).

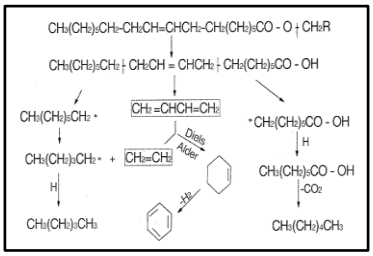

Figure 10 – Reaction Mechanism Illustrating Thermal Decomposition of Triglycerides (Schwab, et al., 1988)

There have been many works that have studied the effects and conditions of pyrolysis on bio-fuel production. Niehaus et al. (1986) and Schwab et al. (1988) pyrolyzed soybean and safflower oil, respectively, in conjunction with a sparged supply of air and nitrogen in a distillation unit. Table 18 illustrates the differences in fuel properties between soybean oil and pyrolyzed soybean oil against diesel fuel.

Table 18 – Comparison of Fuel Properties between Pyrolyzed Oil and Diesel Fuel (Ma & Hanna, 1999)

	Soybean oil		Pyrolyzed soybean oil		Diesel fuel	
	(Niehaus, et al., 1986)	(Schwab, et al., 1988)	(Niehaus, et al., 1986)	(Schwab, et al., 1988)	(Niehaus, et al., 1986)	(Schwab, et al., 1988)
Cetane number	38.0	37.9	43.0	43.0	51.0	40.0
Higher heating value, MJ/kg	39.3	39.6	40.6	40.3	45.6	45.5
Pour point, ℃	-12.2	-12.2	4.4	7.2	-6.7 max	-6.7 max
Viscosity, cSt at 37.8 ℃	32.6	32.6	7.74	10.2	2.82	1.9-4.1

In addition, the process of pyrolysis can accommodate catalysts to speed up the overall reaction process. In the work by, Pioch et al. (1993), copra and palm oil were catalytically cracked under pyrolysis conditions at $450℃$ in the presence of a conventional petroleum catalyst (SiO_2/Al_2O_3) to gases, liquids and solids. Biodiesel and biofuel were produced by fractionation of the condensed organic phase which yielded similar properties to that of petroleum diesel.

2.4.8. Microalgae

Microalgae-based biodiesel is derived from prokaryotic or eukaryotic micro-organisms that are either unicellular or simple multi-cellular in nature. It is widely understood that microalgae-based biodiesel can offer many advantages over traditional feedstocks currently used in the production of biodiesel. The distinct advantage of microalgae is the amount of biodiesel that can be extracted from a very small population of microalgae as compared to the large area required of crop cultivation. In addition, microalgae only requires sunlight and simple nutrients to grow and reproduce, thus completing a life cycle every few days (Sheehan, et al., 1998). Microalgae is easy to cultivate and can grow is almost any environment. There are numerous species of microalgae that can be adapted to live in specific regions and growth can be accelerated by means of nutrients and aeration in the case of aquatic microalgae (Mujeeb, et al., 2016). A comparison between microalgae and traditional feedstocks used for biodiesel production can be seen in Table 19. A vast difference in land use and biodiesel productivity can be seen when high oil content microalgae is used. These differences are due to similar seed oil content values but very different land usage values. Therefore, from a practical point of view, microalgae-based biodiesel seems to be the most economical way of biodiesel production.

Table 19 – Comparison of Microalgae and Traditional Feedstocks (Mujeeb, et al., 2016)

Plant source	Seed oil content ($\%\ oil\ by\ wt\ in\ biomass$)	Oil yield ($L\ oil/ha\ year$)	Land use ($m^2 year/kg\ biodiesel$)	Biodiesel productivity ($kg\ biodiesel/ha\ year$)
Corn/Maize	44	172	66	152
Hemp	33	363	31	321
Soybean	18	636	18	562
Jatropha	28	741	15	656
Canola/Rapeseed	41	974	12	862
Sunflower	40	1070	11	946
Castor	48	1307	9	1156
Palm oil	36	5366	2	4747
Microalgae (low oil content)	30	58700	0.2	51927
Microalgae (medium oil content)	50	97800	0.1	86515
Microalgae (high oil content)	70	136900	0.1	121104

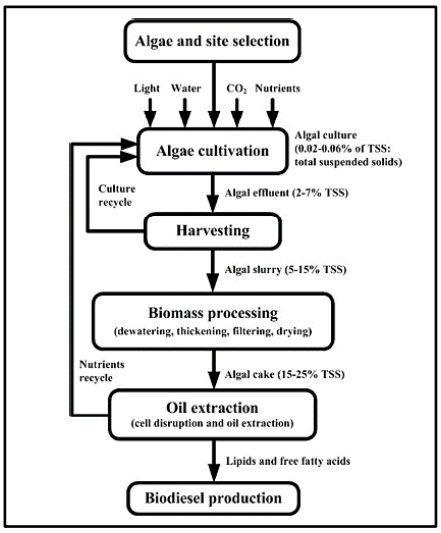

Figure 11 – Microalgae based Oil Extraction (Mujeeb, et al., 2016)

With reference to Figure 11, it can be seen that water and nutrients are necessary for adequate growth of microalgae. Typically, nutrients required are nitrogen-based and usually in the form of chemical or inorganic fertilizers. Chemical fertilizers, however, contaminate water sources easily and are often difficult to remove from wastewater. According to Colosi et al. (2015), secondary and tertiary wastewater treatments are necessary to reduce the amount of nitrates and ortho-phosphates present in chemical fertilizers that are not removed during the primary wastewater treatment process. This will result in approximately $60 - 80\%$ of additional energy utilization by the treatment plant. An attractive solution would be to culture microalgae in wastewater, thus eliminating the need for large amounts of

chemical fertilizer and wastewater purification can occur by the removal of nitrates and ortho-phosphates (Colosi, et al., 2015).

Lipid extraction is achieved depending on the type of microalgae used and on the nature of biodiesel to be produced. Much like terrestrial energy crops, lipid extraction can be achieved by mechanical means using cell homogenizers, bead mills, ultrasound, autoclaves and spray drying. However, due to the thick cell walls present in the microalgae, mechanical press methods are generally not applied as it results in intra-lipid loss. Generally, solvent extraction and supercritical fluid extraction methods are employed for lipid extraction.

Chemical solvent extraction is the most common method in microalgae processes and offers high efficiency in lipid extraction. Moreover, the solvents used are typically n-hexane, methanol and ethanol, which are readily available. These solvents have a high selectivity and solubility towards lipids and can quickly extract lipids from the microalgae. However, the efficiency of extraction strongly depends on the type of microalgae used, more specifically on the thickness of the cell wall as the rate limiting factor in the extraction process is diffusion through the cell wall (Mujeeb, et al., 2016).

Supercritical fluid extraction exploits the single-phase nature of a supercritical system to greatly increase the efficiency of the extraction process in which the fluid used for extraction becomes a super-solvent (Mujeeb, et al., 2016). Carbon dioxide is regarded as the most attractive supercritical fluid as it is able to extract pharmaceutical and health aiding products from microalgae (Plaza, et al., 2009). Carbon dioxide has several advantages over solvent extraction fluids viz., (1) non-oxidizing and non-toxic to prevent the degradation of products, (2) relatively low critical temperature to avoid thermal degradation, (3) higher efficiency of extraction due to increased diffusivity and lower surface tension of carbon dioxide, (4) ease of separation after extraction under atmospheric temperatures and pressures (Mujeeb, et al., 2016; Plaza, et al., 2009). Thereafter, once extraction is complete, transesterification can occur using any suitable method discussed earlier.

2.4.9. Membrane Technology

This process utilizes an organic or inorganic membrane to remove the transesterification reaction products as soon as they are formed, thus eliminating the adverse effects of the alcohol and glycerol present in the reaction system (Aransiola, et al., 2014). According to Cao et al. (2009), the efficiency and selectivity parameter of the membrane employed depends on suitable pore size and chemical affinity. Membrane technology can also be employed in the refinement of crude biodiesel as evident in the work of Cao et al. (2009), who achieved high quality biodiesel from crude biodiesel. Generally, membrane technology is utilized in conjunction with membrane reactors. In the work of Cao et al. (2009), it is evident that a variety of oils may be used in the production of biodiesel. These oils; soybean,

palm and canola oil; are relatively common in the biodiesel environment. They report that the main advantage of membrane reactors and membrane technology is the quality of biodiesel produced, conversely, the size and structure of the membrane is limited as larger membranes would be prone to structural weakness and tearing. Moreover, larger membranes have been employed using ceramic as the material of construction, however, this makes the membrane relatively expensive (Ambat, et al., 2018).

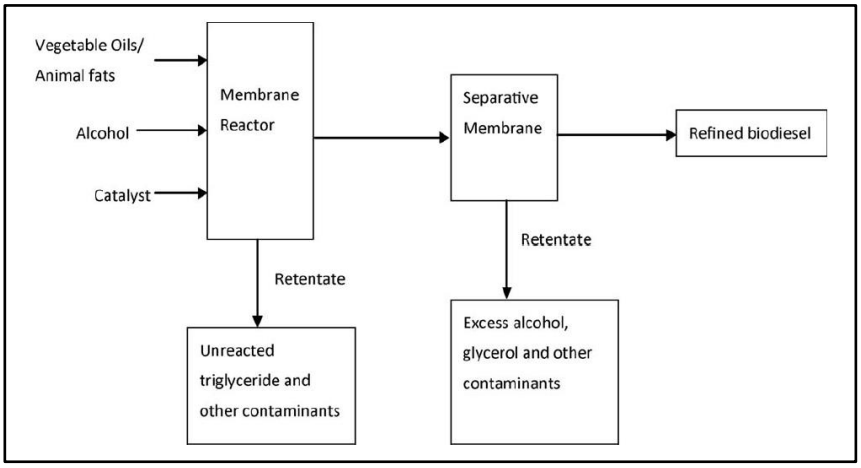

Figure 12 – Biodiesel Production via Membrane Technology (Atadashi, et al., 2010)

Table 20 – Advantages and Disadvantages associated with Catalytic and Non-Catalytic Processes (Ruhul, et al., 2015)

Process	Advantages	Disadvantages
Catalytic	Lower power consumption regarding heating	Higher process cost
	Higher yield is possible	Greater time is required than for non-catalytic method
	Relatively lower temperature and pressure required	Cost involved with catalyst loading
		Preparation of catalyst is quite complex
Non-catalytic	Less water is produced as a by-product and sometimes the presence of water accelerates the conversion rate	Relatively lower yield than for catalytic conventional process
	Simpler purification steps involved	More energy is required, especially in the heating step
	Simpler separation steps involved	High temperature and pressure required
	High quality glycerine produced as a by-product	High alcohol/oil ratio required
	Environmentally friendly as a smaller amount of chemical used	
	Less time required	
	Low quality feedstock can be easily transformed into biodiesel	

2.5. Factors Affecting Biodiesel Production – Esterification & Transesterification

There are various factors that affect the yield of biodiesel, viz. reaction temperature, reaction time, alcohol/oil ratio, catalyst loading and stirrer speed. The aforementioned factors are specific for esterification and transesterification reactions were edible and non-edible oils react with alcohol in the presence of a catalyst.

2.5.1. Temperature

N.i et al. (2018) recorded an increase in biodiesel yield with an increase in reaction temperature up to the boiling point of the alcohol used. This is to be expected as the reaction is endothermic with positive activation energy. Additionally, soap formation was observed when reaction temperature exceeded the boiling point of the alcohol used and this can be attributed to the triglycerides present in the feedstock (waste cooking oil). They also noted the formation of a waxy solution upon addition of alcohol and catalyst (NaOH) when oil temperature was in excess. In such a case, no biodiesel could be synthesised.

Tan et al. (2016) noted an optimal reaction temperature of 65℃ when methanol is used in conjunction with waste cooking oil in the presence of a homogeneous or heterogeneous catalyst in a closed reaction vessel. This is in accordance with literature as it corresponds to the normal boiling point temperature of methanol.

Sheet (2018) investigated the effects of pre-treatment by heating prior to transesterification for waste cooking oil. They concluded that pre-treatment by heating past the alcohol boiling point is not recommended. This may be attributed to an increase in saponification rate by the catalyst during transesterification.

Anguebes-Franseschi et al. (2016) employed the use of Response Surface Methodology (RSM) and Central Composite Design (CCD) to investigate the effects of reaction temperature; among other parameters; on biodiesel production from African crude palm oil. An optimal temperature of 56℃ resulted in a yield of 90 %, with further temperature increase resulting in saponification and reduction in yield.

Dhawane et al. (2018) conducted parametric optimisation to investigate biodiesel production from waste cooking oil. The Taguchi Approach was employed for optimisation which resulted in reaction temperature having the largest effect (71.6 %) on biodiesel yield according to an analysis of variance (ANOVA). The maximum yield and optimal reaction temperature are 95.376 % and 60℃, respectively, when methanol is used in a molar ratio of 12:1 in the presence of 5 $wt\%$ H_2SO_4 for 3 hours.

2.5.2. Acid Value

Generally, a high acid value may be noted when waste cooking oil is used as a feedstock. This is evident in the work of Tchameni et al. (2015) who noted an acid value of $83.07\ mg\ KOH/g\ oil$. This is above the limit of $2\ mg\ KOH/g\ oil$ according to literature (Tchameni, et al., 2015; Freedman & Pryde, 1982). Their solution involved a two-step (1) acid-catalysed esterification and (2) base-catalysed transesterification process to reduce the acid value to $3.32\ mg\ KOH/g\ oil$ and finally to $0.56\ mg\ KOH/g\ oil$. Similarly, Anguebes-Franseschi et al. (2016) followed a two-step process for African crude palm oil with a free fatty acid content of 5.72 %.

Whereas, Sousa et al. (2010) used castor oil with an acid value of $4.7\ mg\ KOH/g\ oil$ and glycerol in a ratio of 1:2, with trace amounts of base-catalyst in a neutralisation reaction to reduce the acid value to $0.44\ mg\ KOH/g\ oil$ under constant heating at $120℃$ for 2 hours. The glycerol was obtained from previous transesterification reactions in the presence of a base catalyst. However, the amount of glycerol necessary for this process is double the amount of castor oil, therefore, this method may not be feasible as first glycerol needs to be produced by transesterification and then used in subsequent neutralisation reactions.

2.5.3. Reaction Time

When waste cooking oil is used as a feedstock in the presence of methanol, the reaction time is typically $60 - 90\ min$. This is evident in the work of N.i et al. (2018) who observed a 5 % difference in biodiesel yield for reaction times of 60 and 90 minutes. The curve of reaction time versus biodiesel yield rises with time, but soon reaches equilibrium around 60 minutes. The reaction time of 60 minutes is in accordance with Samuel et al. (2015), who noted an optimal yield of 97.2 % when Nigerian waste cooking oil is used.

In addition, Sanli & Canakci (2008) who used sunflower oil as a feedstock, noted only a 1 % increase in yield when the reaction time is changed from $1\ h$ to $8\ h$. They concluded that a reaction time of $1\ h$ is appropriate for biodiesel production for low viscosity oils and that an extended reaction time may result in a decrease in yield. Furthermore, a decrease in biodiesel density was noticed when reaction time increased. This effect was more pronounced when soybean oil was used as compared to sunflower oil. They reported an inversely proportional relationship between density and reaction time for soybean oil and observed that all oils tested had reached the standard density for biodiesel even with a reaction time of 30 minutes.

Boz et al. (2015) noted a reaction time of 9 hours during simultaneous esterification and transesterification of waste cooking oil as well as for testing other factors such as alcohol/oil ratio and catalyst (Amberlyst 15 and modified Amberlyst 15) ion-exchange capacity.

2.5.4. Alcohol/Oil Molar Ratio

This ratio represents the molar quantities of alcohol that needs to be added to oil to fully convert the oil into biodiesel. Alcohol is typically present in excess quantities to ensure maximum conversion. N.i et al. (2018) described an alcohol/oil ratio of 6:1 as the optimum. In their work, higher ratios of waste cooking oil to alcohol led to increased glycerine and alcohol in the separation stage which led to decreased purity of biodiesel.

Sanli & Canakci (2008) noted a decrease in biodiesel yield when sunflower oil was used with a decreased oil/alcohol ratio. Initially, the ratio of oil to methanol was 6:1 which resulted in a yield of 97.85 %. Decreasing the alcohol/oil ratio from 6:1 to 3:1 resulted in a 20.3 % decrease in yield. The alcohol/oil ratio of 3:1 is the stoichiometric ratio of oil to alcohol as seen in Figure 13. Factors such as viscosity, density and glycerol production were also negatively affected. The viscosity was found to increase by 1.03 mm^2/s whilst the density and total glycerol production increased by 0.0062 g/cm^3 and 1.1 %, respectively. They concluded that further increase; past 6:1; in alcohol/oil ratio had very little effect on the yield as well as on the physical properties of the product. In this work, however, the oils used were of low density and viscosity which significantly contributed to the conclusion drawn. Further increase in the alcohol/ratio may proof beneficial when high viscosity oils are used as this increases the solubility and contact time of the oil in alcohol (Leung & Guo, 2006).

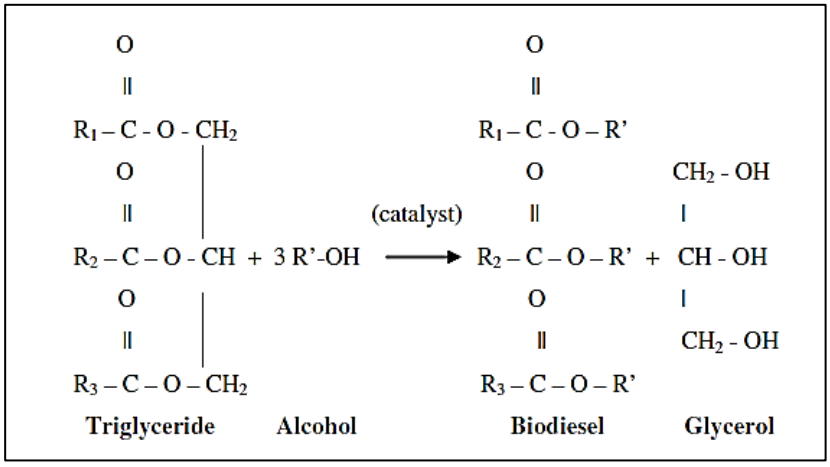

Figure 13 – Stoichiometric Transesterification Reaction (Canakci & Sanli, 2008)

2.5.5. Alcohol Type

According to N.i et al. (2018), methanol is more effective in the conversion of oil to biodiesel than ethanol as the energy required to break the hydroxide bond (OH^-) from methanol is lower than that of ethanol. Therefore, for a transesterification reaction, they concluded that methanol has a higher affinity for waste cooking oil conversion than ethanol.

The work of Sanli & Canakci (2008) highlighted the difficulty associated when ethanol is used in the transesterification reaction. They noted difficulty in separation between biodiesel and glycerol phases

after transesterification due to low purity ethanol (96 %). Furthermore, after physical property testing; density and viscosity; they noticed the similarity between the physical properties of the products and that of the vegetable oil used. This led to the realisation that biodiesel could not be synthesised by the low purity ethanol even at alcohol to oil ratios of 20:1. In addition to ethanol usage, they also investigated the use of propan-2-ol for transesterification. The relative low reactivity of propan-2-ol can be attributed to the branched hydroxide group present. Therefore, biodiesel could not be synthesised when propan-2-ol is used in the presence of an alkaline catalyst, even at unfeasible conditions. Sanli & Canakci (2008) used an acid catalyst after the unsuccessful attempt at biodiesel production using an alkaline catalyst. A similar procedure was noted when butan-1-ol was used.

2.5.6. Type of Catalyst & Catalyst Loading

The type of catalyst and catalyst loading significantly effects the yield of biodiesel produced. This is evident in the work of Fereidooni et al. (2017) whereby an investigation into the effect of bentonite on biodiesel synthesis was conducted. Waste cooking oil, potassium hydroxide and methanol were the reactants. Prior to transesterification, potassium hydroxide ($0.6\ g$) of concentration $21.43\ mg/mL$ was reacted with methanol ($22\ g$) and heated at $60℃$ for 1 hour to form potassium methoxide. Varying amounts of bentonite zeolite were then added to potassium methoxide. They reported a directly proportional relationship between the amount of bentonite added versus biodiesel yield. This may be attributed to the water removing capabilities of bentonite during potassium methoxide synthesis. The reduction in water by bentonite serves to maintain the catalytic activity of the methoxide catalyst.

The effect of catalyst type and loading can generally be seen in works involving biodiesel production. For example, Sanli & Canakci (2008) noted a decrease in yield for an increase in KOH loading from 1 (wt %) to 1.5 (wt %). Excess alkaline catalyst resulted in an increase in saponification. Conversely, when NaOH loading was increased from 0.5 (wt %) to 1 (wt %), a 4.24 % increase in yield was observed under the same reaction conditions. Excess NaOH loading; 1.5 (wt %); resulted in gelling which resulted in no biodiesel being synthesised. In addition, they noted longer dissolving times when NaOH was dissolved in methanol than that of KOH. Acid-catalysed transesterification using H_2SO_4 occurred when propan-2-ol and butan-1-ol were used with sunflower oil. Butan-1-ol at 5 (wt %) catalyst loading and reaction temperature of $110℃$ resulted in biodiesel which was in accordance with EN 14214 standards whereas the biodiesel produced from propan-2-ol could not meet EN 14214 standards, even at 3 (wt %) and 5 (wt %) catalyst loading and reaction temperature of $77℃$. Sanli & Canakci (2008) also noted slow reaction times when using acid-catalysts, which is in accordance with literature.

Boz et al. (2015) investigated the use of Amberlyst 15 and modified Amberlyst 15 catalyst for the simultaneous esterification and transesterification reaction when waste cooking oil with a high free fatty

acid content ($1.04 - 8.04$ %) is used for biodiesel production. Their findings indicated a relatively low biodiesel yield of 78 ± 3.39 %, corresponding to Amberlyst 15 catalyst, which may be attributed to the simultaneous nature of the process whereby water production during esterification resulted in hydrolysis of triglycerides which in turn, led to inhibited biodiesel production. Another factor contributing to lower yield is catalyst loading. This was investigated in the work by Anguebes-Franseschi et al. (2016), who reported that excess catalyst promoted saponification of triglycerides of African crude palm oil and the reversibility of the reaction system may also result in a lower yield if the reaction time is in excess.

2.5.7. Stirrer Speed

Since oil and alcohol are immiscible mixtures, significant agitation is necessary for the transesterification reaction to proceed timeously. N.i et al. (2018) reported highest biodiesel yields for maximum stirrer speeds of 600 and $800\ rpm$ when ethanol and methanol, respectively, is used with waste cooking oil. The speed of the stirrer is important in the mixing of the alcohol and catalyst, in the case of heterogeneous catalysts, the catalyst and alcohol must be mixed under heating, such that the alcohol adsorbs onto the catalyst surface.

Karmakar et al. (2018) reported that stirrer speed is an important parameter in castor oil esterification owing to the high viscosity of castor oil, especially when the reaction temperature is low. They concluded that higher stirrer speeds below the optimum speed leads to an increase in turbulence within the reaction mixture, thus promoting interactions between the reactants at a molecular scale. According to their findings, they report that a stirrer speed of $700\ rpm$ is sufficient to overcome external mass transfer limitations associated with the catalyst, oil and alcohol and does not result in reduced contact time between the aforementioned reactants. In the case of castor oil esterification, an increase in reaction rate and Free Fatty Acid conversion was observed with an increase in stirrer speed up to the optimum speed of $700\ rpm$.

2.6. Biodiesel Optimization

There are a variety of factors that influence the production and optimisation of biodiesel, however, the common factors generally include, temperature, reaction time, alcohol/oil ratio and catalyst loading. These factors are specific to the reaction system and will not be applicable to similar reaction systems with minor differences therefore for the best results, optimisation should occur for every reaction system. Typically, one variable at a time (OVAT), Central Composite Design (CCD) and Box-Behnken Design (BBD) are used for the optimisation of biodiesel production.

2.6.1. One variable at a time (OVAT)

This method of optimisation is regarded in literature as the most basic form of optimisation and functions by fixing specific variables as constants whilst varying the other variable. This method of optimisation makes discovering the optimal conditions much easier as one may be able to see which

variables have produced the largest impact on the yield of biodiesel. Furthermore, since other variables are fixed, when the effect of the changing variable is plotted against yield, it will be clear from the plot where the optimal condition that results in the highest yield lies.

2.6.2. Central Composite Design (CCD)

A Central Composite Design may be regarded as a design comprising a cube and a star portion. This design is recommended for sequential experiments due to its ability to capture information from a properly planned two-level factorial experiment. Furthermore, the CCD can easily estimate regression parameters in a full quadratic regression model and has orthogonal blocks. The design is rotatable or nearly rotatable.

2.6.3. Box-Behnken Design (BBD)

A Box-Behnken Design may be regarded as a cube comprising design points at either the center of the cube or at the midpoints of the lines making up the cube, or a possible combination of the two aforementioned methods. Additionally, this design method does not operate at all design factors at the extremes simultaneously. A key advantage of this design is the efficiency of estimation of regression coefficients in a regression model. The model may be regarded as rotatable or nearly rotatable and the design has orthogonal blocks. Generally, in literature, when compared to Central Composite Design (CCD), it can be seen that BBD has fewer experiments that need to be conducted for the same number of factors. This may be regarded as more economical since fewer resources need to be used to achieve similar results. The following figure provides a visual representation of the Box-Behnken Design.

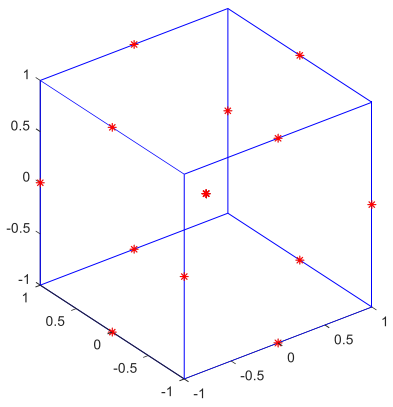

Figure 14 – Box-Behnken Design

According to Ferreira et al. (2007), the Box-Behnken design easily estimates regression parameters for a full quadratic model and permits the building of sequential designs by the use of multiple blocks. In addition, the design is able to determine the lack of fit of the model to the data set. Furthermore, in their work in the comparison between Box-Behnken design, Central Composite design, Doehlert Matrix and

full factorial designs, the Box-Behnken design and Doehlert Matrix was shown to be more efficient than the Central Composite design and very efficient when compared to the full factorial design.

2.7. Summary

As seen in this chapter, there are many ways to produce biodiesel, however, transesterification using a homogeneous base catalyst is mostly used. However, as technology improves and the need for biodiesel becomes greater, emerging technologies such as supercritical methanol transesterification and ultrasonic assisted transesterification may prove vital in meeting the demand of biodiesel. Currently, biodiesel is more expensive than petro-diesel, which may be attributed to the high price of the feedstock used in the production of biodiesel. This may be mitigated by the use of microalgae as a feedstock which do not require large areas for cultivation, however, expensive temperature and environmental controls are required to cultivate the microalgae.

Chapter 3 – Equipment Description

3.1. Introduction

This chapter focuses mainly on providing a concise image of the experimental setup. The optimization methodology chosen for this study is the Box-Behnken Design (BBD). Although two oils, viz. castor oil and sunflower oil, were used, the process of esterification and transesterification of castor oil resulted in effectively three independent experiments. As such, 27 separate experiments were conducted for each of the three feedstocks, i.e. base castor oil, esterified castor oil and sunflower oil.

3.2. Materials Used

The following raw materials were of analytical grade and used without further purification:

Table 21 – Raw Materials

Material	Supplier	Purity
Castor oil	KIWA BCS Oeko-garantie	–
Sunflower oil	LICHRO	–
Methanol	Sigma-Aldrich	≥ 99.8 %
Calcium oxide catalyst (CaO)	Radchem	Analytical Grade (AR)
Sulphuric acid	Radchem	Analytical Grade (98 %)

However, additional materials were necessary for physical property testing according to ASTM standards. Toluene and propan-2-ol were used in conjunction with water in the ratio of $100:99:1$, respectively, to form the titration solvent necessary for the determination of the acid value. Potassium hydroxide was used as the titrant when combined with water to form a $0.1\,M$ solution. Ethanol and hydrochloric acid were used with potassium hydroxide to determine the saponification value of the oils. Hexane was used to wash the catalyst surface during the catalyst reusability study which was conducted independently from the experimental procedure. Finally, kerosene was used in the blending process with biodiesel from the respective oils to produce bio-jet fuel.

Table 22 – Additional Materials Used

Material	Supplier	Purity
Toluene	Merck	Analytical Grade (≥ 99 %)
Propan-2-ol	Radchem	Analytical Grade (AR)
n-Hexane	Sigma-Aldrich	Analytical Grade (AR)
Potassium hydroxide	Radchem	Analytical Grade (AR)
Ethanol	Sigma-Aldrich	Analytical Grade (AR)
Hydrochloric Acid	Sigma-Aldrich	Analytical Grade (AR)
Kerosene	LICHRO	–

3.3. Equipment Used

The following equipment was used to facilitate the esterification and transesterification of castor oil and transesterification of sunflower oil. The figure shown below is to be used in conjunction with the table below:

Table 23 – Equipment Used

Equipment	Key	Description
Burette $(50ml)$		To determine the acid content of the base oil and biodiesel produced by titration against 0.1 M KOH solution
Centrifuge		Facilitates the separation of solid catalyst from the biodiesel and glycerol mixture
Magnetic stirrer and heater $(500ml)$	1	To impart kinetic energy into the reaction vessel whilst providing magnetic stirring via a magnetic stirrer bar
Reflux condenser	2	To condense methanol vapours during the reaction, thus increasing the oil/alcohol contact time and improving yield
Rotary Evaporator		To remove excess water and methanol residuals present in the biodiesel after hot water washing
Separation funnel $(500ml)$	3	Allows biodiesel to easily settle at the top of the funnel for easy removal of the bottom glycerol layer
Stirrer bar	4	Ensures the vigorous mixing of the oil and alcohol with the catalyst
Thermometer	5	To measure the average kinetic energy of the reaction proceedings. To enable suitable temperature adjustments to maintain isothermal conditions
Three-necked flask $(500ml)$	6	To contain the reaction contents and to facilitate the addition of a thermometer and reflux condenser
Water bath	7	Provides cold water to the condenser, which in turn condenses the methanol vapours

3.4. Experimental Setup

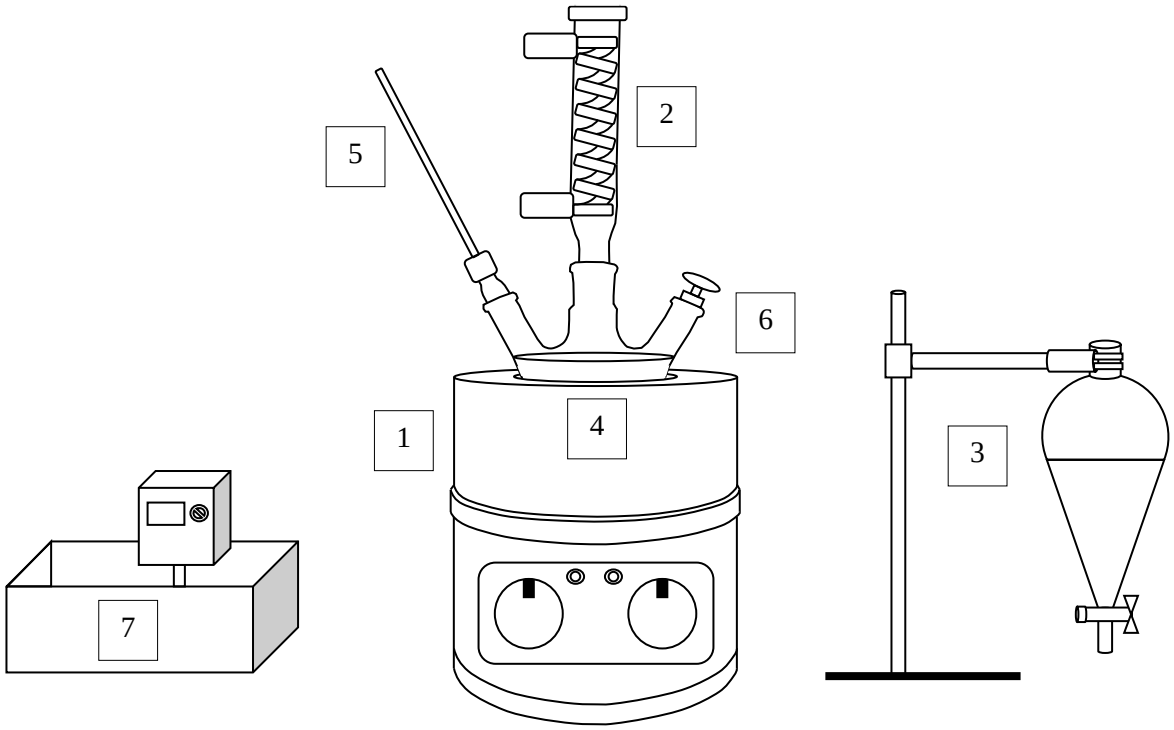

Figure 15 – Experimental Setup (Schematic)

The following picture of the experimental setup may aid to visualise the process:

Figure 16 – Experimental Setup (Picture)

3.5. Summary

In general, the equipment used is in accordance with conventional transesterification equipment. However, minor losses in yield may have occurred during transfer of the sample from the vials used for centrifugation to the separation funnel. Overnight settling coupled with water washing may have also resulted in loss of yield. The evidence of saponification was seen in many experiments, and due to the type of catalyst used, more soap was produced upon water washing. Water washing was necessary to improve the quality of the biodiesel.

Chapter 4 – Experimental Design & Methodology

4.1. Introduction

The experimental design follows a Box-Behnken Design with 4 factorials, viz. reaction temperature, reaction time, alcohol/oil molar ratio and catalyst loading. An acid value limit of $2\ mg\ KOH/g\ oil$ is recommended in literature (Tchameni, et al., 2015; Freedman & Pryde, 1982). Preliminary acid value testing of commercial castor and sunflower oils revealed the need for a two-step esterification and transesterification process for castor oil as the acid number was greater than $2\ mg\ KOH/g$ whereas a single transesterification reaction was sufficient for sunflower oil as it had an acid value lower than the allowed amount. Additionally, it is widely reported in literature that biodiesel produced from castor oil in a single transesterification reaction has a high kinematic viscosity which does not meet ASTM standards.

4.2. Experimental Design

As evident in Table 24, Table 25 and Table 26, the four factors varied were temperature, catalyst loading, reaction time and alcohol/oil ratio. According to the Box-Behnken experimental design conducted on *Minitab*™, there are a minimum of 27 experiments, inclusive of 3 replicates which are highlighted in bold font. The experiments are randomised to minimise experimental error.

The amount of required experiments for optimisation is calculated via the following equation (Srikanth, et al., 2018):

$$N = 2k(k-1) + C$$

Where, N, represents the number of experiments and k represents the number of independent variables or predictors and C represents the central points necessary for model validation and determination of coefficients.

$$N = 2 * 4 * (4-1) + 3 = 27$$

Table 24 – Castor Oil Esterification Experimental Box-Behnken Design

Std Order	Run Order	Pt Type	Blocks	Temperature (℃)	Catalyst Loading ($wt\%$)	Time (min)	Alcohol/Oil Ratio
13	1	2	1	47	0.25	30	9.5
24	2	2	1	47	3.25	75	15
22	3	2	1	47	3.25	75	4
10	4	2	1	64	1.75	75	4
20	5	2	1	64	1.75	120	9.5
2	6	2	1	64	0.25	75	9.5
18	7	2	1	64	1.75	30	9.5

4	8	2	1	64	3.25	75	9.5
6	9	2	1	47	1.75	120	4
3	10	2	1	30	3.25	75	9.5
25	**11**	**0**	**1**	**47**	**1.75**	**75**	**9.5**
9	12	2	1	30	1.75	75	4
1	13	2	1	30	0.25	75	9.5
8	14	2	1	47	1.75	120	15
7	15	2	1	47	1.75	30	15
19	16	2	1	30	1.75	120	9.5
21	17	2	1	47	0.25	75	4
16	18	2	1	47	3.25	120	9.5
26	**19**	**0**	**1**	**47**	**1.75**	**75**	**9.5**
5	20	2	1	47	1.75	30	4
11	21	2	1	30	1.75	75	15
12	22	2	1	64	1.75	75	15
23	23	2	1	47	0.25	75	15
17	24	2	1	30	1.75	30	9.5
15	25	2	1	47	0.25	120	9.5
27	**26**	**0**	**1**	**47**	**1.75**	**75**	**9.5**
14	27	2	1	47	3.25	30	9.5

Table 25 – Castor Oil Transesterification Experimental Box-Behnken Design

Std Order	Run Order	Pt Type	Blocks	Temperature (℃)	Catalyst Loading ($wt\%$)	Time (min)	Alcohol/Oil Ratio
3	1	2	1	30	1.5	75	9.5
1	2	2	1	30	0.5	75	9.5
11	3	2	1	30	1	75	15
21	4	2	1	47	0.5	75	4
5	5	2	1	47	1	30	4
17	6	2	1	30	1	30	9.5
6	7	2	1	47	1	120	4
26	**8**	**0**	**1**	**47**	**1**	**75**	**9.5**
16	9	2	1	47	1.5	120	9.5
20	10	2	1	64	1	120	9.5
25	**11**	**0**	**1**	**47**	**1**	**75**	**9.5**
10	12	2	1	64	1	75	4
15	13	2	1	47	0.5	120	9.5
23	14	2	1	47	0.5	75	15
22	15	2	1	47	1.5	75	4
7	16	2	1	47	1	30	15
13	17	2	1	47	0.5	30	9.5
9	18	2	1	30	1	75	4
19	19	2	1	30	1	120	9.5
12	20	2	1	64	1	75	15
27	**21**	**0**	**1**	**47**	**1**	**75**	**9.5**

8	22	2	1	47	1	120	15
18	23	2	1	64	1	30	9.5
24	24	2	1	47	1.5	75	15
2	25	2	1	64	0.5	75	9.5
4	26	2	1	64	1.5	75	9.5
14	27	2	1	47	1.5	30	9.5

Table 26 – Sunflower Oil Transesterification Experimental Box-Behnken Design

Std Order	Run Order	Pt Type	Blocks	Temperature (℃)	Catalyst Loading $(wt\%)$	Time (min)	Alcohol/Oil Ratio
14	1	2	1	47	1.5	30	9.5
7	2	2	1	47	1	30	15
16	3	2	1	47	1.5	120	9.5
27	**4**	**0**	**1**	**47**	**1**	**75**	**9.5**
21	5	2	1	47	0.5	75	4
20	6	2	1	64	1	120	9.5
26	**7**	**0**	**1**	**47**	**1**	**75**	**9.5**
24	8	2	1	47	1.5	75	15
17	9	2	1	30	1	30	9.5
22	10	2	1	47	1.5	75	4
8	11	2	1	47	1	120	15
15	12	2	1	47	0.5	120	9.5
2	13	2	1	64	0.5	75	9.5
12	14	2	1	64	1	75	15
6	15	2	1	47	1	120	4
13	16	2	1	47	0.5	30	9.5
5	17	2	1	47	1	30	4
1	18	2	1	30	0.5	75	9.5
10	19	2	1	64	1	75	4
18	20	2	1	64	1	30	9.5
23	21	2	1	47	0.5	75	15
11	22	2	1	30	1	75	15
4	23	2	1	64	1.5	75	9.5
25	**24**	**0**	**1**	**47**	**1**	**75**	**9.5**
9	25	2	1	30	1	75	4
19	26	2	1	30	1	120	9.5
3	27	2	1	30	1.5	75	9.5

4.3. Experimental Method

The following experimental method was followed for esterification of castor oil:

1. Weight exactly $286.5\ g$ of castor oil in the 3-neck flask which corresponds to a volume of $300\ ml$
2. Proceed to preheat the oil to the desired operating temperature as determined by the Box-Behnken Design
3. Weight the alcohol in an appropriate measuring cylinder depending on the alcohol/oil molar ratio
4. Weight the catalyst in a smaller beaker or measuring cylinder depending on the catalyst loading
5. Mix and heat the catalyst and alcohol prior to addition into the reaction flask
6. Once the oil has reached the desired temperature, proceed with the addition of the catalyst and alcohol mixture
7. Carefully maintain the reaction temperature using the temperature controller at the desired temperature
8. Once complete, empty contents into separation funnel for gravity separation overnight
9. Proceed with decantation of the bottom glycerol, unreacted oil, alcohol and catalyst layer
10. Follow with hot water washing using hot tap water several times until the bottom wash water layer is clear
11. Proceed with rotary evaporation at $90℃$ and $150\ mbar$ to remove water and alcohol
12. Measure out the biodiesel produced and calculate the yield via the following equation:

    $$Yield = \frac{mass\ of\ biodiesel}{mass\ of\ oil}$$
13. Proceed with acid value testing according to ASTM D974
14. Proceed with the optimization of esterification of castor oil and determine the optimal conditions
15. Conduct castor oil esterification at the optimal conditions for model validation

A similar procedure was followed for transesterification of esterified castor oil and sunflower oil with minor differences:

1. Calculate the adjusted amount of esterified castor oil biodiesel produced and sunflower oil which is to be used as the feedstock for the transesterification process
2. Proceed with calcination of Calcium Oxide (CaO) catalyst at $600℃$ for 3 hours and store in a desiccator under vacuum conditions with potassium hydroxide (KOH) pellets to remove moisture from the catalyst sample
3. Mix the catalyst and alcohol under heating to the required conditions and thermostat the esterified castor oil/sunflower oil to the required conditions separately. Add approximately

0.2 ($wt\ \%\ oil$) water to the catalyst and alcohol mixture and leave for a period of 30 $mins$, after which time the esterified castor oil/sunflower oil may be added and the timer can start

4. Proceed with neutralisation of the base catalyst by a calculated amount of acid
5. Proceed with high speed centrifugation separation then transfer to a separating funnel for overnight gravity separation
6. Proceed with hot tap water washing and decantation until the bottom layer is clear
7. Proceed with rotary evaporation at 90℃ and 150 $mbar$ to remove residual water and alcohol
8. Calculate the yield via the following equation:

$$Yield = \frac{mass\ of\ biodiesel\ produced}{mass\ of\ esterified/sunflower\ oil}$$

4.4. Analytical Method – Gas Chromatography Analysis

In this work, biodiesel synthesized from esterified castor oil and sunflower oil at the optimal conditions was subject to GC-MS analysis. An Ultra Alloy column type was used with a diameter, length and thickness of 0.25 mm, 30 m and 0.25 μm, respectively, within a Shimadzu Gas Chromatography Mass Spectroscopy (GC-MS) machine. An injection temperature of 250℃ and column oven temperature of 120℃ were set. The injection mode of split ratio was selected and a split ratio of 30 was used for a 0.1 μL injection and a solvent cut time of 1 min was employed. Helium carrier gas was used with a linear velocity of 37.5 cm/s whilst the total flow, column flow and pressure were set to 34 mL/min, 1 mL/min and 80.6 kPa, respectively. The temperature program for the column oven temperature was as follows, (1) an initial temperature of 120℃ which increases at a rate of 10℃/min to a temperature of 180℃, (2) the temperature of 180℃ is held for 1 min, (3) after which a final temperature of 240℃ is achieved by heating at a rate of 2℃/min. In addition, a purge flow of 3 mL/min was employed. The above settings resulted in a run-time of 37 $mins$ and were specific to the Gas Chromatography machine (Warra, 2015).

With reference to the Mass Spectroscopy machine, an ion source temperature and interface temperature of 250℃ and 280℃ was selected. The run-time for the Mass Spectroscopy machine was also 37 $mins$ with an event time of 0.5 s and a scan speed of 1428. The aforementioned settings are adapted from the work of Warra (2015), however, modifications were necessary depending on the type of oil used and chromatogram produced.

4.5. Summary

The experimental design was conducted on *Minitab*™ using the Box-Behnken response surface methodology. A total of 27 experiments is to be conducted for each of the three different feedstocks, i.e. base castor oil, esterified castor oil and sunflower oil. The resulting biodiesel is then analysed by gas chromatography and mass spectroscopy to identify the compounds present.

Chapter 5 – Results & Discussion: Castor Oil Esterification

5.1. Introduction

This chapter focuses mainly on the esterification of castor oil using sulphuric acid as a catalyst to reduce the acid value of castor oil. Box-Behnken response surface methodology has been employed to design and optimise for the conditions necessary to achieve the lowest possible acid value of the castor oil. The resulting esterified castor oil; at the optimal conditions; was then subject to transesterification via heterogeneous catalyst as discussed in the next chapter. The design, optimisation and statistical analysis was performed on *Minitab*™. In this section, A, B, C and D represent Temperature, Catalyst loading, Reaction time and Methanol/Oil molar ratio, respectively.

5.2. Statistical Models

Upon the completion of the design and conduction of the experiments, the values of the response variable; Free Fatty Acid (FFA % oleic acid); was entered into the software. Table 27 shows the statistical models that were tested. At first glance, it can be seen that the full quadratic model provides the best description for the current experimental data. Furthermore, the F-Value is the highest for the full quadratic model, which means that the model can sufficiently predict the responses associated with the data. In addition, the linear models could not predict some of the coefficients in the model and had to be omitted, whereas the full quadratic model was able to predict the coefficients for all the terms used in the model. The R-Squared value is also the highest for the full quadratic model which means that the goodness of fit of the data by the quadratic model is sufficient. Furthermore, the difference in the R-Squared and R-Squared adjusted value is less than 0.1, therefore the full quadratic model may be assumed suitable for the determination of the optimal conditions for esterification (Halder, et al., 2015).

Table 27 – Statistical Model Testing for Castor Oil Esterification

Model Summary	Sum of Squares	R-squared	R-squared (adjusted)	F-Value	Suggestion
Linear	184.714	62.11 %	55.23 %	9.02	Not Suggested
Linear + Squares	246.578	82.92 %	75.33 %	10.92	Not Suggested
Linear + Interactions	233.172	78.41 %	64.92 %	5.81	Not Suggested
Full Quadratic	295.036	99.21 %	98.29 %	107.98	Suggested

5.3. Statistical Analysis

With reference to Table 28, it can be seen that the full quadratic model is very significant with a high F-Value and very low P-Value (Halder, et al., 2015). Additionally, it can be seen that the alcohol/oil molar ratio has the biggest influence on the data analysis because it has the highest F-Value, followed by catalyst loading, temperature and finally reaction time. Furthermore, the P-Value for all linear factors is very significant and well below the confidence interval used for the statistical analysis of 95%.

Therefore, it can be said that the observations recorded in the experiments did not happen by chance as the probability of that happening is very low, as indicated by the low P-Value of the model.

Table 28 – Analysis of Variance (ANOVA) for Castor Oil Esterification (Full Quadratic Model)

Analysis of Variance (ANOVA)					
Source	DF	Adjusted Sum of Squares	Adjusted Mean of Squares	F-Value	P-Value
Model	14	295.036	21.074	107.98	< 0.0001
Linear	4	184.714	46.178	236.61	< 0.0001
A	1	12.506	12.506	64.08	< 0.0001
B	1	46.306	46.306	237.26	< 0.0001
C	1	3.799	3.799	19.46	0.001
D	1	122.103	122.103	625.62	< 0.0001
Square	4	61.864	15.466	79.24	< 0.0001
A*A	1	2.251	2.251	11.54	0.005
B*B	1	5.117	5.117	26.22	< 0.0001
C*C	1	6.638	6.638	34.01	< 0.0001
D*D	1	27.439	27.439	140.59	< 0.0001
2-Way Interaction	6	48.458	8.076	41.38	< 0.0001
A*B	1	5.924	5.924	30.35	< 0.0001
A*C	1	0.242	0.242	1.24	0.287
A*D	1	22.468	22.468	115.12	< 0.0001
B*C	1	1.315	1.315	6.74	0.023
B*D	1	9.11	9.11	46.68	< 0.0001
C*D	1	9.399	9.399	48.16	< 0.0001
Error	12	2.342	0.195		
Lack-of-Fit	10	2.326	0.233	28.83	0.034
Pure Error	2	0.016	0.008		
Total	26	297.378			

The factors that have the largest influence on the process are the linear terms of alcohol/oil molar ratio followed by catalyst loading and the quadratic effects of alcohol/oil molar ratio which is followed by the interaction between temperature and alcohol/oil molar ratio.

Table 29 – Coded Coefficients for Castor Oil Esterification (Full Quadratic Model)

Coded Coefficients						
Term	Effect	Coefficient	SE Coefficient	T-Value	P-Value	VIF
Constant		5.97	0.255	23.4	< 0.0001	
A	-2.042	-1.021	0.128	-8	< 0.0001	1
B	3.929	1.964	0.128	15.4	< 0.0001	1
C	-1.125	-0.563	0.128	-4.41	0.001	1
D	-6.38	-3.19	0.128	-25.01	< 0.0001	1
A*A	-1.299	-0.65	0.191	-3.4	0.005	1.25
B*B	-1.959	-0.979	0.191	-5.12	< 0.0001	1.25
C*C	-2.231	-1.116	0.191	-5.83	< 0.0001	1.25

D*D	4.536	2.268	0.191	11.86	< 0.0001	1.25
A*B	-2.434	-1.217	0.221	-5.51	< 0.0001	1
A*C	0.492	0.246	0.221	1.11	0.287	1
A*D	-4.74	-2.37	0.221	-10.73	< 0.0001	1
B*C	-1.147	-0.573	0.221	-2.6	0.023	1
B*D	3.018	1.509	0.221	6.83	< 0.0001	1
C*D	-3.066	-1.533	0.221	-6.94	< 0.0001	1

Table 30 – Model Summary for Castor Oil Esterification (Full Quadratic Model)

Model Summary			
S	R-squared	R-squared (adjusted)	R-squared (predicted)
0.441781	99.21 %	98.29 %	95.48 %

As evident by Table 30, the R-Squared value is very close to unity which means that the model gives a true representation of the data from the experiments. In addition, the optimal values may be found easily because the model may be used for interpolation within the experimental range.

The full quadratic model is shown in the following equation (Halder, et al., 2015):

$$Y = \beta_o + \sum_{i=1}^{k} \beta_i X_i + \sum_{i=1}^{k} \beta_{ii} {X_i}^2 + \sum_{i<j} \beta_{ij} X_i X_j \tag{5.1}$$

Where, the constant, linear, linear and squares and two-way interaction terms are captured by the first, second, third and fourth terms of Eq. (5.1), respectively. The fully expanded version of Eq. (5.1) is shown below:

$$\begin{aligned} Y = {} & \beta_o + \beta_1 X_1 + \beta_2 X_2 + \beta_3 X_3 + \beta_4 X_4 + \beta_{11} {X_1}^2 + \beta_{22} {X_2}^2 + \beta_{33} {X_3}^2 + \beta_{44} {X_4}^2 \\ & + \beta_{12} X_1 X_2 + \beta_{13} X_1 X_3 + \beta_{14} X_1 X_4 + \beta_{23} X_2 X_3 + \beta_{24} X_2 X_4 + \beta_{34} X_3 X_4 \end{aligned} \tag{5.2}$$

The regression equation obtained via multiple regression analysis is shown below in coded units, where A, B, C and D represent Temperature, Catalyst loading, Reaction time and Methanol/Oil molar ratio, respectively.

$$\begin{aligned} Y = {} & -6.28 + 0.4515 * A + 3.976 * B + 0.1287 * C - 0.669 * D - 0.002248 * A^2 \\ & -0.4353 * B^2 - 0.000551 * C^2 + 0.07498 * D^2 - 0.04772 * AB + 0.000322 * AC \\ & -0.02535 * AD - 0.00850 * BC + 0.1829 * BD - 0.006194 * CD \end{aligned} \tag{5.3}$$

5.4. The Individual Effects of Process Parameters on FFA (% Oleic Acid)

The objective of this study was to determine the optimal conditions necessary to reduce the acid value of castor oil via esterification in the presence of methanol and sulphuric acid. Therefore, it is crucial to evaluate the effects that each variable has on the response variable. The individual effects can be seen by the Analysis of Variance (ANOVA) in Table 28, whereas the interaction of two parameters and the resulting effect on the response variable can be visualised by a surface plot. The design and optimisation methodology for this work is the Box-Behnken Design, which employs the use of response surfaces to visualise the effects and interaction between parameters on the response variable. For the purposes of consistency, the constant setting for all variables was kept at the midpoints, i.e. temperature of 47℃, catalyst loading of 1.75 $wt\%$, time of 75 $mins$ and alcohol/oil molar ratio of 9.5.

5.4.1. The Effect of Temperature on FFA (% Oleic Acid)

The temperature values employed for this work are 30 ℃, 47 ℃ and 64 ℃. Although higher temperature ranges were employed in similar works, this range was chosen to give the best possible result as the optimised temperature should certainly fall within this range. Furthermore, it is reported in literature that the reaction temperature should not exceed that of the boiling point of the alcohol used (N.i, et al., 2018). In this work, the alcohol chosen was methanol which has a normal boiling point temperature of 64.7 ℃ (Kundu, et al., 2016).

In addition, should the reaction temperature exceed that of the boiling point of the alcohol, saponification and a reduction in yield may be observed as in the case of (N.i, et al., 2018; Tan, et al., 2016). A similar conclusion was drawn by Halder et al. (2015) who noted that an increase in temperature results in a decrease in the conversion of FFAs in castor oil. Ultimately, they concluded that when all other variables are kept constant whilst temperature is varied, lower temperatures; 40 ℃; favoured the conversion of FFAs and higher temperatures; 80 ℃; past the boiling point of methanol were inefficient in the conversion of FFAs.

According to the work by Halder et al. (2015), the parameter that has the biggest influence on castor oil esterification in the presence of sulphuric acid and methanol is reaction temperature, which is followed by alcohol/oil molar ratio, catalyst loading and lastly reaction time. However, temperature may influence the FFA content when high temperatures are used, as in the case of Halder et al. (2015) who employed a temperature range of $50 - 70$℃, whereas the temperature range for this work was much milder and was in the range of $30 - 64$℃. Higher operating conditions may have also led to the conclusion drawn earlier. Furthermore, despite different operating conditions and raw materials, similar conclusions were drawn by Khan et al. (2010) who conducted acid esterification on crude palm oil and rubber seed oil blend. Similar to the works cited above, this work also determined that reaction time has the smallest effect on the process.

As shown in Figure 17, a contradiction between the work of Halder et al. (2015) and this work was observed in the case of temperature effects. This may be as a result of the baseline of the other three variables. Simply put, the other variables may have influenced the FFAs much more at their baselines, which may have negated the effects of temperature variation on the FFAs. This suggestion is validated by the ANOVA analysis found in Table 28 which shows the vast differences between the respective F-Values. The F-Values of alcohol/oil molar ratio, catalyst loading and temperature are 625.62, 237.26 and 64.08, respectively.

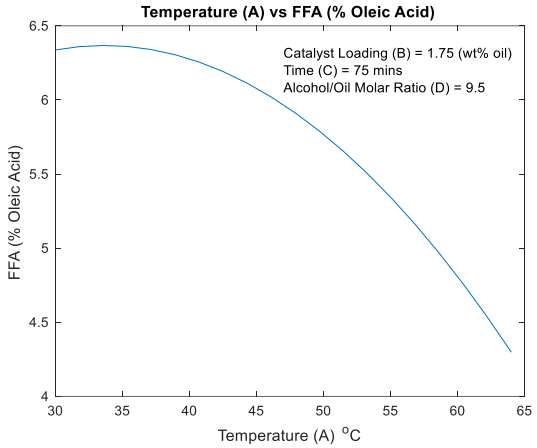

Figure 17 – Effect of Temperature (A) on FFA (% Oleic Acid)

As mentioned previously, a high F-Value implies that the parameter is statistically significant to the process. Therefore, the effect of temperature may have been minimal due to its relatively low F-Value as compared to alcohol/oil molar ratio and catalyst loading. Furthermore, Kundu et al. (2016) reported that lower temperatures have a higher effect on FFA conversion than alcohol/oil molar ratio when castor oil esterification is conducted in the presence of sulphuric acid and methanol. However, it is reported in literature that higher temperatures below the boiling point of the alcohol serve to increase the reaction rate during transesterification and lower temperatures require longer reaction times (Kundu, et al., 2016). Similarly, in this work for esterification, the high temperature limit of 64℃ may have caused an increase in reaction rate which led to the conversion of FFAs in the castor oil.

Higher operating temperatures may also result in a positive effect on the physical properties of the esterified castor oil/biodiesel produced in the case of esterification. Deshpande et al. (2012) noted that an increase in reaction temperature results in a decrease in the physical properties of the biodiesel produced from castor oil in the presence of sulphuric acid. In their work, when temperature increased from 30℃ to 50℃, the kinematic viscosity of the products decreased by 25.9 %. In addition, a decrease in the density and FFA of the products was reported with an increase in reaction temperature.

In addition, while other works may have focused on producing biodiesel via acid-catalysed esterification, this work focused on conducting esterification for the purposes of FFA reduction and to

find the optimal conditions at which the FFAs are minimised, which will later be trans-esterified via heterogeneous base catalysis to produce biodiesel. Therefore, the reaction time for esterification was relatively low at $30 - 120\ mins$ whilst reaction times of $(0 - 4\ h)$ are reported by Halder et al. (2015) and Kundu et al. (2016) who conducted castor oil esterification using sulphuric acid and methanol. As such, deviations from literature is to be expected as the process conditions as well as the end products are different. However, Deshpande et al. (2012) noted a decrease in FFA content with an increase in temperature for castor oil esterification in the presence of sulphuric acid and methanol which is in accordance with this work.

5.4.2. The Effect of Catalyst Loading on FFA (% Oleic Acid)

The catalyst loading for this section was in the range of $0.25 - 3.25\ (wt\%)$ of the oil used Halder et al. (2015). The lower limit of the catalyst loading allowed for the optimal conditions for esterification to be found due to the relatively large operation range whilst minimising catalyst loading during experiments.

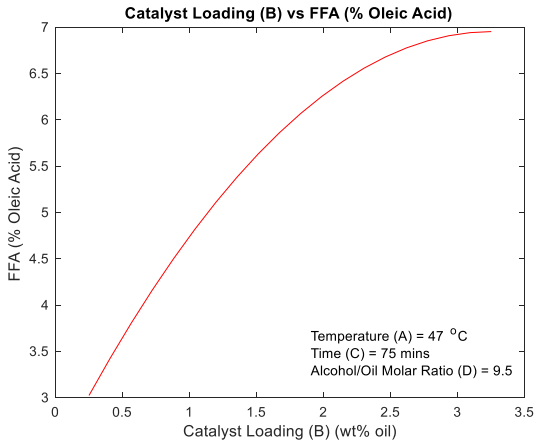

Figure 18 – Effect of Catalyst Loading (B) on FFA (% Oleic Acid)

Sulphuric acid is among the most common acid catalyst for esterification due to its relatively low cost and availability (Hayyan, et al., 2011). Furthermore, sulphuric acid is highly efficient at high temperatures and in the case of esterification, is less likely to result in saponification (Hayyan, et al., 2011). As can be seen from Figure 18, when the catalyst loading increases so does the FFA content. This result is expected as higher catalyst ratios promote water formation during esterification. Furthermore, water present in the feedstock may have aided in the result shown in Figure 18. Similar observations were noticed in the work of Agra & Warnijati (1996) who produced motor oil via castor oil esterification in the presence of ethanol and sulphuric acid.

Furthermore, similar results were recorded by Kundu et al. (2016) who found the optimal conditions of catalyst loading at 1 $(wt\%)$ of the mass of castor oil used in esterification. They concluded that as catalyst loading increased past 1 $(wt\%)$, the conversion of FFAs were minimal, hence further increase

in catalyst loading would only result in higher operating costs. However, the opposite observation was reported by Ferdous et al. (2013) who conducted acid catalysed castor oil esterification in the presence of methanol and sulphuric acid. They reported that as catalyst loading increases, the FFA conversion also increases up to a certain constant value.

The base castor oil used in the work of Ferdous et al. (2013) had a similar acid value to the castor oil used in this work, however, the conditions at which they evaluated the effect of catalyst loading on FFA was very different to this work. In particular, the alcohol/oil molar ratio and reaction temperature of 9.5: 1 and 47℃, respectively, was employed in this work whilst a ratio and reaction temperature of 6: 1 and 60℃, respectively, was employed in their work. According to the statistical analysis in this work, the alcohol/oil molar ratio may have resulted in the difference between their results and the literature results. The results shown in Figure 18 is in accordance with Halder et al. (2015) and Deshpande et al. (2012).

Another benefit of operation at lower catalyst loadings would be the positive effect on the kinematic viscosity of the product. Deshpande et al. (2012) reported that higher catalyst loadings resulted in biodiesel with higher viscosities. This may lead to biodiesel which does not fulfil ASTM fuel standards. Therefore, catalyst loading should be kept at a minimum for an economical process as well as for the production of biodiesel with a kinematic viscosity in the range of ASTM fuel standards.

With reference to Figure 18, it can be seen that an increase in catalyst loading has a negative effect of FFA conversion. This may be as a result of the base castor oil having a high amount of FFAs which when combined with the increased acid catalyst loading serve to inhibit the catalytic activity of the catalyst as the catalyst cannot provide suitable activity when the acid concentration is beyond a specific concentration within the reaction vessel (Banani, et al., 2015).

5.4.3. The Effect of Time on FFA (% Oleic Acid)

The reaction time for this section was chosen to be in the range of $30 - 120\ mins$. As mentioned previously, longer reaction times may be employed if biodiesel is to be produced via acid catalysed esterification, however, since the purpose of this section is to minimise the FFA content of castor oil, shorter reaction times may be employed as biodiesel does not need to be produced. The reaction time range was selected such that enough time for a reduction in acid content may be achieved without producing biodiesel as biodiesel would be produced via heterogeneous base catalysis at the optimal esterification conditions.

As seen in Figure 19, initially the FFA content increases with an increase in reaction time until approximately $1\ hr$ has elapsed. This result is to be expected as initially the acid content and the acid

catalyst combine to yield a mixture of higher acid content. This higher acid content inhibits the catalytic activity of the catalyst as the catalyst cannot be effective past a critical acid concentration in the reaction mixture, as mentioned by Banani et al. (2015). However, past a reaction time of $1\ hr$, the catalyst seems to become effective and reduce the acid content of the reaction mixture.

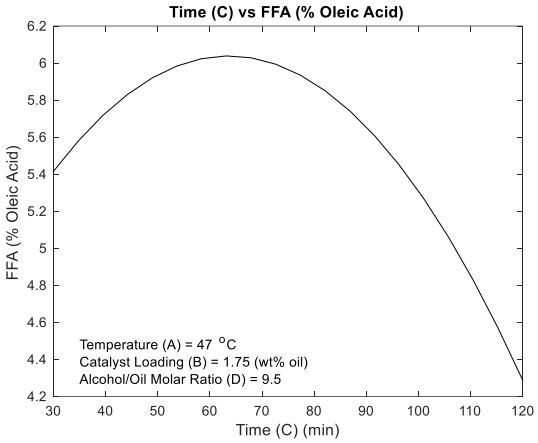

Figure 19 – Effect of Time (C) on FFA (% Oleic Acid)

However, as mentioned earlier, as discovered in this work and literature, reaction time in the case of castor oil esterification proves to be statistically insignificant. The F-Value for the linear model reaction time according to this work was 19.46 with a P-Value of 0.001 whilst the F-Values in the linear model for alcohol/oil molar ratio, catalyst loading and reaction temperature are 625.62, 237.26 and 64.08, respectively, with P-Values less than 0.0001. Simply put, although reaction time is an important parameter during experimental design, statistically it showed to be insignificant in comparison to the other parameters which may have negated the effects of reaction time because the other parameters influence the FFAs more.

Hence, if a slightly different alcohol/oil molar ratio is chosen whilst all other factors are kept constant, the resulting plot of time and FFA may be completely different. However, reaction time proved to be statistically insignificant relative to the other parameters but is statistically relevant due to the low P-Value which is below the 95% confidence interval used for the ANOVA which indicates that the values obtained did not occur by chance.

Kundu et al. (2016) reported that initially FFA decreases with increasing reaction time until equilibrium is achieved in the case of castor oil esterification using sulphuric acid as a catalyst. In their work, however, the effect of reaction time on FFA content was explored in the time domain of $60 - 120\ mins$. Therefore, their conclusions are incomplete because it is based on a starting reaction time of $1\ hr$. Similar conclusions were drawn by Halder et al. (2015) for the case of castor oil esterification in the presence of sulphuric acid and methanol.

In this work, it is shown that the FFA content increased until a reaction time of $1\ hr$, after which there was a reduction in acid content of the reaction mixture which is in accordance with the works cited above. An equilibrium was not achieved because the reaction time was relatively short in comparison to other works which employed reaction times of $0 - 4\ h$. This short reaction time and low reaction temperature of $47℃$ meant that equilibrium would not be achieved at the current operating conditions.

However, it can be seen from Figure 19 that longer reaction times; past $1\ hr$; resulted in a decrease in FFA content which is the objective of this study. Longer reaction times, however, are not economical as there would be more heating costs and less volume of products produced per day. Furthermore, it is reported by Goyal et al. (2012) that longer reaction times promote water formation during esterification which serves to inhibit the catalytic activity of the sulphuric acid catalyst.

Deshpande et al. (2012) conducted castor oil esterification in the presence of sulphuric acid to reduce the FFA content as well as explore the effects that the different parameters had on the density and kinematic viscosity of the biodiesel produced. An initial decrease in kinematic viscosity was associated with an increase in reaction time, however, at a reaction time of $45\ mins$ the kinematic viscosity began to increase to time. They reported a marginal decrease in the specific gravity of the biodiesel produced as time increased.

5.4.4. The Effect of Alcohol/Oil Molar Ratio on FFA (% Oleic Acid)

The alcohol/oil molar ratio employed for this work was in the range of 4:1 to 15:1 with the middle ratio at a value of 9.5:1. The lower limit of 4:1 was selected to explore the lowest possible alcohol/oil molar ratio that would facilitate the esterification reaction. Furthermore, the minimum allowed stoichiometric ratio is 3:1, therefore, operation at a ratio of 4:1 would be regarded as the minimum allowed ratio that would negate the reverse reaction. The upper limit of 15:1 was selected as operation at ratios higher than 15:1 would marginally lower the FFA content but substantially increase the overall process cost.

As cited by Kundu et al. (2016) for the case of castor oil esterification using sulphuric acid, operation at ratios higher than 15:1 would lead to difficulties and higher costs that may be associated with heating as the entire reaction volume has to be heated to the required temperature and maintained for the entire duration of the reaction. Furthermore, they report that lower alcohol/oil molar ratios would promote the reverse reaction as higher ratios negate the reverse reaction by shifting the reaction equilibrium towards the forward desired reaction. It is with excess alcohol/oil molar ratios that the reaction set can be assumed pseudo-first order irreversible.

However, if the alcohol/oil molar ratio is greater than 15:1, the excess methanol in the reaction vessel would drive the forward reaction towards the generation of products. For an esterification reaction, the main reaction set comprises oil and alcohol reacting in the presence of an acid catalyst to form biodiesel

and water (Kundu, et al., 2016). The excess methanol will therefore drive the forward reaction faster than usual which would lead to an increase in reaction rate. Therefore, more biodiesel would be generated but at the same time, more water is generated which tends to inhibit the reaction rate and lower the catalytic activity. Furthermore, Halder et al. (2015) reported that in the case of castor oil esterification, water tends to promote the reverse reaction as well as increase the separation time of the products.

As seen in this work, in Table 28, the F-Value for alcohol/oil molar ratio for the linear model is the highest throughout the data set, which is indictive of the most important parameter that affects the FFA content in the reaction system. From Figure 20, it is clear that the largest range of FFA values; shown on the y-axis; is captured by the variations of the alcohol/oil molar ratio. The results depicted in the figure is in accordance with the literature values. Similar results were obtained by Halder et al. (2015) and Kundu et al. (2016) for castor oil esterification via sulphuric acid. According to Karmakar et al. (2018), alcohol/oil molar ratio is the most significant parameter that affects the process, which is in accordance with this work.

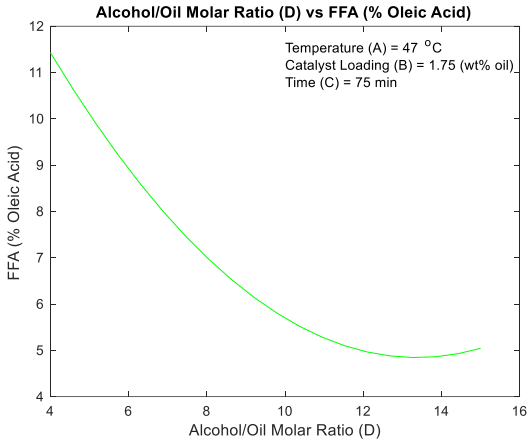

Figure 20 – Effect of Alcohol/Oil Molar Ratio (D) on FFA (% Oleic Acid)

According to Deshpande et al. (2012), an increase in alcohol/oil molar ratio would lower the kinematic viscosity of the biodiesel produced but would have marginal or no effect on the specific gravity of the product. In addition, in their work with high acid value castor oil esterification, a decrease in FFA content was as a result of an increase in alcohol/oil molar ratio which conforms to the literature and this work.

Figure 21 shown below represents the combined main effects of temperature, catalyst loading, reaction time and alcohol/oil molar ratio. The Box-Behnken Design allows for the use of three levels for a specific parameter and these levels are coded -1, 0 and 1. With -1 representing the lower limits of the parameters, 0 representing the mid-points of the data range of the parameters and 1 representing the upper limits of the parameters.

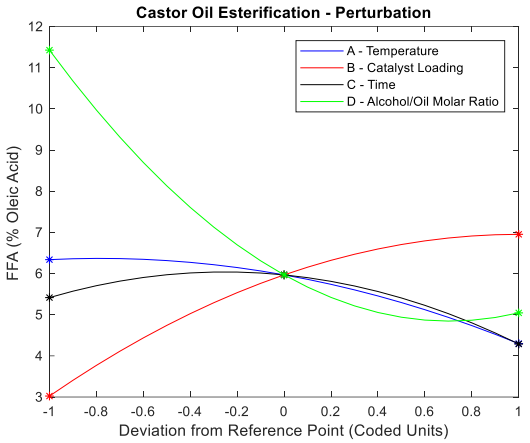

Figure 21 – Castor Oil Esterification – Perturbation

Obviously, to show the effect of one variable, the other three variables must be kept constant. Therefore, all four variables were kept at their mid-points whilst one of the four variables was varied. The mid-points or 0 reference point for temperature, catalyst loading, time and alcohol/oil molar ratio was 47℃, 1.75 ($wt\%$) oil, 75 $mins$ and 9.5, respectively. The upper and lower limits of the variables may be found in Table 24.

5.5. Response Surface Plots

Response surface plots help show the interaction of two parameters on one response variable, i.e. FFA. The combination of these parameters in conjunction with the ANOVA analysis help determine which parameters and interactions are important to the process. The regression equation (Eq. (5.3)) stated previously was used to plot the response surfaces and contour plots shown below. As mentioned previously, when trying to determine the relationship between two parameters and the resulting effect of the response variable, the other two factors need to be kept constant. For the purposes of consistency, the constant setting for all variables was kept at the midpoints, i.e. temperature of 47℃, catalyst loading of 1.75 $wt\%$, time of 75 $mins$ and alcohol/oil molar ratio of 9.5.

5.5.1. The Effect of Temperature & Catalyst Loading on FFA (% Oleic Acid)

The 3-D response surface for the interaction between temperature and catalyst loading is shown in Figure 22 and the contour plot between temperature and catalyst loading is shown in Figure 23 whilst the reaction time and alcohol/oil molar ratio were set at 75 $mins$ and 9.5: 1, respectively, in the regression equation. With reference to the response surface plot, it can be seen that low temperatures of 30℃ and low catalyst loading of 0.25 ($wt\%$) of oil resulted in the lowest FFA reading of approximately 2.1 % obtained in this plot. However, the lowest reading of 2.1 % by itself is not sufficient to reduce the allowed FFA content for base catalysed transesterification, thus validating the use of response surface optimisation to achieve the lowest possible value.

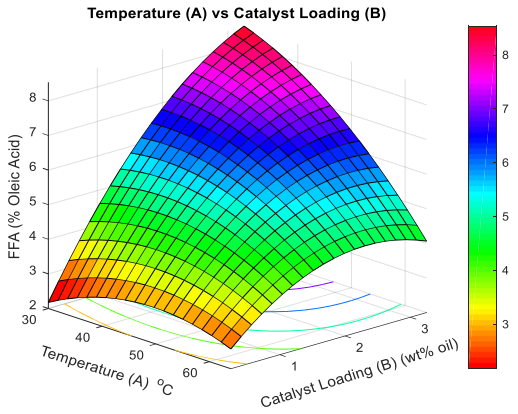

Figure 22 – Esterification Response Surface (A) vs (B)

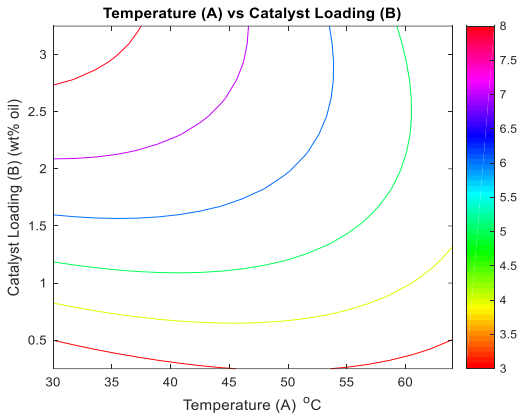

Figure 23 – Esterification Contour (A) vs (B)

Furthermore, from Table 28 it can be seen that the interaction between temperature and catalyst loading has a relatively high F-Value of 30.35 with a P-Value that is less than 0.0001. This is indictive of an interaction that is statistically significant where both parameters affect the response variable. The subtle effects of temperature variations may be seen on the temperature axis in Figure 22 which shows that catalyst loading is the dominant parameter as it influences a wider range of FFA values than temperature. It can therefore be said that the interactions between temperature and catalyst loading did not occur by chance as indicated by the low P-Value.

The maximum FFA value recorded in this plot was approximately 8.4 % which occurs at the upper limit of catalyst loading and lower limit of temperature. It is therefore important to highlight that both the minimum and maximum values of FFA lie at the boundary conditions of temperature and catalyst loading, hence the optimal values for temperature and catalyst loading should lie inside the response surface. However, due to the high coefficient of determination (R^2) of the full quadratic model, the model may be able to minimise the FFA to values below zero, which is impractical. Therefore, as mentioned before, in the case of optimisation, the values of temperature and catalyst loading will be constrained to their specific domains, such that the values obtained lie within the response surface and do not result in an FFA value that is below zero.

By inspection of Figure 22, it can be seen that the lower limits of temperature and catalyst result in the highest conversion of FFAs. This may be as a result of the low catalyst loading employed. The lower limit of catalyst loading of 0.25 ($wt\%$) may have combined with the existing acid content in the oil and the resulting acid concentration in the reaction mixture may have increased, which led to a high conversion of FFAs within the allowed time limit. In that case the reaction temperature of 30℃ may have been sufficient to facilitate the esterification reaction. Conversely, at the catalyst loading upper limit of 3.25 ($wt\%$) with a reaction temperature of 30℃, there may have been an excess of acid in the reaction system which required longer reaction times to reduce the FFA content at such a low temperature. In addition, the acid concentration may have exceeded the critical acid concentration

allowed for esterification, after which the catalytic activity is reduced (Banani, et al., 2015). Furthermore, due to the low reaction temperature, the reaction rate may have simply been too low for an esterification reaction to proceed timeously.

Considering the upper limit of temperature, it can be seen that at the lower catalyst limit, the conversion of FFAs is not as high as it was for the lower temperature limit. This may be due to the reaction mixture having the correct acid concentration, but the reaction temperature may have been too high, which increased the rate of the forward reaction. As the forward reaction proceeds, water is produced as a by-product which serves to inhibit the catalytic activity. A similar observation can be made about the upper limits of temperature and catalyst loading. However, in this case the acid concentration may have exceeded the critical acid concentration but due to the high temperature, the reaction rate may have increased which led to the conversion of FFAs, thereby reducing the overall acid concentration of the reaction mixture.

The boundary effects of the parameters are more clearly seen in Figure 23 which shows the different curvatures or contours of the interactions between temperature and catalyst loading. In addition, it can be seen that an FFA value of $4\ \%$ was determined when both parameters are at their upper limits. Similar, but less obvious response surfaces were obtained by Halder et al. (2015) in the case of castor oil esterification via sulphuric acid and methanol using a Central Composite Design (CCD) approach. However, in their work, reaction temperature exhibited the largest effect on FFA content. Nevertheless, the resulting response surface depicts the same general shape as this work and any differences may be due to the operating conditions employed in their work, viz. a reaction temperature and catalyst loading of $50 - 70℃$ and $1 - 2.5\ (wt\%)$ of oil, respectively. Very few works involving response surface methodology of castor oil esterification using sulphuric acid have been done therefore this work is in agreement with the work done by Halder et al. (2015).

5.5.2. The Effect of Temperature & Time on FFA (% Oleic Acid)

The 3-D response surface for the interaction between temperature and time is shown in Figure 24 and the contour plot between temperature and time is shown in Figure 25 whilst the catalyst loading and alcohol/oil molar ratio were set at $1.75\ (wt\%)$ of oil and $9.5{:}\ 1$, respectively, in the regression equation. The lowest FFA value of $2.9\ \%$ can be seen on the response surface and contour plot. It can be seen that the highest conversion of FFAs; which corresponds to the lowest FFA percentage; occurs at the upper limits of temperature and time.

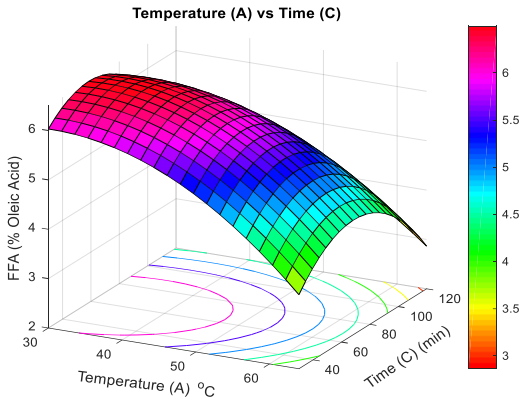

Figure 24 – Esterification Response Surface (A) vs (C)

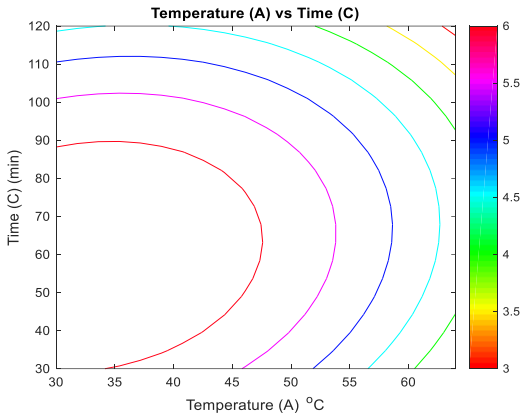

Figure 25 – Esterification Contour (A) vs (C)

However, according to Table 28, the F-Value and P-Value corresponding to the interaction between temperature and time is 1.24 and 0.287, respectively. The F-Value for this interaction is the lowest amongst the interaction between the other variable, hence the F-Value for temperature and time is regarded as low for this work. Furthermore, the P-Value is greater than the confidence interval of 95 % used in this work, which means that the probability that these results occurred by chance is 0.287. It can therefore be said that the interaction between temperature and time is statistically insignificant as it did not fall within the confidence interval of this work. However, for the purposes of consistency in employing the full quadratic model, the interaction between temperature and time was included in the regression model equation.

However, the trend observed in the response surface and contour plot is in keeping with the individual effects of temperature on FFA and time on FFA. As the reaction temperature increases, the rate of the reaction increases which results in a reduction in the FFA values. A similar observation can be made about an increase in reaction time. Whilst the interaction between temperature and time is statistically insignificant, it is worthwhile to understand why this occurs. The conclusion drawn is as a result of the only parameter that changed settings from the previous work, i.e. response surface plots of temperature and catalyst loading on FFA. From that work, it can be seen that temperature and catalyst loading was varied whilst time and alcohol/oil molar ratio were kept constant at 75 $mins$ and 9.5, respectively. In this section temperature and time are varied whilst catalyst loading and alcohol/oil molar ratio are kept constant at 1.75 ($wt\%$) of oil and 9.5, respectively. Therefore, similar to the conclusions drawn earlier, the effect of temperature and time was negated by the catalyst loading base setting of 1.75 ($wt\%$) of oil.

5.5.3. The Effect of Temperature & Alcohol/Oil Molar Ratio on FFA (% Oleic Acid)

The 3-D response surface for the interaction between temperature and alcohol/oil molar ratio is shown in Figure 26 and the contour plot between temperature and alcohol/oil molar ratio is shown in Figure 27 whilst the catalyst loading and time were set at 1.75 ($wt\%$) of oil and 75 $mins$, respectively, in the

regression equation. It can be seen from the response surface that the minimum FFA value of 2 % occurs at the upper limits of temperature and alcohol/oil molar ratio. This FFA value of 2 % is not constrained to only the upper limit values as indicated by the contour plot, the domain of temperature and alcohol/oil molar ratio that allows the minimum FFA is $60 - 64℃$ and $12.5 - 15$, respectively.

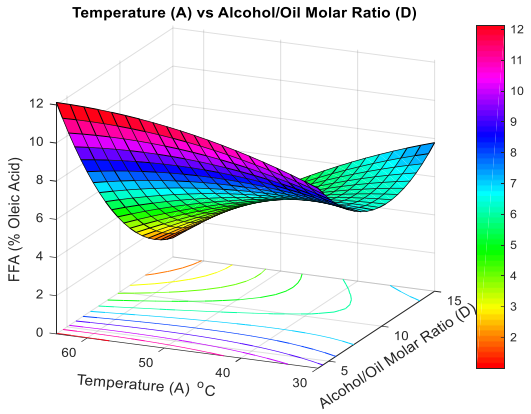

Figure 26 – Esterification Response Surface (A) vs (D)

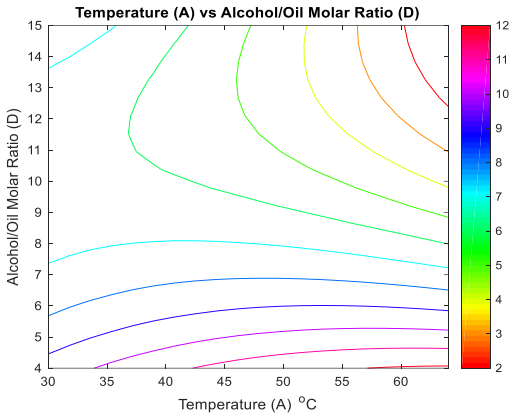

Figure 27 – Esterification Contour (A) vs (D)

As mentioned previously, the alcohol/oil molar ratio is the dominant parameter in this work with an F-Value of 625.62. Therefore, any parameter interacting with it will have a much more profound effect on the response variable with respect to the other parameter and a negative effect on the response variable will be noted with respect to alcohol/oil molar ratio. As such, the F-Value for the interaction between temperature and alcohol/oil molar ratio is 115.12 with a P-Value that is less than 0.0001 which signifies that the interaction is statistically significant and did not occur by chance. Furthermore, as stated earlier, catalyst loading has a larger influence over the response variable than temperature whilst reaction time has the smallest influence, however, the interaction between temperature and alcohol/oil molar ratio has a much larger effect on the response variable than the interaction between catalyst loading and alcohol/oil molar ratio and time and alcohol/oil molar ratio. The latter observation is expected. Whilst temperature may not have been as dominant as the other parameters, the interaction between temperature and alcohol/oil molar ratio has the largest effect on the FFA content than other interactions.

With reference to Figure 26, it can be seen that the upper limits of temperature and alcohol/oil molar ratio yield the highest conversion of FFAs because the FFA value of 2 % is the lowest at those conditions. This may be due to an increased reaction rate associated with an increase in temperature. The excess methanol in the reaction vessel allows for the increased reaction rate to proceed towards the formation of products, thereby reducing the FFA content. The results obtained by Halder et al. (2015) who conducted castor oil esterification via sulphuric acid and methanol is not in agreement with this work.

This may be due to the operating conditions employed in their work, of which, two parameters are different. Firstly, the temperature range of $50 - 70℃$ is regarded as too high. They concluded that an increase in temperature resulted in an increase in FFA content due to methanol loss. Obviously then their effect of temperature and alcohol/oil molar ratio on FFA results may be somewhat misleading as the aim is to investigate the interaction effects of the two parameters on the FFA content which may be hard to do if one parameter is depleting continuously at a reaction temperature of $70℃$. Secondly, the base reaction time setting of $2\ hrs$ was employed. As mentioned previously, longer reaction times lead to reduced FFA values.

Focusing on the upper limit and lower limit of temperature and alcohol/oil molar ratio, respectively, the highest FFA value of $12\ \%$ may be noted. This may be due to the evaporative loss of a marginal amount of methanol at $64℃$ which may have led to the promotion of the reverse reaction as it is understood that a large excess of methanol is required to drive the forward reaction to equilibrium. There is very little effect of the FFA content when the reaction temperature is $30℃$ and the alcohol/oil molar ratio is 4 or 15. An FFA value of $8\ \%$ was obtained with a reaction temperature of $30℃$ and alcohol/oil molar ratio of 15 whilst a value of $10\ \%$ was obtained at the same temperature but alcohol/oil molar ratio of 4. The difference may be explained by the difference in methanol amounts between the two cases.

5.5.4. The Effect of Catalyst Loading & Time on FFA (% Oleic Acid)

The 3-D response surface for the interaction between catalyst loading and time is shown in Figure 28 and the contour plot between catalyst loading and time is shown in Figure 29 whilst the temperature and alcohol/oil molar ratio were set at $47℃$ and $9.5{:}\,1$, respectively, in the regression equation. The lowest value of FFA is approximately $2\ \%$ which occurs at both the upper and lower limits of time when the catalyst loading is $0.25\ (wt\%)$ of oil.

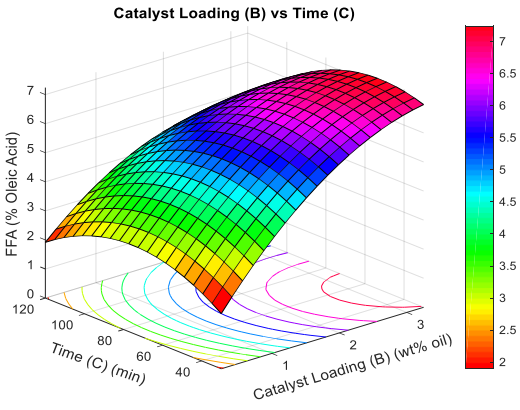

Figure 28 – Esterification Response Surface (B) vs (C)

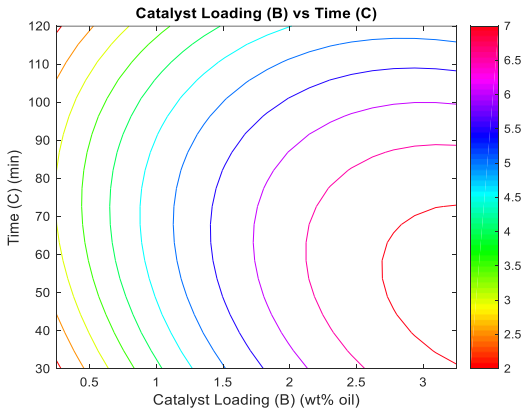

Figure 29 – Esterification Contour (B) vs (C)

According to Table 28, the F-Value and P-Value of the interaction between catalyst loading and time is 6.74 and 0.023, respectively. Whilst both these values are relatively low, the P-Value is above the

confidence interval of 95 % used in this work which signifies the results obtained are statistically significant and did not occur by chance. In addition, the relatively low F-Value is indictive that the interaction between the respective parameters may have resulted in only a marginal effect on the response variable.

From Figure 28 the time effects can be seen on the time axis which leads to the conclusion that as time increases so does the FFA until the turning point which occurs at approximately $1\ hr$, after which the FFA decreases for a catalyst loading of $0.25\ (wt\%)$ of oil, whilst only a decrease in FFA content may be noted at a catalyst loading of $3.25\ (wt\%)$ of oil. This observation may be explained by the relative lower catalyst concentration in the reaction vessel, as a result, the reaction takes longer to proceed at lower catalyst concentrations. However, once the catalyst has fully combined with the reaction mixture, the esterification reaction can proceed which results in a reduction in FFA as time increases. This is justified by considering the catalyst loading at the upper limits where the FFA response has no turning point, i.e. there is only a decrease in FFA with an increase in time.

This decrease in FFA values with increasing time for both upper and lower catalyst loading limits is in accordance with Halder et al. (2015), however in their work with castor oil esterification, the lower time limit of $1\ hr$ was employed, as such no turning points may been seen on their time axis response surface. They however, report an increase in FFA, beyond a reaction time of $120\ mins$, which was not explored in this work. As such, at a time of $120\ mins$, the FFA content begins to increase which may be attributed to an increase in water formation due to the forward reaction. The increased water in the reaction mixture promotes the reverse reaction as well as inhibits the catalytic activity (Karmakar, et al., 2018).

As such, a positive conclusion may be drawn from the aforementioned results as lower catalyst amounts may be employed to achieve a greater reduction in FFA with time as compared to higher catalyst amounts. Nevertheless, the effect of catalyst concentration has a more profound effect on the response variable according to the statistical analysis, therefore, it may be suitable to have slightly higher catalyst loadings with reduced time than lower catalyst loadings with longer reaction times as throughput of products will far outweigh the cost of the catalyst. Furthermore, shorter reaction times will result in lower thermal heating costs. Therefore, keeping the previously mentioned factors in mind, there should be a trade-off between catalyst loading and reaction time.

5.5.5. The Effect of Catalyst Loading & Alcohol/Oil Molar Ratio on FFA (% Oleic Acid)

The 3-D response surface for the interaction between catalyst loading and alcohol/oil molar ratio is shown in Figure 30 and the contour plot between catalyst loading and alcohol/oil molar ratio is shown in Figure 31 whilst the temperature and time were set at $47℃$ and $75\ mins$, respectively, in the regression equation. The lower limit of catalyst loading and upper limit of alcohol/oil molar ratio yield an FFA value of approximately 0.8 % which is the lowest FFA value recorded in this work.

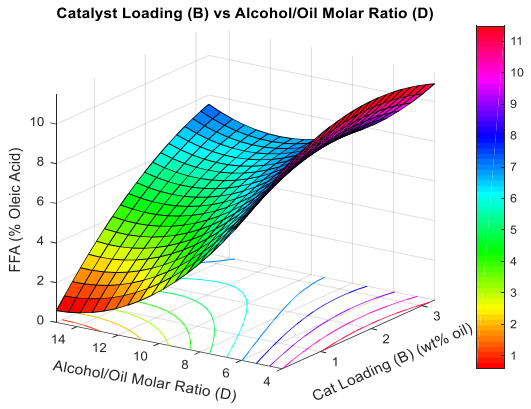

Figure 30 – Esterification Response Surface (B) vs (D)

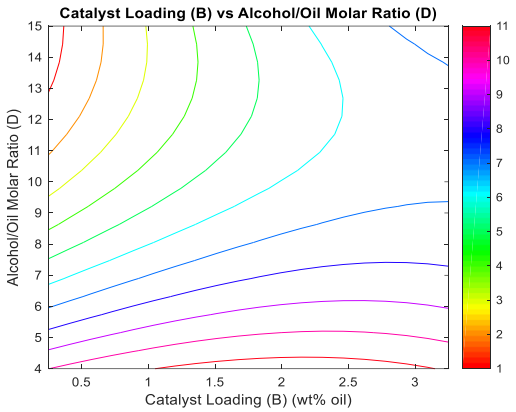

Figure 31 – Esterification Contour (B) vs (D)

This low value of 0.8 % FFA is to be expected as catalyst loading and alcohol/oil molar ratio have the largest individual effect on the response variable in terms of the linear model, whereas the effect of the interaction between these two parameters seems somewhat diminished with an F-Value and P-Value of 46.68 and less than 0.0001, respectively. This may be as a result of the interaction between these two parameters.

With reference to Figure 30, the highest FFA value of 11 % is recorded for the upper limit of catalyst loading and lower limit of alcohol/oil molar ratio whereas the lower limit of catalyst loading and lower limit of alcohol/oil molar ratio resulted in the second highest FFA value of 10 %. The common denominator in both cases is the lower limit of alcohol/oil molar ratio. As shown in Figure 20, lower alcohol/oil molar ratios result in higher FFAs. This may be due to insufficient methanol present in the reaction mixture which is necessary to drive the forward reaction to equilibrium. The reaction, however, may still occur but at a very reduced reaction rate which is validated by the difference in the FFA values obtained for the upper and lower catalyst loadings.

However, considering the upper limits of both catalyst loading and alcohol/oil molar ratio, it can be seen that the resulting FFA value is approximately 7.6 %. This value is in accordance with this work as mentioned previously, higher alcohol/oil molar ratios and lower catalyst loadings result in a drastic reduction in the FFA. Since alcohol/oil molar ratio is more statistically significant than catalyst loading, a value of 7.6 % FFA is reasonable because the reductive tendencies on FFAs of an increase in alcohol/oil molar ratio become less profound as the catalyst loading increases.

The general shape and slope of the surface plot from the upper limit of catalyst loading reveals that as catalyst loading decreases, so does the FFA. This trend, however, is not followed throughout the surface as at the upper limit of catalyst, there is a turning point at an alcohol/oil molar ratio of approximately 9.5 which results in an FFA value of 6.4 %. This may be as a result of an increase in the alcohol/oil molar ratio which drives the forward reaction to equilibrium. The turning point could signify that under

those conditions, the lowest possible FFA reduction has been achieved, after which further increase in alcohol/oil molar ratio causes an increase in reaction rate and water production becomes more significant thus promoting the reverse reaction.

5.5.6. The Effect of Time & Alcohol/Oil Molar Ratio on FFA (% Oleic Acid)

The 3-D response surface for the interaction between time and alcohol/oil molar ratio is shown in Figure 32 and the contour plot between time and alcohol/oil molar ratio is shown in Figure 33 whilst the temperature and catalyst loading were set at $47℃$ and 1.75 $(wt\%)$ of oil, respectively, in the regression equation. The lowest FFA value of approximately 2 % occurs at the upper limit of time and alcohol/oil molar ratio as shown by the contour plot in Figure 33.

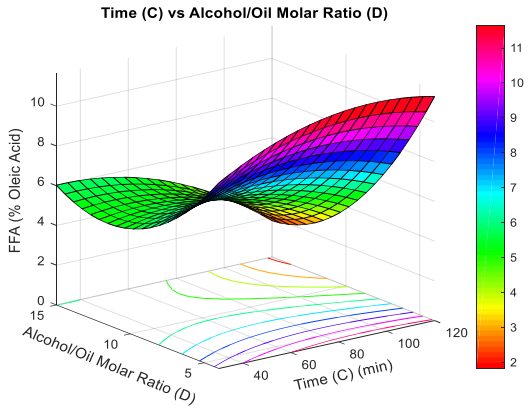

Figure 32 – Esterification Response Surface (C) vs (D)

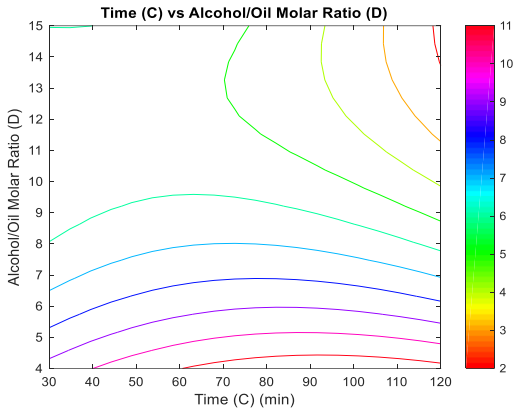

Figure 33 – Esterification Contour (C) vs (D)

The interaction between time and alcohol/oil molar ratio is shown in the figures above with an F-Value of 48.16. This is the second highest F-Value in terms of interaction effects apart from the interaction between temperature and alcohol/oil molar ratio. Obviously then alcohol/oil molar ratio is the dominant parameter which causes a more significant effect than reaction time on the response variable. The P-Value for this interaction is less than 0.0001 which indicates that the results obtained are statistically significant and did not occur by chance.

The odd-twisting response surface may be attributed to the time parameter. As mentioned earlier, there is a difference in this work and the work of Halder et al. (2015) in the case of castor oil esterification. More specifically, in their work, a reaction time starting from 1 hr was employed and as shown in this work, there is a turning point between the start of the reaction and the first hour. Furthermore, they concluded that there is a gradual reduction in FFA as time and alcohol/oil molar ratio increases. A similar trend may be noticed in the surface plot with the lowest FFA value of 2 % recorded at the upper limit of time and alcohol/oil molar ratio.

Consider the lower limit of alcohol/oil molar ratio and the time axis. As time increases an initial decrease in FFA may be observed up until a time of approximately $60\ mins$. This may be due to the forward reaction occurring and resulting in a decrease in FFA content, however, past a time of $60\ mins$, the FFA begins to increase implying that the reverse reaction is occurring due to water formation generated previously by the forward reaction.

Focusing on the contour plot, it can be seen that as time increases and for alcohol/oil molar ratios greater than 8, there is minimal change in the FFA content which remains constant at $5\ \%$. This effect remains true up until a reaction time of $70\ mins$, after which the FFA content decreases with increasing time and increasing alcohol/oil molar ratios. A possible explanation for this observation may be due to water present in the oil as this may cause the reverse reaction to occur. In addition, it is stated earlier that reaction time first causes an increase in FFA up to a time of $1\ hr$, after which there is a decrease in FFA content. This observation is not visible in the region in question, indicating that the tendency of the FFA to increase when reaction time is less than $1\ hr$, has been reduced by the increasing alcohol/oil molar ratios which has a tendency to reduce the FFAs at high ratios.

The following table illustrates the actual FFAs and the predicted FFAs from the regression equation associated with the coded units; A, B, C and D which represent temperature, catalyst loading, time and alcohol/oil molar ratio, respectively.

Table 31 – Box-Behnken Design Matrix for Castor Oil Esterification in Coded Units

Run Order	A	B	C	D	Actual FFA (%)	Predicted FFA (%)
1	47	0.25	30	9.5	1.850	1.90
2	47	3.25	75	15	7.800	7.54
3	47	3.25	75	4	10.437	10.90
4	64	1.75	75	4	11.934	12.13
5	64	1.75	120	9.5	3.176	2.86
6	64	0.25	75	9.5	2.638	2.57
7	64	1.75	30	9.5	3.701	3.50
8	64	3.25	75	9.5	3.791	4.07
9	47	1.75	120	4	11.786	11.28
10	30	3.25	75	9.5	8.588	8.54
11	47	1.75	75	9.5	6.073	5.97
12	30	1.75	75	4	9.610	9.43
13	30	0.25	75	9.5	2.567	2.18
14	47	1.75	120	15	1.530	1.83
15	47	1.75	30	15	5.636	6.03
16	30	1.75	120	9.5	4.030	4.41
17	47	0.25	75	4	9.550	9.99
18	47	3.25	120	9.5	4.826	4.70
19	47	1.75	75	9.5	5.927	5.97

20	47	1.75	30	4	9.760	9.34
21	30	1.75	75	15	8.056	7.78
22	64	1.75	75	15	0.900	1.00
23	47	0.25	75	15	0.876	0.59
24	30	1.75	30	9.5	5.540	6.03
25	47	0.25	120	9.5	1.679	1.92
26	47	1.75	75	9.5	5.909	5.97
27	47	3.25	30	9.5	7.291	6.97

Figure 34 shows the similarities between the actual results obtained via experiments versus the predicted results from the regression equation. The resulting data may be fitted to a linear model indicating a strong relationship between the two parameters.

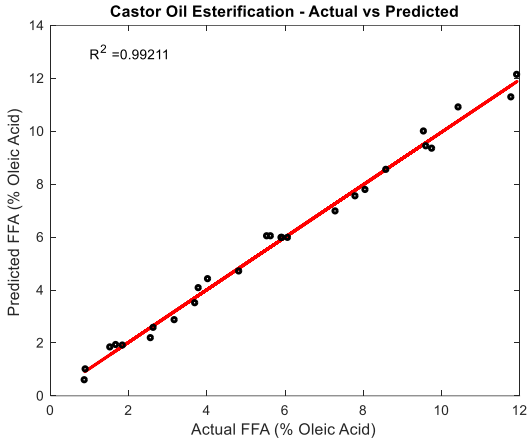

Figure 34 – Predicted FFA vs Actual FFA

The optimisation of the castor oil esterification Box-Behnken Design using a full quadratic model was conducted on *Minitab*™ where all the parameters where constrained to their respective domains as to avoid FFA minimisation below zero. As mentioned earlier, a trade-off between catalyst loading and alcohol/oil molar ratio was necessary to reduce the FFA below 0.8 %. Furthermore, the results of the optimisation are in direct agreement with the factors previously mentioned. The model validation experiments were conducted in triplets and the average is represented in Table 32. The optimisation conditions is deemed suitable as there is a 0.7 % difference between the actual and predicted values.

Table 32 – Optimum Conditions for Castor Oil Esterification – FFA Minimisation

Parameter	Optimum Value
Temperature (A)	58 ℃
Catalyst Loading (B)	0.865 $(wt\% \ oil)$
Time (C)	100.58 min
Alcohol/Oil Molar Ratio (D)	12.54
FFA (% Oleic Acid) (Predicted)	0.720
FFA (% Oleic Acid) (Actual)	0.715

5.6. Summary

Castor oil esterification was conducted using sulphuric acid as a catalyst in the presence of methanol. The Box-Behnken experimental design was used on *Minitab*™ to design the experiments with the fewest number of experiments to reduce operating costs and save resources. A total of 27 experiments were conducted inclusive of 3 replicates which is necessary for the determination of the regression coefficients. The resulting data was then tested and fitted to suitable models, of which, the full quadratic model was chosen. Alcohol/oil molar ratio was determined to be the most significant parameter which influenced the reduction of FFAs which was followed by catalyst loading whilst temperature and time had minimal effects on the reduction of FFAs. The response surface of the interaction between alcohol/oil molar ratio and catalyst loading showed the largest reduction in FFA content with a value of 0.8 % after which the optimisation for the minimisation of FFAs further reduced the FFAs to the optimal value of 0.72 by lowering the reaction time, alcohol/oil molar ratio and catalyst loading and increasing the reaction temperature. The FFA value of 0.72 was validated by the conduction of a series of three identical experiments at the optimal conditions to result in an FFA value of 0.715.

Chapter 6 – Results & Discussion: Castor Oil Transesterification

6.1. Introduction

This chapter is the second step in the production of biodiesel from castor oil. In the previous chapter, castor oil underwent acid-catalysed esterification via sulphuric acid and methanol to reduce the FFA content from a base value of 12 % to 0.715 % at the optimal conditions. Therefore, a large volume of castor oil with this FFA content was produced and stored for use in transesterification where calcium oxide is used as a heterogeneous base catalyst in the presence of methanol. The design of the experiment, statistical analysis and optimisation was conducted on *Minitab*™ using the Box-Behnken response surface methodology. In this section, A, B, C and D represent Temperature, Catalyst loading, Reaction time and Methanol/Oil molar ratio, respectively.

6.2. Statistical Models

The Box-Behnken model is generally associated with response surfaces, however, other models such as linear or a combination thereof may be employed provided that the model can sufficiently predict the data within the experimental range. With reference to Table 33, it can be seen that the linear model is not suitable for such prediction, simply because the coefficient of determination (R^2) value is too low. This means that the experimental data does not follow a linear or directly proportion trend which is expected in the case of a reacting system, as equilibrium should be reached at some point in time. The coefficient of determination indicates the goodness of fit between the data and the model, hence a full quadratic model is suggested in this work. Another observation that can be made would be the difference in (R^2) values between the linear plus squares and linear plus interactions models. This indicates that the interactions between the parameters is outweighed by the parameters interacting with themselves. In addition, the full quadratic model allows for all the model terms to be included in the regression equation, a characteristic not applicable in the other models, to result in the highest coefficient of determination and F-Value. According to Halder et al. (2015), if the difference between the R-Squared and R-Squared adjusted value is less than 0.1, the model is suitable for prediction of values within the data range. The difference between these two values is 0.049.

Table 33 – Statistical Model Testing for Castor Oil Transesterification

Model Summary	Sum of Squares	R-squared	R-squared (adjusted)	F-Value	Suggestion
Linear	0.519683	59.70 %	52.37 %	8.15	Not Suggested
Linear + Squares	0.750888	86.26 %	80.15 %	14.13	Not Suggested
Linear + Interactions	0.602983	69.27 %	50.06 %	3.61	Not Suggested
Full Quadratic	0.834188	95.83 %	90.96 %	19.69	Suggested

6.3. Statistical Analysis

As mentioned previously, the full quadratic model was chosen for this section which resulted in an F-Value and P-Value of 19.69 and less than 0.0001, respectively. Previously, it was stated that the interaction of the parameters with themselves are stronger than the interaction between the parameters which is shown to be valid even in the case of the full quadratic model. According to Halder et al. (2015), a high F-Value and low P-Value below the 95 % confidence interval is indictive of a model or parameter that strongly influences the response variable, which in this case is biodiesel yield. Therefore, to determine which individual parameters influence the yield, the linear model is used to make the following observation. It can be seen from Table 34 that temperature has the largest effect on yield which is followed by time then catalyst loading and lastly alcohol/oil molar ratio. An observation made from the table below would be the low P-Value of the model, which indicates that the model is significant and that the results observed did not occur by chance.

Table 34 – Analysis of Variance (ANOVA) for Castor Oil Transesterification (Full Quadratic Model)

Analysis of Variance (ANOVA)					
Source	DF	Adjusted Sum of Squares	Adjusted Mean of Squares	F-Value	P-Value
Model	14	0.834188	0.059585	19.69	< 0.0001
Linear	4	0.519683	0.129921	42.94	< 0.0001
A	1	0.304008	0.304008	100.48	< 0.0001
B	1	0.080033	0.080033	26.45	< 0.0001
C	1	0.118008	0.118008	39	< 0.0001
D	1	0.017633	0.017633	5.83	0.033
Square	4	0.231205	0.057801	19.1	< 0.0001
A*A	1	0.115379	0.115379	38.13	< 0.0001
B*B	1	0.151126	0.151126	49.95	< 0.0001
C*C	1	0.002601	0.002601	0.86	0.372
D*D	1	0.059737	0.059737	19.74	0.001
2-Way Interaction	6	0.0833	0.013883	4.59	0.012
A*B	1	0.009025	0.009025	2.98	0.11
A*C	1	0.015625	0.015625	5.16	0.042
A*D	1	0.000625	0.000625	0.21	0.658
B*C	1	0.0289	0.0289	9.55	0.009
B*D	1	0.021025	0.021025	6.95	0.022
C*D	1	0.0081	0.0081	2.68	0.128
Error	12	0.036308	0.003026		
Lack-of-Fit	10	0.036242	0.003624	108.72	0.009
Pure Error	2	0.000067	0.000033		
Total	26	0.870496			

As evident from Table 34 it can be seen that the parameters which influence the yield the most is the linear parameter of temperature, which is followed by the interaction of catalyst loading with itself and the linear term of reaction time is followed by the interaction of temperature with itself.

Table 35 – Coded Coefficients for Castor Oil Transesterification (Full Quadratic Model)

Coded Coefficients						
Term	Effect	Coefficient	SE Coefficient	T-Value	P-Value	VIF
Constant		0.9267	0.0318	29.18	< 0.0001	
A	0.3183	0.1592	0.0159	10.02	< 0.0001	1
B	0.1633	0.0817	0.0159	5.14	< 0.0001	1
C	0.1983	0.0992	0.0159	6.25	< 0.0001	1
D	0.0767	0.0383	0.0159	2.41	0.033	1
A*A	-0.2942	-0.1471	0.0238	-6.18	< 0.0001	1.25
B*B	-0.3367	-0.1683	0.0238	-7.07	< 0.0001	1.25
C*C	-0.0442	-0.0221	0.0238	-0.93	0.372	1.25
D*D	-0.2117	-0.1058	0.0238	-4.44	0.001	1.25
A*B	0.095	0.0475	0.0275	1.73	0.11	1
A*C	-0.125	-0.0625	0.0275	-2.27	0.042	1
A*D	-0.025	-0.0125	0.0275	-0.45	0.658	1
B*C	-0.17	-0.085	0.0275	-3.09	0.009	1
B*D	0.145	0.0725	0.0275	2.64	0.022	1
C*D	-0.09	-0.045	0.0275	-1.64	0.128	1

Table 36 – Model Summary for Castor Oil Transesterification (Full Quadratic Model)

Model Summary			
S	R-squared	R-squared (adjusted)	R-squared (predicted)
0.0550063	95.83 %	90.96 %	76.00 %

From Table 36 it can be seen that there is a good agreement between the R-Squared and R-Squared adjusted values. The difference between these two values is 0.049, thus making it suitable for the optimisation procedure because the model can sufficiently interpolate values within the data range.

The full quadratic model is shown in the following equation (Halder, et al., 2015):

$$Y = \beta_o + \sum_{i=1}^{k} \beta_i X_i + \sum_{i=1}^{k} \beta_{ii} {X_i}^2 + \sum_{i<j} \beta_{ij} X_i X_j \tag{6.1}$$

Where, the constant, linear, linear and squares and two-way interaction terms are captured by the first, second, third and fourth terms of Eq. (6.1), respectively. The fully expanded version of Eq. (6.1) is shown below:

$$\begin{aligned} Y = {} & \beta_o + \beta_1 X_1 + \beta_2 X_2 + \beta_3 X_3 + \beta_4 X_4 + \beta_{11} {X_1}^2 + \beta_{22} {X_2}^2 + \beta_{33} {X_3}^2 + \beta_{44} {X_4}^2 \\ & + \beta_{12} X_1 X_2 + \beta_{13} X_1 X_3 + \beta_{14} X_1 X_4 + \beta_{23} X_2 X_3 + \beta_{24} X_2 X_4 + \beta_{34} X_3 X_4 \end{aligned} \tag{6.2}$$

The regression equation obtained via multiple regression analysis is shown below in coded units, where A, B, C and D represent Temperature, Catalyst loading, Reaction time and Methanol/Oil molar ratio, respectively.

$$Y = -2.330 + 0.05901 * A + 1.280 * B + 0.01318 * C + 0.0670 * D - 0.000509 * A^2 \\ -0.6733 * B^2 - 0.000011 * C^2 - 0.003499 * D^2 + 0.00559 * AB - 0.000082 * AC \\ -0.000134 * AD - 0.00378 * BC + 0.0264 * BD - 0.000182 * CD \quad (6.3)$$

6.4. The Individual Effects of Process Parameters on Yield

In order to determine which parameters have the largest effect on the yield of biodiesel produced, the individual effects of each parameter need to be discussed whereas the combination effects of two parameters on the biodiesel yield may be seen in a surface plot. Whilst the ANOVA analysis in Table 34 shows which parameters and interactions effect the entire data set by analysing the variance of the data within the specified confidence interval, the individual and interaction effects of the parameters may be visualised by plots to quantify and understand the results of the statistical analysis. For the purposes of consistency, the constant setting for all variables was kept at the midpoints, i.e. temperature of 47℃, catalyst loading of 1 $wt\%$, time of 75 $mins$ and alcohol/oil molar ratio of 9.5.

6.4.1. The Effect of Temperature on Yield

Similar to the esterification procedure highlighted earlier, the temperatures employed in this section are 30℃, 47℃ and 64℃. These values were the same for esterification as the optimal temperature should not exceed that of the boiling point of methanol which has a normal boiling point of 64.7℃ (Kundu, et al., 2016). According to N.i et al. (2018) who conducted transesterification on waste cooking oil in the presence of sodium hydroxide catalyst, no biodiesel could be synthesised when the temperature of the oil was in excess.

Anguebes-Franseschi et al. (2016) noted similar observations in the case of African crude palm oil transesterification where an optimal temperature of 56℃ resulted in a biodiesel yield of 90 % and further increase in temperature resulted in a reduction in yield and saponification. The lower temperature limit of 30℃ was chosen such that low temperature transesterification could be investigated which may result in a reduction in thermal heating costs, should the optimisation reveal that yield is maximised at low temperatures. It can therefore be said that the temperature conditions were chosen in accordance with literature.

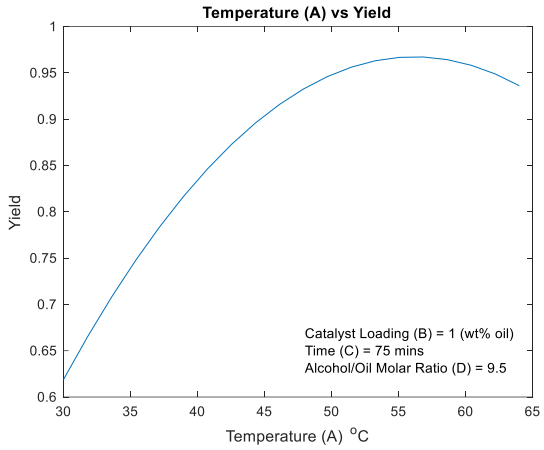

Figure 35 – Effect of Temperature (A) on Yield

According to the ANOVA analysis presented in Table 34, temperature has the largest effect on biodiesel yield with an F-Value and P-Value of 100.48 and less than 0.0001, respectively. The low P-Value indicates that the parameter is statistically significant.

However, in the work of Pradhan et al. (2012) in the case of biodiesel production from calcium oxide by reactive extraction of castor seed, temperature effects were somewhat negated by the extreme alcohol/oil molar ratio of 225: 1, employed in their work. They ultimately conclude that the process is feasible due to the short time between raw material and product as the extraction and purification of castor oil from castor seed has been omitted by the reactive extraction process. In their work, it is reported that temperatures above the boiling point of methanol were avoided.

They concluded that higher temperatures led to methanol loss which proves difficult in product extraction as well as increase the rate of saponification. Saponification is a side reaction that may occur during the transesterification reaction and the rate of saponification increases with an increase in temperature when alkali catalysts are employed (Pradhan, et al., 2012). In addition, they also noted that yield was highest when the reaction temperature was close to that of the boiling point temperature of the alcohol used. As seen in Figure 35, the temperature which facilitates the maximum yield of 96 % is approximately 56℃. This observation is in accordance with the works cited previously.

However, according to Figure 35, three regions can be seen in the graph, (1) increasing, (2) maximum or turning point and (3) decreasing regions. Firstly, the transesterification reaction is known to be endothermic which means that temperature must be added to the system in order to overcome the activation energy and begin the reaction. Therefore, as temperature increases, so does the reaction rate, which drives the forward reaction towards the production of biodiesel and glycerol, provided that the reaction occurs in an excess of methanol. Similar conclusions were drawn by Chaudhary et al. (2018) in the case of castor oil transesterification using methanol and sulphuric acid as a catalyst via the Central Composite Design (CCD) response surface methodology approach. In addition, due to the high

kinematic viscosity of esterified castor oil, higher temperatures may be necessary to effectively reduce the kinematic viscosity and thus increase the solubility of the castor oil in methanol, thereby increasing the yield produced.

The decreasing region of the graph which occurs between temperatures of 57℃ and 64℃ may be explained by methanol loss due to the temperature increase close to the boiling point temperature of methanol. Although a reflux condenser circulating chilled water was utilised, the temperature at which methanol returned to the reaction vessel after condensation may have produced an adverse effect on the reaction rate, which resulted in a decrease in yield. Furthermore, it is reported by Liu et al. (2008) that a 0.2 $wt\%$ of oil addition of water into the reaction vessel results in an increase in yield, a procedure that was followed in this work. However, as temperature increased, the frequency of side reactions may have also increased. In particular, the production of soap by saponification or water by esterification. Therefore, with an increase in temperature and the resulting methanol depletion, the amount of water in the reaction system may have resulted in partial hydrolysis of FAMEs, which led to a decrease in yield. This justification is validated by Liu et al. (2008) in the case of soybean oil transesterification using calcium oxide, methanol and 0.2 $wt\%$ addition of water.

6.4.2. The Effect of Catalyst Loading on Yield

The catalyst loadings, with reference to the amount of esterified castor oil, were 0.5 $wt\%$, 1 $wt\%$ and 1.5 $wt\%$. The catalyst chosen was calcium oxide which readily deactivates when exposed to atmospheric conditions due to carbon dioxide and water in the air that act as poisons for the catalyst. As such, calcination at 600℃ for 3 hrs inside a muffle furnace was necessary to fully activate the catalyst. These conditions resulted in the decomposition of hydroxides and carbonates as well as an increase in the basicity of the catalyst as shown by (Esipovich, et al., 2014).

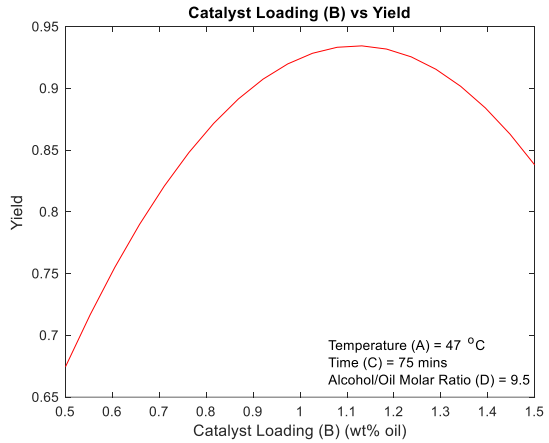

Figure 36 – Effect of Catalyst Loading (B) on Yield

As seen in Table 34, the F-Value and P-Value for catalyst loading according to the linear model is 26.45 and less than 0.0001, respectively. It can therefore be said that catalyst loading has the third highest

effect on yield. This may be due to the immediate deactivation of the catalyst upon exposure with the atmosphere which occurred during weighing and loading of the catalyst into the reaction vessel.

Furthermore, it is reported by Veljković et al. (2009) in the case of transesterification, that the catalyst and alcohol should be mixed and heated under stirring for a period of $30\ mins$ before the addition of oil that has been thermostated separately. This procedure was followed in this work, however, after the addition of esterified oil, $0.2\ wt\%$ of water was added which may have initially deactivated the catalyst and inhibited the forward reaction.

However, as catalyst loading increases, so does the yield of biodiesel. This increase in yield is maximised at a catalyst loading of $1.1\ wt\%$ which produces a yield of 93 %. This trend is to be expected as an increase in catalyst loading effectively increases the number of basic sites that a reaction may occur on. Similar observations are made in the work of Win & Khine (2017) in the case of palm oil transesterification using calcium oxide doped with potassium fluoride. In their work, they conclude that as the amount of potassium fluoride doping increases, so does the yield because the number of basic sites increases.

Considering the maximum or turning point shown in Figure 36, it can be said that at those conditions the maximum yield possible was achieved. Therefore, from an optimisation point of view, it can be noted that lower catalyst loadings result in higher yields up to the maximum point, therefore the amount of catalyst added should be kept moderately low as excess catalyst leads to a reduction in yield. This is seen at a catalyst loading past $1.1\ wt\%$ and may be attributed to an excess amount of basic sites present in the reaction vessel which may promote side reactions like saponification.

6.4.3. The Effect of Time on Yield

Similar to the procedure outlined in the previous chapter, the reaction time values are $30\ mins$, $75\ mins$ and $120\ mins$. This range was selected to fully explore the effect of reaction time on yield to allow a suitable optimisation time to be determined. Heterogeneous base catalysts are known to have a faster reaction rate than their acid catalyst counterparts (Refaat, 2011), therefore a maximum reaction time of $120\ mins$ is deemed sufficient to allow for maximum biodiesel production without the reverse reaction or saponification occurring. The lower time limit was employed mainly to reduce the high operating costs associated with longer reaction times.

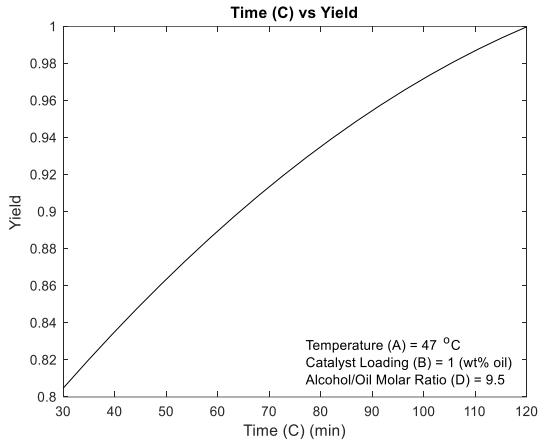

Figure 37 – Effect of Time (C) on Yield

With reference to Figure 37, at a reaction time of $120\ mins$, a yield of $100\ \%$ is observed to occur. This combination of parameters did not occur experimentally and may be attributed to over-prediction from the regression model.

As seen in Table 34, reaction time is a significant parameter in the production of biodiesel according to the linear model with an F-Value and P-Value of 39 and less than 0.0001, respectively. Although, through statistical analysis of the data, reaction time is deemed significant, the effect of reaction time on yield seems somewhat linear, which is an unusual observation due to the high reaction rate characteristics of heterogeneous base catalysts and high basicity of calcinated calcium oxide catalyst.

This high reaction rate in conjunction with sufficient reaction time should result in the reaction reaching equilibrium or a maximum point should have occurred, indicating that the reverse reaction or saponification is occurring. However, with reference to Figure 37, a steady increase in yield is observed with an increase in reaction time. This may be justified by the reaction temperature, which is the parameter that has the largest influence on the yield. Basically, if the reaction temperature is low, the rate of the reaction will be low as temperature is necessary for an endothermic reaction. Therefore, a longer reaction time is necessary to achieve equilibrium or induce the reverse reaction. This is justified by Figure 38 which shows that at elevated temperatures for the same reaction conditions, there exists a turning point at which the yield is maximised and the reverse reaction or saponification becomes significant. Furthermore, Figure 38 shows a much more realistic maximum yield of $95\ \%$ which is achieved at a reaction time of $110\ mins$.

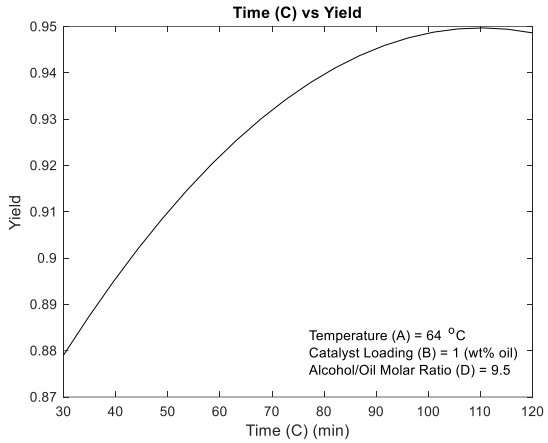

Figure 38 – Effect of Time (C) on Yield (Elevated Temperature)

6.4.4. The Effect of Alcohol/Oil Molar Ratio on Yield

This section employed the use of alcohol/oil molar ratios of $4:1$, $9.5:1$ and $15:1$. The lower limit was regarded as the minimum ratio employed because according to stoichiometry, 3 $mols$ of alcohol reacts with 1 mol of triglyceride to form 3 $mols$ of FAMEs and 1 mol of glycerol, therefore employing a minimum ratio of $4:1$ should theoretically drive the reaction in the forward direction towards the production of biodiesel. However, using a ratio of $4:1$ should reduce the reaction rate as methanol will not be in excess, therefore a lower catalyst loading would be necessary to achieve effective transesterification as seen in this work. The upper limit of alcohol/oil molar ratio was selected to avoid high operating costs as there is no appreciable change in yield with an increase in alcohol/oil molar ratio at moderate temperatures. Similar conclusions were drawn by Chaudhary et al. (2018) in the case of castor oil transesterification in the presence of sulphuric acid and methanol. In their work, alcohol/oil molar ratios as high as $30:1$ were employed and appreciable changes in yield were noted only in the case of high temperatures and high catalyst loadings.

The alcohol/oil molar ratio must be in excess to drive the forward reaction to equilibrium otherwise the reverse reaction may occur, or the reaction simply may not occur if the temperature is low. It is with the assumption of excess methanol that the reversibility of the reaction set may be negated and the reaction may be assumed pseudo-first order. Whilst this assumption is theoretically valid, the reverse reaction may still occur for many of the reasons discussed previously.

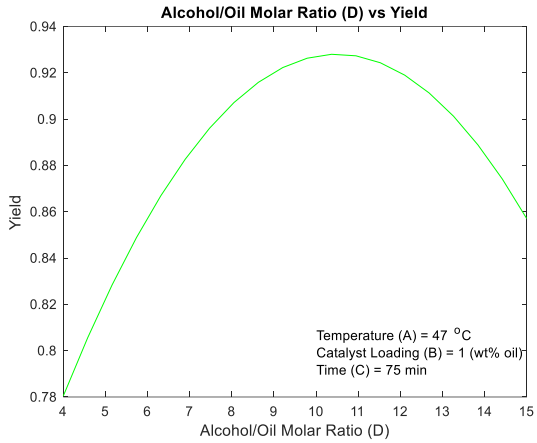

Figure 39 – Effect of Alcohol/Oil Molar Ratio (D) on Yield

In this work, alcohol/oil molar ratio was shown to have the smallest influence on the yield according to the linear model presented in Table 34. The relatively low F-Value of 5.83 and P-Value of 0.033 indicate that although the parameter has a small effect on the response variable, it is still statistically significant because the P-Value is below the confidence interval of 95 % employed in this work. With reference of Figure 39, it can be seen that a maximum or turning point occurs at an alcohol/oil molar ratio of 10.5: 1 which corresponds to a maximum yield of 92.5 %. The increasing region of the graph may be attributed to the increase in alcohol/oil molar ratio which drives the forward reaction, thereby increasing the reaction rate. Additionally, an increase in methanol will allow the surface of the catalyst to become fully saturated, thus increasing the frequency of reactions.

Furthermore, an increase in methanol would effectively lower the overall kinematic viscosity of the reaction mixture, thus making it easier for the triglyceride molecules to be transferred via mass transfer across the methanol layer covering the catalyst surface. However, the maximum point achieved using these conditions is relative to the conditions and may not exist if other conditions are employed. For example, in the work of Chaudhary et al. (2018), higher reaction temperatures resulted in an increase in biodiesel yield at higher alcohol/oil molar ratios.

After an alcohol/oil molar ratio of 10.5: 1, a reduction in yield can be noted. This may be attributed to excess methanol in the reaction system. According to Win & Khine (2017), who conducted palm oil transesterification using calcium oxide catalyst and calcium oxide doped with potassium fluoride, glycerol produced in the reaction would dissolve in a large excess of methanol. This would effectively reduce the amount of methanol available for transesterification as glycerol would inhibit the interaction between the methanol and catalyst. They conclude by stating that the aforementioned tends to promote the reverse reaction, as shown in Figure 39.

Figure 40 shown below represents the combined main effects of temperature, catalyst loading, reaction time and alcohol/oil molar ratio. The Box-Behnken Design allows for the use of three levels for a

specific parameter and these levels are coded -1, 0 and 1. With -1 representing the lower limits of the parameters, 0 representing the mid-points of the data range of the parameters and 1 representing the upper limits of the parameters.

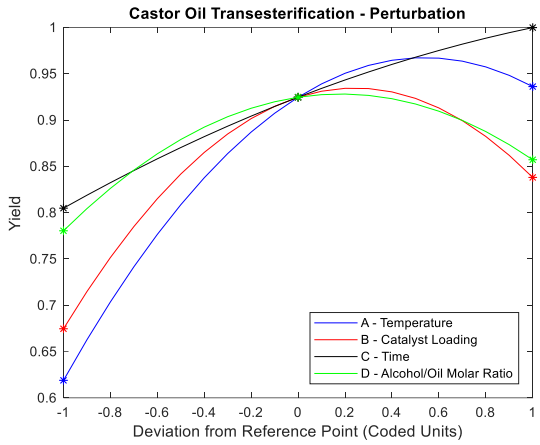

Figure 40 – Castor Oil Transesterification – Perturbation

6.5. Response Surface Plots

The regression equation (Eq. (6.3)) stated previously was used to plot the response surfaces and contour plots shown below. As mentioned previously, when trying to determine the relationship between two parameters and the resulting effect of the response variable, the other two factors need to be kept constant. For the purposes of consistency, the constant setting for all variables was kept at the midpoints, i.e. temperature of 47℃, catalyst loading of 1 $wt\%$, time of 75 $mins$ and alcohol/oil molar ratio of 9.5.

6.5.1. The Effect of Temperature & Catalyst Loading on Yield

The 3-D response surface for the interaction between temperature and catalyst loading is shown in Figure 41 and the contour plot between temperature and catalyst loading is shown in Figure 42 whilst the reaction time and alcohol/oil molar ratio were set at 75 $mins$ and $9.5{:}\,1$, respectively, in the regression equation. With reference to the response surface, a maximum yield of approximately 90 % may be seen which is unlike the esterification process because the values of interest are found inside the response surface and not at the extrema. The response surface also indicates a large range of values that result in 90 % yield which may be more clearly seen in the contour plot shown in Figure 42.

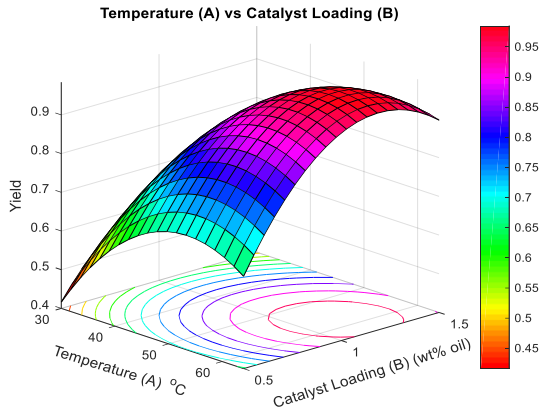

Figure 41 – Transesterification Response Surface (A) vs (B)

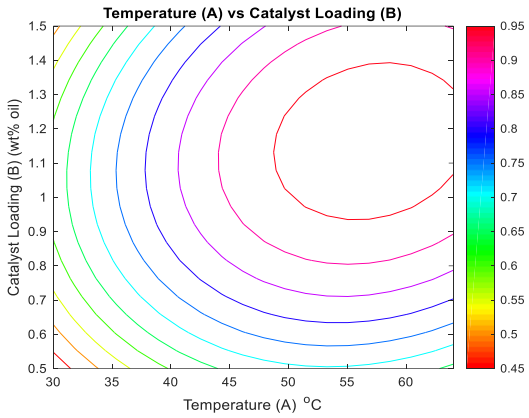

Figure 42 – Transesterification Contour (A) vs (B)

With reference to Table 34 for the interaction between temperature and catalyst loading, an F-Value and P-Value of 2.98 and 0.11, respectively, can be seen. Therefore, the interaction between these two parameters are regarded as being statistically insignificant because the interaction resulted in a P-Value that is not within the confidence interval of 95 % (Pradhan, et al., 2012). However, omitting all of the terms presented in Table 34 which are statistically insignificant resulted in an increase in standard deviation from 0.0550063 to 0.0595080 and a decrease in the coefficient of determination (R^2) from 95.83 % to 93.49 %. Clearly then, the omitted terms had a positive effect on the model used which may be attributed to the type of model used initially, which was the full quadratic model.

The ranges of temperature and catalyst loading which result in a yield of approximately 90 % are 47℃ to 64℃ and 0.95 $wt\%$ to 1.4 $wt\%$, respectively. In addition, the model predicts that temperatures above the boiling point of methanol may be employed to result in a 90 % yield, however, this may prove incorrect as methanol loss will result in decreased contact time between the triglycerides and catalyst (N.i, et al., 2018). Furthermore, depletion of methanol may induce the reverse reaction as an excess amount of methanol is necessary to drive the forward reaction to equilibrium.

The lowest yield reported by the response surface is 40 % which occurred at the lower limits of temperature and catalyst loading. This may be attributed to the low reaction temperature as temperature was found to have the largest influence on the yield of biodiesel produced according to the ANOVA. As such, the low reaction rate coupled with minimal catalyst resulted in a low yield. This suggestion may be justified as a slightly higher yield of 45 % may be noticed at a temperature and catalyst loading of 30℃ and 1.5 $wt\%$, respectively.

However, at the upper limits of temperature and catalyst loading, a slight decrease in yield may be noticed. This may be due to a decrease in temperature caused by methanol condensing back into the reaction vessel at the temperature of the chilled water bath. The results of this work is in accordance

with Pradhan et al. (2012) who conducted reactive extraction of castor seed in the presence of calcium oxide catalyst and methanol in a molar ratio to oil of 225: 1.

6.5.2. The effect of Temperature & Time on Yield

The 3-D response surface for the interaction between temperature and time is shown in Figure 43 and the contour plot between temperature and time is shown in Figure 44 whilst the catalyst loading and alcohol/oil molar ratio were set at 1 $wt\%$ and 9.5: 1, respectively, in the regression equation. The maximum yield of 98.5 % which is close to the theoretical yield of 100 % occurs at a temperature range and reaction time range of 47℃ to 57℃ and 105 $mins$ to 120 $mins$, respectively.

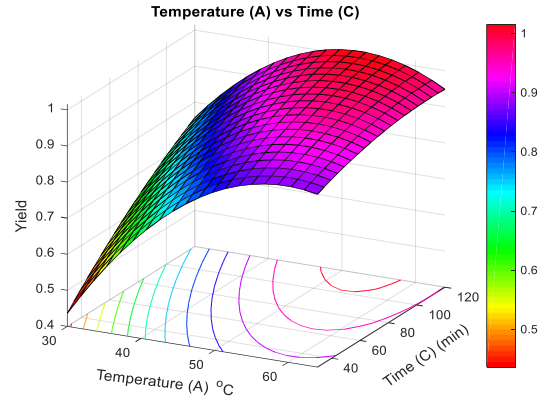

Figure 43 – Transesterification Response Surface (A) vs (C)

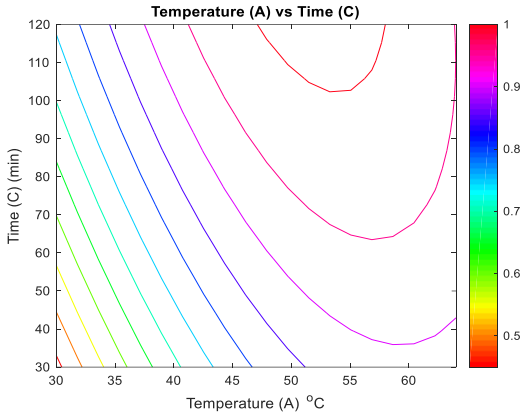

Figure 44 – Transesterification Contour (A) vs (C)

With reference to Table 34, it can be seen that according to the linear model, temperature and time have the largest influence on the yield of biodiesel produced, therefore, the interaction between the two parameters should have a large impact on the yield. The F-Value and P-Value of the interaction between these parameters are 5.16 and 0.042, respectively. Overall, it can be seen that the F-Value and P-Value is the third highest among the interaction effects which means that the combined effect of temperature and time has a negative effect on the yield. The interaction, however, is statistically significant as the P-Value is above the 95 % confidence interval used in this work.

Consider the lower limit of temperature and time which results in a yield of 45 %. This may be attributed to the reaction temperature being too low which causes the reaction rate for transesterification to be too slow. Furthermore, this seems like a valid assumption because a yield of 70 % is achieved when the reaction temperature is 30℃ and the reaction time is 120 $mins$, thereby indicating that the reaction rate was too slow, and a longer reaction time was required by the transesterification reaction.

A yield of approximately 85 % and 95 % was achieved when the reaction time was 30 $mins$ and 120 $mins$, respectively, for a temperature of 64℃. This result is expected as longer reaction times are necessary for effective conversion of triglycerides. It is also important to note the maxima which occurs in the temperature and time range highlighted earlier. This resulted in a yield of approximately 98.5 %,

after which when temperature or time were increased or decreased, a decrease in yield was observed. This may be due to temperature increase beyond 57℃ which resulted in methanol loss. The reaction temperature may have been lowered by condensed methanol; at the temperature of the chilled water; falling back into the reaction vessel. The methanol loss may have resulted in insufficient coverage of the catalyst surface on which the reaction occurs, as such the rate of the reaction may have been lowered (Lukić, et al., 2013).

6.5.3. The Effect of Temperature & Alcohol/Oil Molar Ratio on Yield

The 3-D response surface for the interaction between temperature and alcohol/oil molar ratio is shown in Figure 45 and the contour plot between temperature and alcohol/oil molar ratio is shown in Figure 46 whilst the catalyst loading and reaction time were set at 1 $wt\%$ and 75 $mins$, respectively, in the regression equation. With reference to the following plots, a maximum yield of 95 % can be seen to occur within the temperature and alcohol/oil molar ratio range of 50℃ to 62℃ and 8: 1 to 12.5: 1, respectively.

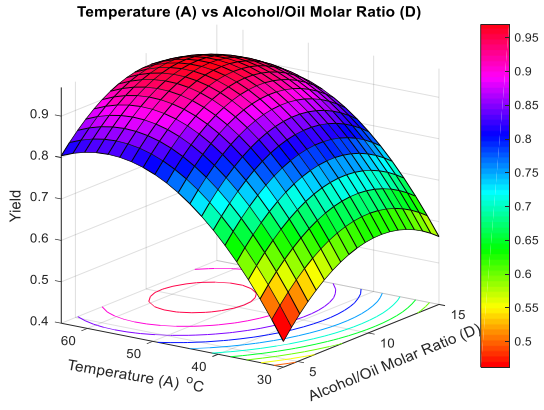

Figure 45 – Transesterification Response Surface (A) vs (D)

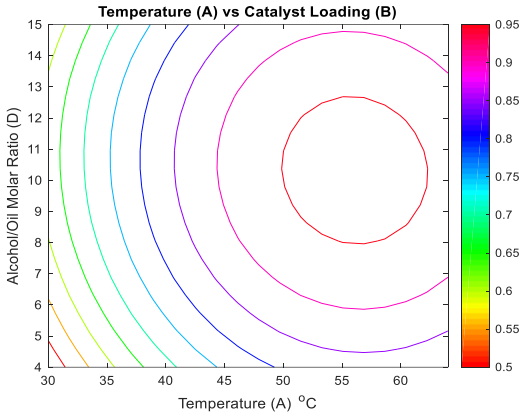

Figure 46 – Transesterification Contour (A) vs (D)

From Table 34 it can clearly be seen that the interaction between temperature and alcohol/oil molar ratio is statistically insignificant as the P-Value is above the 95 % confidence interval employed in this work. Furthermore, the F-Value of 0.21 and P-Value of 0.658 clearly indicate that the interaction between temperature and alcohol/oil molar ratio has the lowest influence over the response variable. Nevertheless, the response surface and contour plot between temperature and alcohol/oil molar ratio are in accordance with the literature, as discussed below.

A local maximum may be seen occurring in the temperature and alcohol/oil molar ratio ranges outlined earlier. This result is highly expected as yield increases with an increase in temperature as the rate of the reaction increases for a constant alcohol/oil molar ratio, as seen in the temperature axis of the response surface plot, but as the temperature approaches close to the boiling point of methanol, the yield decreases slightly indicating methanol loss.

In addition, this effect is seen in the work of Bharti et al. (2019) who conducted transesterification of soybean oil in the presence of methanol and nano-calcium oxide catalysts prepared using the Sol-Gel method using the Box-Behnken response surface methodology. However, in their work, a catalyst loading of 3.675 $wt\%$ was employed to produce a similar response surface to that of this work. Bojan et al. (2011) reported similar response surfaces for the interaction between temperature and alcohol/oil ratio in the case of transesterification with high content free fatty acid Jatropha Curcas oil using potassium hydroxide as a catalyst. However, in their work, a maximum yield of 76 % was recorded which may be attributed to saponification occurring due to the high free fatty acid content of the base oil.

With reference to castor oil, Deb et al. (2017) conducted a saponification reaction and acidification reaction to produce FFAs, then esterification reaction to obtain similar response surfaces to this work. Similar temperature ranges were employed but a maximum alcohol/oil molar ratio of $9{:}1$ was employed. Lastly, similar results were obtained in the work of Chaudhary et al. (2018) in the case of castor oil transesterification using sulphuric acid and a Central Composite Design approach. It can therefore be said that the results of this work, especially the interaction between temperature and alcohol/oil molar ratio which was shown to be statistically insignificant, is in accordance with the literature cited above.

6.5.4. The Effect of Catalyst Loading & Time on Yield

The 3-D response surface for the interaction between catalyst loading and time is shown in Figure 47 and the contour plot between catalyst loading and time is shown in Figure 48 whilst the reaction temperature and alcohol/oil molar ratio were set at 47℃ and $9.5{:}1$, respectively, in the regression equation. A maximum yield of 95 % may be seen to occur within the catalyst loading and time ranges of 0.75 $wt\%$ to 1.25 $wt\%$ and 88 $mins$ to 120 $mins$, respectively.

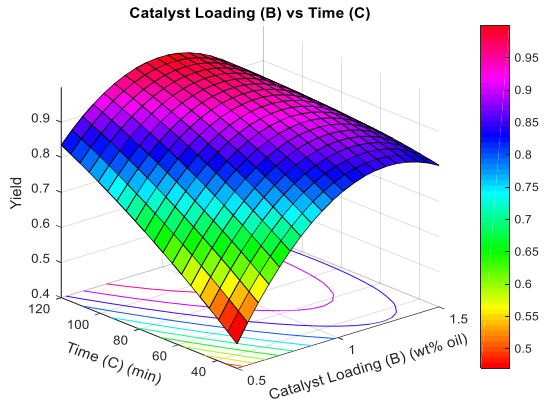

Figure 47 – Transesterification Response Surface (B) vs (C)

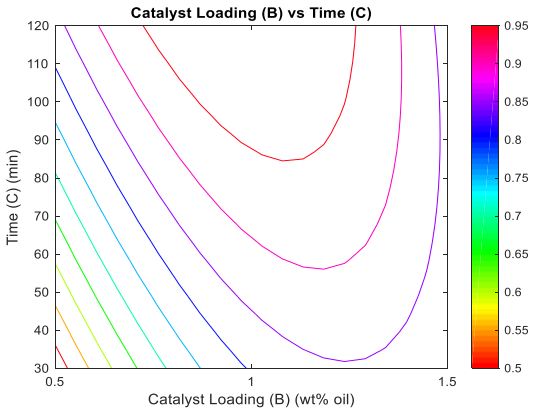

Figure 48 – Transesterification Contour (B) vs (C)

According to Table 34, the interaction between catalyst loading and time is the most significant among the interactions because it has the highest F-Value of 9.55 and lowest P-Value of 0.009. As shown by the response surface in Figure 47, reaction time has a larger influence over the yield, covering values from 50 % to 83 % whilst catalyst loading only influences the yield within a range of 50 % to 80 %. Therefore, reaction time is shown to have a larger influence over the response variable in comparison to catalyst loading, which is in accordance with the ANOVA presented in Table 34.

The range of values highlighted previously which result in a yield of 95 % is relatively large, indicating that the process is not too sensitive with respect to the two parameters. However, it is expected that lower catalyst loadings require longer reaction times in the case of transesterification which is shown more clearly in the contour plot in Figure 48. As shown in the contour plot, as catalyst loading increases the time required to maintain the 95 % yield decreases. This result is expected as more catalyst means that there are more active sites for reactions to occur and the process will reach the maximum conversion faster. This effect is observed until a catalyst loading of 1.1 $wt\%$ and a reaction time of 88 $mins$ where a turning point is observed.

This turning point may indicate that those conditions are the minimum conditions necessary to achieve a yield of 95 %. Further increase in catalyst loading past 1.1 $wt\%$ results in longer reaction times which indicate that the excess amount of catalyst in the reaction vessel has led to the occurrence of side reactions, i.e. saponification. This however, does not lower the yield immediately, probably due to the reaction temperature of 47℃, which may not be high enough to promote the increase in reaction rate of the saponification reaction. However, as catalyst loading increased past 1.3 $wt\%$, the saponification reaction becomes more significant and a reduction in yield is observed.

With reference to Figure 47, an almost linear relationship may be seen at the reaction time axis for the catalyst loading of 0.5 $wt\%$. This result is expected as lower catalyst loadings require longer reaction times and the linearity suggests that saponification or the reverse reaction did not occur. Similar results for the interaction between catalyst loading and reaction time were noted by Malpani et al. (2016) in the case of biodiesel production from algae oil using calcium oxide with titanium dioxide as a catalyst and methanol. In their work, however, a much gentler response surface is noticed which may be attributed to the difference in operating conditions employed.

6.5.5. The Effect of Catalyst Loading & Alcohol/Oil Molar Ratio on Yield

The 3-D response surface for the interaction between catalyst loading and alcohol/oil molar ratio is shown in Figure 49 and the contour plot between catalyst loading and alcohol/oil molar ratio is shown in Figure 50 whilst the reaction temperature and time were set at 47℃ and 75 $mins$, respectively, in the regression equation. A maximum yield of 90 % is achieved when the catalyst loading and alcohol/oil molar ratio are within the ranges of 0.9 $wt\%$ to 1.4 $wt\%$ and 8: 1 to 14.5: 1, respectively. It

is important to note that the range to obtain a relatively high yield is the largest between the interaction of catalyst loading and alcohol/oil molar ratio.

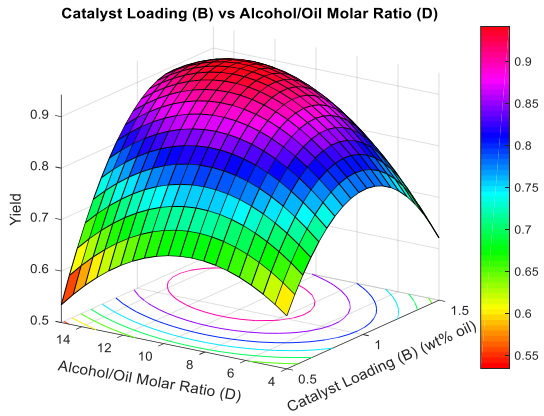

Figure 49 – Transesterification Response Surface (B) vs (D)

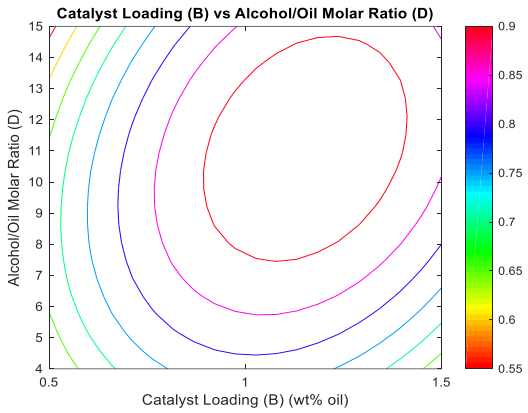

Figure 50 – Transesterification Contour (B) vs (D)

This wide range is in accordance with the ANOVA conducted in Table 34, which indicates that according to the linear model, catalyst loading and alcohol/oil molar ratio are among two of the lowest parameters that influence the yield, therefore, the range of the parameters should not have a drastic influence over the yield. However, the interaction between these two parameters has the second highest impact on the yield. The F-Value and P-Value of 6.95 and 0.022 indicate that the interaction is statistically significant, and the values obtained did not occur by chance as the probability of that happening is relatively low because the interaction of the parameters falls within a 95 % confidence interval.

Similar results were reported by Chumuang & Punsuvon (2017) who conducted transesterification of waste cooking oil in the presence of calcium methoxide as a catalyst and tetrahydrofuran as a cosolvent. In their work, the addition of tetrahydrofuran influenced the response surface obtained and different operating conditions were employed, nevertheless, similar results to this work was observed. This may be attributed to tetrahydrofuran lowering the overall viscosity of the reaction mixture and increasing the solubility between the oil, methanol and catalyst.

In this work, water was used instead of tetrahydrofuran. According to Liu et al. (2008), the addition of 0.2 $wt\%$ of oil of water increases the yield of biodiesel produced. This was validated by Esipovich et al. (2014) in the case of calcium oxide catalysts, who suggested that water forms active hydroxide sites (OH^-) on the catalyst surface which leads to an increase in methoxide anion formation, thereby increasing the yield by promoting the formation of methoxide anions. In addition, the addition of water was found to increase the solubility of the reacting species and the calcium oxide catalyst because the reaction is catalysed by diluted active calcium oxide rather than active calcium oxide (Kouzu, et al., 2009).

With reference to Figure 49, considering the lower limit of catalyst loading and upper limit of alcohol/oil molar ratio, a yield of 54 % was achieved. This is due to excess methanol in the reaction system which readily dissolves with glycerol produced via the forward reaction, thereby leading to a decrease in methanol coverage on the catalyst surface (Win & Khine, 2017). This may lead to blockage of active sites by the triglyceride or glycerol molecules which lowers the reaction rate.

6.5.6. The Effect of Time & Alcohol/Oil Molar Ratio on Yield

The 3-D response surface for the interaction between time and alcohol/oil molar ratio is shown in Figure 51 and the contour plot between time and alcohol/oil molar ratio is shown in Figure 52 whilst the reaction temperature and catalyst loading were set at 47℃ and 1 $wt\%$, respectively, in the regression equation. A maximum yield of 95 % was found to occur in the ranges of 88 $mins$ to 120 $mins$ and 5.5: 1 to 13: 1 for reaction time and alcohol/oil molar ratio, respectively.

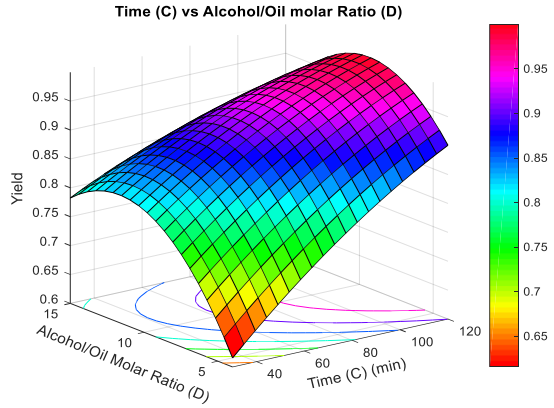

Figure 51 – Transesterification Response Surface (C) vs (D)

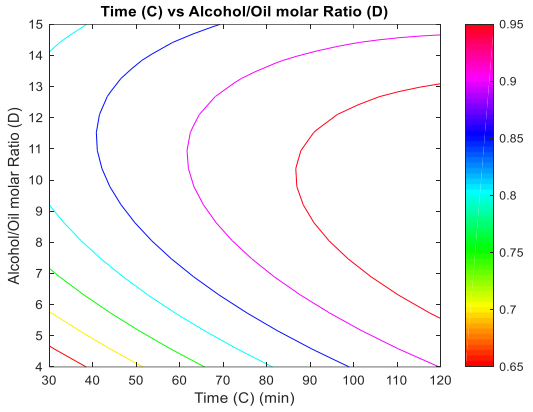

Figure 52 – Transesterification Contour (C) vs (D)

As seen in Figure 51, the reaction time parameters displays a much larger influence over alcohol/oil molar ratio because it influences a wider range of the response variable as compared to alcohol/oil molar ratio. However, the interaction between the two parameters are deemed statistically insignificant because the P-Value of 0.128 is above the 95 % confidence interval employed in this work. Furthermore, the F-Value of 2.68 reveals that the interaction has relatively small effect on the response variable.

As expected, the lower limits of time and alcohol/oil molar ratio result in a yield of 60 %, which is the lowest value recorded by the response surface. This may be due to insufficient methanol necessary to drive the forward reaction timeously, as such, the reaction rate is rather low which results in a low yield of biodiesel. In addition, the reaction time may simply be too short for the reaction to result in a high yield as the conversion of triglycerides into biodiesel requires sufficient reaction time. Considering the lower limit of reaction time and upper limit of alcohol/oil molar ratio, the above statement appears valid as higher ratios promote the forward reaction as indicated by a yield of 78 %.

The linearity of the effect of time can be seen quite clearly on the time axis for an alcohol/oil molar ratio of $4{:}\,1$, which indicates that at low ratios, the reaction time may be increased to result in higher yields produced. The overall shape of the response surface indicates that the system responds better to high reaction times and as time decreases, so does the yield, which is an effect that is particularly visible at low alcohol/oil molar ratios. Similar results were recorded by Chumuang & Punsuvon (2017) in the case of waste cooking oil transesterification using calcium methoxide as a catalyst and tetrahydrofuran as a cosolvent. However, in their response surface, there is minimal variation between the two parameters in question which may be due to the difference in reaction time. For this work, the reaction time started at $30\ mins$ whilst in their work, a starting reaction time of $60\ mins$ was employed. The following table illustrates the actual yield and the predicted yield from the regression equation associated with the coded units; A, B, C and D which represent temperature, catalyst loading, time and alcohol/oil molar ratio, respectively.

Table 37 – Box-Behnken Design Matrix for Castor Oil Transesterification in Coded Units

Run Order	A	B	C	D	Actual Yield	Predicted Yield
1	30	1.5	75	9.5	0.46	0.48
2	30	0.5	75	9.5	0.40	0.42
3	30	1	75	15	0.56	0.56
4	47	0.5	75	4	0.60	0.60
5	47	1	30	4	0.64	0.62
6	30	1	30	9.5	0.50	0.44
7	47	1	120	4	0.91	0.90
8	47	1	75	9.5	0.93	0.92
9	47	1.5	120	9.5	0.91	0.83
10	64	1	120	9.5	0.91	0.95
11	47	1	75	9.5	0.92	0.92
12	64	1	75	4	0.84	0.80
13	47	0.5	120	9.5	0.87	0.83
14	47	0.5	75	15	0.60	0.53
15	47	1.5	75	4	0.58	0.62
16	47	1	30	15	0.73	0.78
17	47	0.5	30	9.5	0.42	0.47
18	30	1	75	4	0.45	0.46
19	30	1	120	9.5	0.76	0.76
20	64	1	75	15	0.90	0.86
21	47	1	75	9.5	0.93	0.92
22	47	1	120	15	0.82	0.89
23	64	1	30	9.5	0.90	0.88
24	47	1.5	75	15	0.87	0.84
25	64	0.5	75	9.5	0.62	0.64
26	64	1.5	75	9.5	0.87	0.90
27	47	1.5	30	9.5	0.80	0.80

Figure 53 shows the actual yield plotted against the predicted yield obtained from the regression equation. As seen below, a linear regression equation can be fitted to the data set and the regression coefficient of determination (R^2) is 0.95826 which indicates a very strong relationship between the actual experimental data and the predicted data from the regression equation. Therefore, the use of the full quadratic model is valid for optimisation where interpolation between the different parameters can occur to maximise the yield.

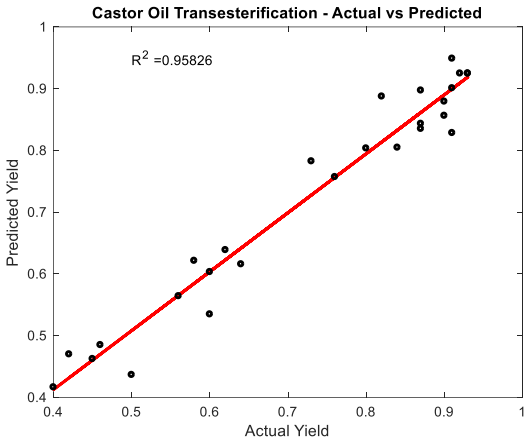

Figure 53 – Predicted Yield vs Actual Yield

The optimisation of the castor oil transesterification Box-Behnken Design using a full quadratic model was conducted on *Minitab*™ where all the parameters where constrained to their respective domains as to avoid maximisation of the response variable beyond 100 %. The parameter that has the largest influence over the response variable is temperature, therefore temperature is expected to be high because higher temperatures promote the forward reaction by increasing the reaction rate. Secondly, catalyst loading is expected to be high and reaction time is expected to be low to prevent saponification and alcohol/oil molar ratio should be relatively high as the reverse reaction should not occur at any point in time. Three model validation experiments were conducted and the average yield of 97.2 % is presented in the table below. The results of the optimisation are deemed suitable as saponification did not occur and the difference between the predicted and actual yields are 1.4 %.

Table 38 – Optimum Conditions for Castor Oil Transesterification – Yield Maximisation

Parameter	Optimum Value
Temperature (A)	61 ℃
Catalyst Loading (B)	1.368 ($wt\%\ oil$)
Time (C)	31.8 min
Alcohol/Oil Molar Ratio (D)	12.8
Yield (Predicted)	0.986
Yield (Actual)	0.972

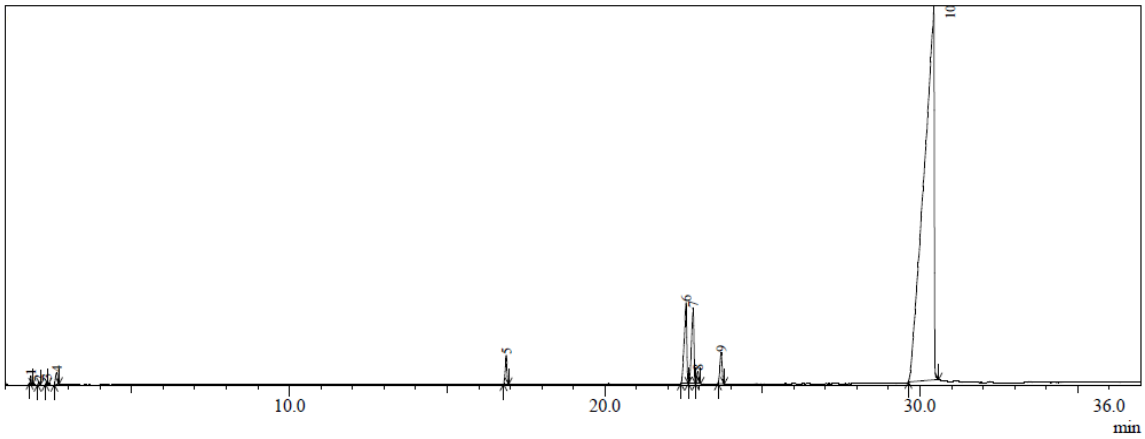

Figure 54 – Castor Oil Biodiesel (Optimal Conditions) Chromatogram

Table 39 – Castor Oil Biodiesel (Optimal Conditions) GCMS

Peak Number	Retention Time (min)	Area (%)	Name
1	1.802	0.13	Methyl alcohol
2	2.057	0.07	Acetone
3	2.300	0.07	Furfural
4	2.625	0.52	Heptanal
5	16.879	1.17	Hexadecenoic acid, methyl ester
6	22.583	4.75	11-Octadecenoic acid, methyl ester
7	22.805	4.08	Methyl stearate
8	22.954	0.54	Methyl palmitate
9	23.696	1.51	9-Octadecenoic acid, methyl ester
10	30.441	87.16	Methyl linoleate

6.6. Summary

Castor oil transesterification was conducted using esterified castor oil at the optimal conditions in the presence of calcium oxide and methanol with the addition of 0.2 $wt\%$ of oil of water. Response surface methodology using Box-Behnken design was employed to design and analyse the experimental results. A total of 27 experiments were conducted inclusive of 3 replicates which are necessary for the determination of the regression coefficients by *Minitab*™. Statistical analysis in the form of an ANOVA revealed that temperature was the most important parameter according to the full quadratic model chosen. Reaction time, catalyst loading and alcohol/oil molar ratio were ranked second, third and fourth, respectively, in terms of influence on yield according to the linear part of the full quadratic model. The response surface between temperature and time showed the largest influence over the yield, with a maximum predicted yield of 98.5 %. The optimisation revealed a maximum predicted yield of 98.6 % which is in accordance with the factors discussed earlier. The actual yield attained at the optimal conditions was 97.2 % which proves that the model and optimisation is valid.

Chapter 7 – Results & Discussion: Sunflower Oil Transesterification

7.1. Introduction

This section focuses on the production of biodiesel from sunflower oil by transesterification using calcium oxide catalyst and methanol. One of the reasons for this section was to evaluate the performance of the calcium oxide catalyst to determine if the results produced via the transesterification of esterified castor oil was as a result of the activity of the calcium oxide or as a result of esterification of the base castor oil by sulphuric acid catalyst. Furthermore, the physical properties of sunflower oil make it desirable for the production of biodiesel and jet fuel thereafter. The design of the experiment, statistical analysis and optimisation was conducted on *Minitab*™ using the Box-Behnken response surface methodology. In this section, A, B, C and D represent Temperature, Catalyst loading, Reaction time and Methanol/Oil molar ratio, respectively.

7.2. Statistical Models

As mentioned previously, the Box-Behnken response surface methodology was used to design the experiments. However, a choice of four different models is given in *Minitab*™ with the full quadratic model usually selected for response surfaces (Halder, et al., 2015). In this work, the full quadratic model is suggested for use as the coefficient of determination (R^2) is the highest among the other models and the linear model with interactions has the second highest coefficient of determination value. This suggests that the interaction between the parameters are significant and therefore validates the use of the full quadratic model as with the other models, the interaction between the parameters will be omitted in the regression equation. The linear model is ranked the lowest and the full quadratic model the highest because of the coefficient of determination values. It is vital to note that the coefficient of determination value increases with increasing model complexity. According to Halder et al. (2015), if the difference between the R-Squared and R-Squared adjusted value is less than 0.1, the model is suitable for prediction of values within the data range. The difference between these two values is 0.051.

Table 40 – Statistical Model Testing for Sunflower Oil Transesterification

Model Summary	Sum of Squares	R-squared	R-squared (adjusted)	F-Value	Suggestion
Linear	0.202566	57.66 %	49.97 %	7.49	Not Suggested
Linear + Squares	0.241445	68.73 %	54.84 %	4.95	Not Suggested
Linear + Interactions	0.296945	84.53 %	74.86 %	8.74	Not Suggested
Full Quadratic	0.335824	95.60 %	90.46 %	18.62	Suggested

7.3. Statistical Analysis

According to Halder et al. (2015), a high F-Value and low P-Value below the confidence interval employed is indictive of a model or parameter that is statistically significant. The F-Value and P-Value for the full quadratic model employed is 18.62 and less than 0.0001, respectively. It can therefore be

said that the full quadratic model is statistically significant and the values obtained thereafter did not occur by chance. Furthermore, the full quadratic model accounts for the linearity of the parameters, which is useful when trying to determine the individual effects of each parameter on the response variable. As such, based on the linear part of the full quadratic model, it can be seen that alcohol/oil molar ratio has the largest influence on the yield of biodiesel produced. Reaction temperature, catalyst loading and reaction time and ranked second, third and fourth, respectively.

Table 41 – Analysis of Variance (ANOVA) for Sunflower Oil Transesterification (Full Quadratic Model)

Analysis of Variance (ANOVA)					
Source	DF	Adjusted Sum of Squares	Adjusted Mean of Squares	F-Value	P-Value
Model	14	0.335824	0.023987	18.62	< 0.0001
Linear	4	0.084167	0.021042	16.33	< 0.0001
A	1	0.034112	0.034112	26.48	< 0.0001
B	1	0.033583	0.033583	26.07	< 0.0001
C	1	0.001002	0.001002	0.78	0.395
D	1	0.05858	0.05858	45.47	< 0.0001
Square	4	0.038879	0.00972	7.54	0.003
A*A	1	0.015213	0.015213	11.81	0.005
B*B	1	0.034398	0.034398	26.7	< 0.0001
C*C	1	0.006053	0.006053	4.7	0.051
D*D	1	0.008223	0.008223	6.38	0.027
2-Way Interaction	6	0.094379	0.01573	12.21	< 0.0001
A*B	1	0.000445	0.000445	0.35	0.568
A*C	1	0.003872	0.003872	3.01	0.109
A*D	1	0.053565	0.053565	41.58	< 0.0001
B*C	1	0.004621	0.004621	3.59	0.083
B*D	1	0.021347	0.021347	16.57	0.002
C*D	1	0.010529	0.010529	8.17	0.014
Error	12	0.01546	0.001288		
Lack-of-Fit	10	0.015021	0.001502	6.84	0.134
Pure Error	2	0.000439	0.00022		
Total	26	0.351284			

Considering the full quadratic model and ranking of parameters based on their F-Values, it can be seen in Table 41 that the linear term of alcohol/oil molar ratio has the largest influence on the yield and is followed by the interaction between temperature and alcohol/oil molar ratio, which is expected as these are the two parameters that has the largest effect on the response variable. In addition, the interaction of catalyst loading with itself is followed by the linear model temperature term.

Table 42 – Coded Coefficients for Sunflower Oil Transesterification (Full Quadratic Model)

Coded Coefficients						
Term	Effect	Coefficient	SE Coefficient	T-Value	P-Value	VIF
Constant		2.613	0.261	10.02	< 0.0001	
A	-0.06243	-0.03122	0.00607	-5.15	< 0.0001	99.08
B	-1.859	-0.93	0.182	-5.11	< 0.0001	77.21
C	-0.00339	-0.0017	0.00192	-0.88	0.395	69.88
D	-0.2143	-0.1071	0.0159	-6.74	< 0.0001	71.12
A*A	0.00037	0.000185	0.000054	3.44	0.005	70.04
B*B	0.6425	0.3212	0.0622	5.17	< 0.0001	37.25
C*C	0.000033	0.000017	0.000008	2.17	0.051	26.25
D*D	0.002596	0.001298	0.000514	2.53	0.027	28.1
A*B	0.00248	0.00124	0.00211	0.59	0.568	35.93
A*C	-0.000081	-0.000041	0.000023	-1.73	0.109	32.26
A*D	0.002475	0.001238	0.000192	6.45	< 0.0001	32.88
B*C	-0.003021	-0.001511	0.000798	-1.89	0.083	21.33
B*D	0.05313	0.02656	0.00653	4.07	0.002	21.95
C*D	0.000415	0.000207	0.000073	2.86	0.014	18.28

Table 43 – Model Summary for Sunflower Oil Transesterification (Full Quadratic Model)

Model Summary			
S	R-squared	R-squared (adjusted)	R-squared (predicted)
0.0358933	95.60 %	90.46 %	75.09 %

It can be seen in Table 43 that there is a good agreement between the R-Squared and R-Squared adjusted values. The difference between the two values is 0.051. As such, the full quadratic model may be assumed valid for optimisation as the model can sufficiently model and predict the data.

The full quadratic model is shown in the following equation (Halder, et al., 2015):

$$Y = \beta_o + \sum_{i=1}^{k} \beta_i X_i + \sum_{i=1}^{k} \beta_{ii} {X_i}^2 + \sum_{i<j} \beta_{ij} X_i X_j \tag{7.1}$$

Where, the constant, linear, linear and squares and two-way interaction terms are captured by the first, second, third and fourth terms of Eq. (7.1), respectively. The fully expanded version of Eq. (7.1) is shown below:

$$\begin{aligned} Y = {} & \beta_o + \beta_1 X_1 + \beta_2 X_2 + \beta_3 X_3 + \beta_4 X_4 + \beta_{11} {X_1}^2 + \beta_{22} {X_2}^2 + \beta_{33} {X_3}^2 + \beta_{44} {X_4}^2 \\ & + \beta_{12} X_1 X_2 + \beta_{13} X_1 X_3 + \beta_{14} X_1 X_4 + \beta_{23} X_2 X_3 + \beta_{24} X_2 X_4 + \beta_{34} X_3 X_4 \end{aligned} \tag{7.2}$$

The regression equation obtained via multiple regression analysis is shown below in coded units, where A, B, C and D represent Temperature, Catalyst loading, Reaction time and Methanol/Oil molar ratio, respectively.

$$Y = 2.613 - 0.03122 * A - 0.930 * B - 0.00170 * C - 0.1071 * D + 0.000185 * A^2 + 0.3212 * B^2 + 0.000017 * C^2 + 0.001298 * D^2 + 0.00124 * AB - 0.000041 * AC + 0.001238 * AD - 0.001511 * BC + 0.02656 * BD + 0.000207 * CD \quad (7.3)$$

7.4. The Individual Effects of Process Parameters on Yield

The individual effects of the parameters and their effect on the yield of biodiesel produced is found by keeping all other parameters at their midpoints and varying the parameter in question for the entire data range. The interaction between two parameters and the resulting effect on the response variable may be visualised in a surface plot. For the purposes of consistency, the constant setting for all variables was kept at the midpoints, i.e. temperature of 47℃, catalyst loading of $1\,wt\%$, time of $75\,mins$ and alcohol/oil molar ratio of 9.5.

7.4.1. The Effect of Temperature on Yield

The temperature range of values are inclusive of temperatures of 30℃, 47℃ and 64℃. This range was the same as the previous two sections mainly because the boiling point temperature of methanol is 64.7℃ and for consistency (Kundu, et al., 2016). The point of consistency was to evaluate the performance of the catalyst used, hence identical conditions were used in the transesterification of sunflower oil as compared to the transesterification of esterified castor oil. The lower limit of temperature was chosen such that low temperature optimisation may be achieved which would result in reduced thermal costs.

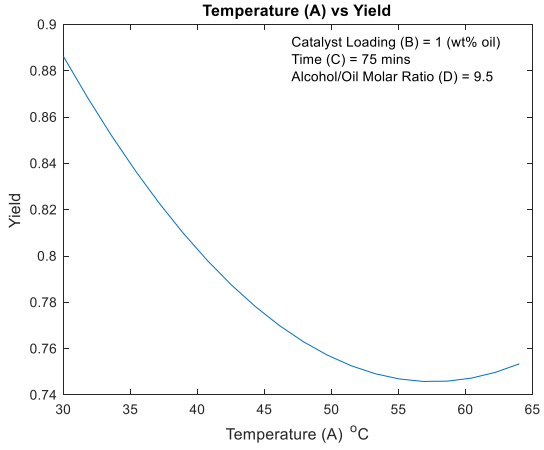

Figure 55 – Effect of Temperature (A) on Yield

In the work of Anastopoulos et al. (2013), an increase in sunflower oil biodiesel yield was observed with an increase in temperature for the case of sunflower oil transesterification using lithium nitrate loaded on calcium oxide as a catalyst in the presence of methanol. They concluded that an optimal temperature of 60℃ resulted in approximately 98 % yield of FAMEs. A contradiction to their work may be seen in this work as temperature increase was found to result in a reduction in yield.

This may be attributed to a multitude of factors, the primary factor being the type of catalyst used as in this work, neat calcium oxide catalyst was used instead of lithium nitrate loaded on calcium oxide. Furthermore, in their investigation of the parameters which affect the yield, temperature was not included as a parameter that affects the yield. The optimal conditions based on parametric optimisation (one-variable-at-a-time) was found for catalyst loading, reaction time and alcohol/oil molar ratio and then the effects of temperature was explored using those optimal conditions. As such, the effects of temperature variations may have been negated by the other variables. In this work, the baseline for the other variables was at their midpoints, hence, the alcohol/oil molar ratio; which has the largest effect on yield; may have influenced the yield much more at its baseline than temperature.

Unlike the castor oil section, in this section temperature is shown to have a negative impact on the yield of biodiesel produced as indicated by the negative shape of the plot in Figure 55. Temperature was found to have the second strongest influence over the yield according to the ANOVA presented in Table 41, with an F-Value and P-Value of 26.48 and less than 0.0001, respectively. As such, it can be said that the results of the temperature effects on yield did not occur by chance and that temperature is shown to be statistically significant as the P-Value is well below the 95 % confidence interval used in this work.

Furthermore, the shape of plot may be justified in the sense that the reaction system preferred to operate at low temperatures based on the baseline of the other variables. Simply put, the baseline of the other variables were relatively low, but sufficient to sustain a process that produces a high yield at low temperatures as indicated by the 88.5 % yield which occurs at a temperature of 30℃. Further increase in the reaction temperature led to a reduction in yield, of which a minimum yield of 75 % is noted at a temperature of 57℃. This reduction may be explained by the occurrence of side reactions which may occur with an increase in temperature due to an increase in reaction rate. Side reactions such as esterification and saponification result in a reduction in yield by consuming the catalyst (Anastopoulos, et al., 2013).

Clearly, the aforementioned factors are valid because using a higher alcohol/oil molar ratio completely reverses the effect that temperature has on the yield, as shown below, proving that the plots shown are relative to the conditions used. Furthermore, it can be said that the results of this work are in accordance with Anastopoulos et al. (2013). Similar results were noted in work of Veličković et al. (2016) in the

work of sunflower oil transesterification using calcium oxide and ethanol. In addition, as reaction temperature increased, the kinematic viscosity of the resulting sunflower oil biodiesel produced in the presence of methanol and calcium oxide catalyst decreased in the work of Son & Kusakabe (2011). Similar observations were noted in this work, as such, it can be said that the findings in this work are in accordance with the literature cited above.

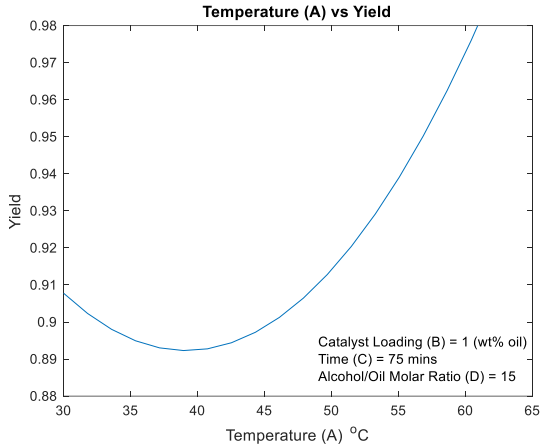

Figure 56 – Effect of Temperature (A) on Yield (Elevated Alcohol/Oil Molar Ratio)

7.4.2. The Effect of Catalyst Loading on Yield

As mentioned earlier the catalyst loading values were kept constant with respect to the transesterification of esterified castor oil section, as such, catalyst loadings of $0.5\ wt\%$, $1\ wt\%$ and $1.5\ wt\%$ was employed. The catalyst loadings for this work are relatively low as compared to Veljković et al. (2009) who employed calcium oxide loadings of $1\ wt\%$ to $10\ wt\%$. However, due to the high calcination temperature of $600℃$ employed in this work, which is noted to be the optimal calcination temperature for calcium oxide by Esipovich et al. (2014), and the addition of $0.2\ wt\%$ of oil of water employed in this work, which is noted to be the optimal amount of water to be added into the reaction vessel by Liu et al. (2008), the relatively low catalyst loadings should produce biodiesel without the saponification reaction occurring.

In addition, for the transesterification of soybean oil, Esipovich et al. (2014) showed that the use of $1.3\ wt\%$ calcined calcium oxide catalyst was sufficient to result in a yield of approximately $98\ \%$ biodiesel. Therefore, the use of the current catalyst loadings are valid as the optimal catalyst loading should be found to somewhere in the upper catalyst loading range. Furthermore, an optimal catalyst loading of $1\ wt\%$ of calcium oxide using sunflower oil as a feedstock for transesterification may be seen in many works (Granados, et al., 2007; Veljković, et al., 2009; Vujicic, et al., 2010).

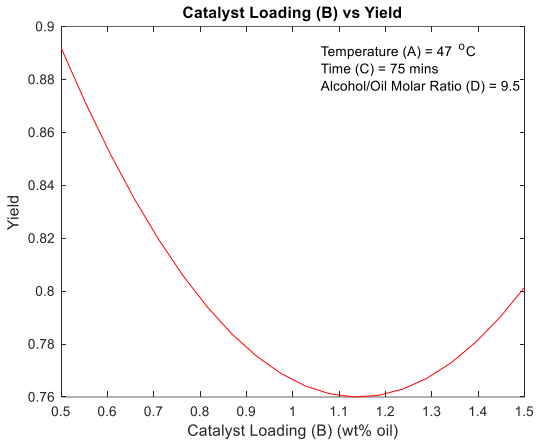

Figure 57 – Effect of Catalyst Loading (B) on Yield

As seen in Table 41, the effect of catalyst loading on yield is significant with an F-Value and P-Value of 26.07 and less than 0.0001, respectively, according to the linear section of the full quadratic model. Additionally, the effect of catalyst loading has a very similar effect to that of reaction temperature, however both result in a negative impact on the yield, therefore the interaction between these two parameters should produce a negative impact on the yield.

Nevertheless, a decreasing trend may be noticed as catalyst loading increases up until 1.15 $wt\%$. This may be attributed to insufficient catalyst in the reaction system which increases the overall mass transfer resistance between the reacting species and catalyst surface. The amount of water added to the reaction system was kept constant at 0.2 $wt\%$ of oil of water which may have led to the partial hydrolysis of FAMEs into free fatty acids, as indicated by Liu et al. (2008). Simply put, the amount of water added was constant (during experiments) whilst the amount of catalyst was varied (in the regression equation) which may have led to an excess amount of water in the reaction system because the catalyst loading was low. Furthermore, due to the low reaction time of 75 $mins$, Todorović et al. (2019) report that mass transfer limitations are more pronounced during the initial reaction period, as such 75 $mins$ may be regarded as the initial reaction period as transesterification reactions generally require reaction times longer than 75 $mins$ for completion.

However, an increase in the yield may be noticed as catalyst loading increases past 1.2 $wt\%$. This may be due to the system favouring higher catalyst loadings for the production of biodiesel, which is an expected result and is in accordance with the works cited above.

7.4.3. The Effect of Time on Yield

The reaction time values are inclusive of 30 $mins$, 75 $mins$ and 120 $mins$. The lower limit of time was selected to allow for the option of low reaction time during optimisation which would result in reduced operating expenses. Furthermore, it is reported by Samuel et al. (2015) that a reaction time of 60 $mins$ is sufficient for the transesterification of Nigerian waste cooking oil. Similar results were noted

by N.i et al. (2018) in the case of transesterification using waste cooking oil and methanol. In their work, a 5 % difference in yield was noted when reaction time increased from 60 $mins$ to 90 $mins$, therefore a reaction time of 120 $mins$ is deemed suitable for complete transesterification.

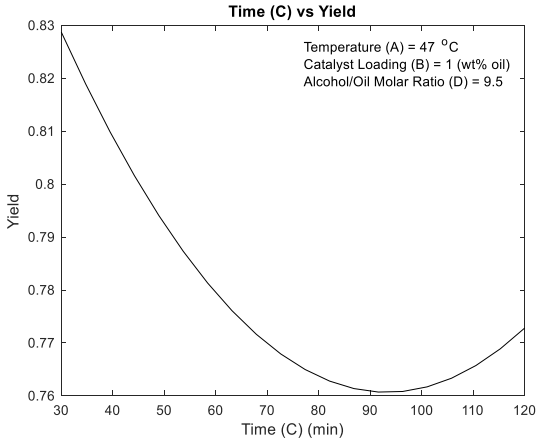

Figure 58 – Effect of Time (C) on Yield

According to the ANOVA presented in Table 41, the effect of time on the response variable is less significant that the other parameters as indicated by the lowest F-Value of 0.78 and highest P-Value of 0.395. This value is above the 95 % confidence interval employed in this work and is deemed statistically insignificant. However, in the work of El-Gendy et al. (2014) in the case of transesterification of sunflower oil and waste sunflower oil using calcium oxide as a catalyst, reaction time proved to be the most significant parameter that had the largest effect on the yield of biodiesel produced.

In their work, a reaction time range of 1 hr to 3 hrs was employed with a catalyst loading range of 6 $wt\%$ to 12 $wt\%$. The higher catalyst loading may have led to an increase in the rate of the reaction which in turn, led to the occurrence of side reaction such as esterification or side reactions which is highly probable considering the high free fatty acid content of the waste cooking sunflower oil. Furthermore, longer reaction times are necessary when higher catalyst loadings are employed because excess catalyst in the reaction system results in an increase in mass transfer resistance because of insufficient coverage of the catalyst surface by methanol (Todorović, et al., 2019).

According to Figure 58, a decrease in yield is observed to occur with an increase in reaction time which signifies that the reverse reaction, saponification or esterification is occurring. Furthermore, the amount of water added to the reaction system may also play a role in the response observed. The water in the system may result in partial hydrolysis of the FAMEs to produce free fatty acids which when combined with methanol undergoes esterification to yield FAME and more water (Son, et al., 2010). Simply put, the amount of water in the system may be increasing with time due to partial hydrolysis and esterification.

However, at a reaction time of 95 $mins$, the yield reaches a minimum and a turning point is observed, after which further increase in time results in an increase in yield. In keeping with the previously developed idea, the amount of water in the system may have also led to this increase in yield. According to Kouzu et al. (2009), water increases the solubility between the reacting species thereby leading to an increase in reaction rate. Furthermore, the time of 95 $mins$ could signify that all of the free fatty acids present in the sunflower oil have been consumed and the transesterification reaction can proceed. In addition, the increasing amount of water in the system would lead to a reduction in yield as stated previously. This reduction in yield is accompanied by the reverse reaction occurring and more reactants are formed. Therefore, the concentration of reactants increases whilst the concentration of products decreases, which leads to the promotion of the forward reaction due to concentration differentials according to *Le Chatelier's* principle.

7.4.4. The Effect of Alcohol/Oil Molar Ratio on Yield

The alcohol/oil molar ratio values employed in this work are 4: 1, 9.5: 1 and 15: 1. The lower limit of alcohol/oil molar ratio was regarded as the minimum ratio that would allow for the transesterification of sunflower oil because theoretically 3 $mols$ of alcohol are required to react with 1 mol of triglyceride to form 3 $mols$ of FAMEs and 1 mol of glycerol. However, the yield is expected to be low when low alcohol/oil molar ratios are employed because an excess of alcohol is required to drive the forward reaction to equilibrium. The upper limit was selected such that excess methanol was not used which would readily dissolve in glycerol, thus limiting the amount of methanol available for transesterification. The yield was found to increase with increasing alcohol/oil molar ratio which was expected and is in accordance with Kostić et al. (2016) in the case of sunflower oil transesterification using calcium oxide and methanol.

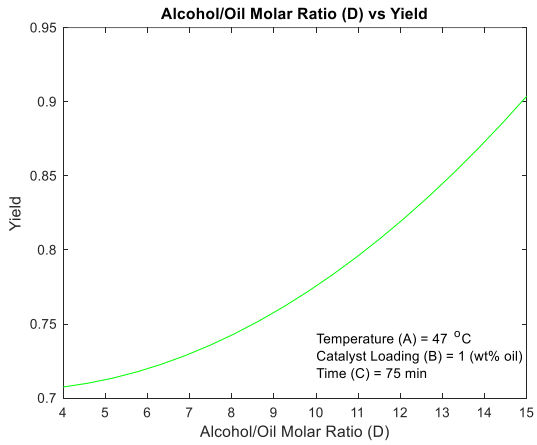

Figure 59 – Effect of Alcohol/Oil Molar Ratio (D) on Yield

According to Table 41, alcohol/oil molar ratio has the largest effect on the yield of biodiesel produced with an F-Value and P-Value of 45.47 and less than 0.0001, respectively. This observation is validated

by the very low P-Value which means that the results did not occur by chance. Unlike the other parameters, changing the value of the alcohol/oil molar ratio will not result in a drastic change in Figure 59 because alcohol/oil is the most significant parameter.

In the work of El-Gendy et al. (2014) in the case of transesterification using sunflower oil and waste cooking sunflower oil, alcohol/oil molar ratio was shown to have the second highest impact on the yield of biodiesel. This may be due to the catalyst loadings of 6 $wt\%$ to 12 $wt\%$ employed as higher catalyst loadings may require higher alcohol/oil molar ratios to promote the forward reaction as well as completely form a layer around the catalyst surface to reduce mass transfer limitation and increase the reaction rate. The highest alcohol/oil molar ratio employed in their work was 9: 1, which may have been insufficient for the amount of catalyst in the reaction vessel.

With reference to Figure 59, it can be seen that for the entire alcohol/oil molar ratio range, the yield ranges from 70 % to 90 %. Therefore, optimisation using higher alcohol/oil molar ratios and lower reaction temperatures may be possible due to their individual effects discussed earlier.

Figure 60 shown below represents the combined main effects of temperature, catalyst loading, reaction time and alcohol/oil molar ratio. The Box-Behnken Design allows for the use of three levels for a specific parameter and these levels are coded -1, 0 and 1. With -1 representing the lower limits of the parameters, 0 representing the mid-points of the data range of the parameters and 1 representing the upper limits of the parameters.

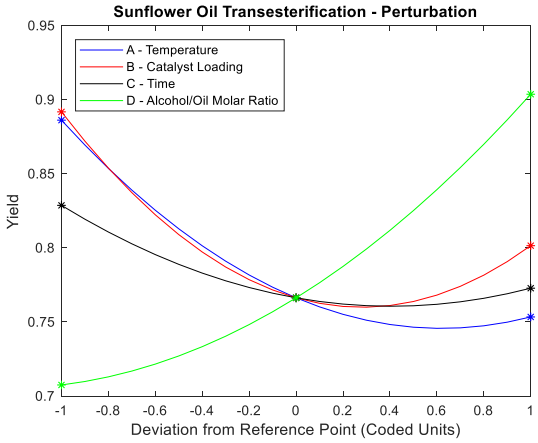

Figure 60 – Sunflower Oil Transesterification – Perturbation

7.5. Response Surface Plots

The regression equation (Eq. (7.3)) stated previously was used to plot the response surfaces and contour plots shown below. As mentioned previously, when trying to determine the relationship between two parameters and the resulting effect of the response variable, the other two factors need to be kept constant. For the purposes of consistency, the constant setting for all variables was kept at the midpoints, i.e. temperature of 47℃, catalyst loading of 1 $wt\%$, time of 75 $mins$ and alcohol/oil molar ratio of 9.5.

7.5.1. The Effect of Temperature & Catalyst Loading on Yield

The 3-D response surface for the interaction between temperature and catalyst loading is shown in Figure 61 and the contour plot between temperature and catalyst loading is shown in Figure 62 whilst the reaction time and alcohol/oil molar ratio were set at 75 $mins$ and 9.5: 1, respectively, in the regression equation. A maximum yield which is close to the theoretical yield of 100 % is predicted by the regression model for a temperature and catalyst loading of 30℃ and 0.5 $wt\%$, respectively. As achieving a yield of 100 % is impractical, the conclusion drawn is due to over-prediction of the response variable by the regression equation. These conditions fell within the experimental range as determined by the Box-Behnken experimental design and a yield of 97 % was achieved. The coefficient of determination (R^2) value of 95.60 % means that 4.4 % of the total variations are not explained by the full quadratic model.

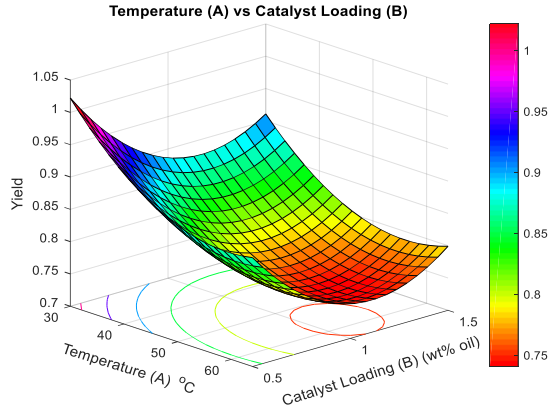

Figure 61 – Sunflower Oil Response Surface (A) vs (B)

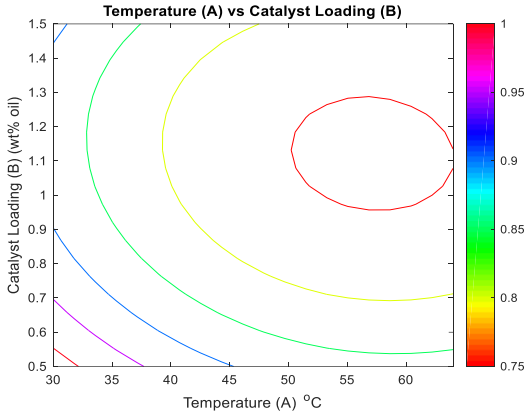

Figure 62 – Sunflower Oil Contour (A) vs (B)

According to Table 41, the interaction between temperature and catalyst loading is not significant due to the low F-Value of 0.35 and high P-Value of 0.568. In fact, the interaction is ranked the least important among the other interactions according to the F-Values and P-Values shown in the ANOVA. This result is to be expected because of the relatively small reaction time of 75 $mins$ employed.

Avramović et al. (2015) showed that for sunflower transesterification in the presence of calcium oxide and ethanol, operation at high temperatures and catalyst loadings results in higher yields produced. In their work, temperature ranges of 65℃ to 75℃ and catalyst loadings in the range of 10 $wt\%$ to 20 $wt\%$

were employed but the key parameter was the reaction time of 420 $mins$ which was employed. This long reaction time may have completely negated any reduction in yield that may have occurred at the start of the reaction and during the initial reaction period.

As highlighted previously, in this work, the alcohol/oil molar ratio proved to have a much larger effect on the yield than temperature, therefore this response surface is not in accordance with literature because it was produced relative to the other parameters that have a much larger influence on the yield at their baselines than temperature. However, temperature variations aside, the effects of catalyst loading can be seen by the response surface. It can be seen that as catalyst loading increases, the yield initially decreases and then increases, which is an effect that is shown at both temperature limits.

This could signify that the system prefers operation at lower catalyst limits, but as catalyst concentration increases, the reaction rate increases which may lead to an increase in the occurrence of side reactions. However, as the catalyst loading passes 1 $wt\%$, there is sufficient catalyst to sustain both the forward reaction and side reaction, but as the forward reaction progresses the amount of triglycerides present in the reaction vessel decrease, thereby decreasing the occurrence of side reactions such as saponification.

7.5.2. The Effect of Temperature & Time on Yield

The 3-D response surface for the interaction between temperature and time is shown in Figure 63 and the contour plot between temperature and time is shown in Figure 64 whilst the catalyst loading and alcohol/oil molar ratio were set at 1 $wt\%$ and 9.5: 1, respectively, in the regression equation. A maximum yield of 92 % was found to occur at a temperature of 30 ℃ and a reaction time of 120 $mins$. Therefore, a trend of low reaction temperature that results in high yields is seen by the previous response surface and Figure 63 which implies that low temperature optimisation is possible. The minimum yield of 74 % is seen to occur at a temperature and time range of 53℃ to 64℃ and 80 $mins$ to 120 $mins$, respectively.

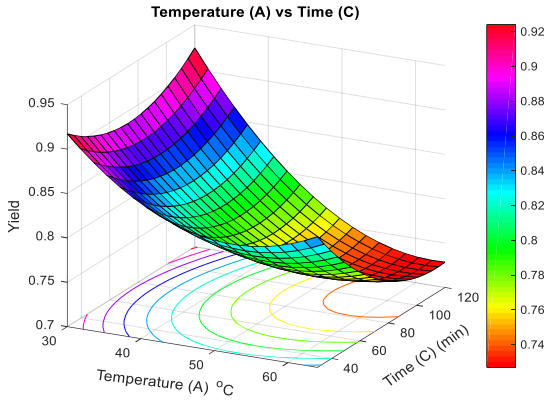

Figure 63 – Sunflower Oil Response Surface (A) vs (C)

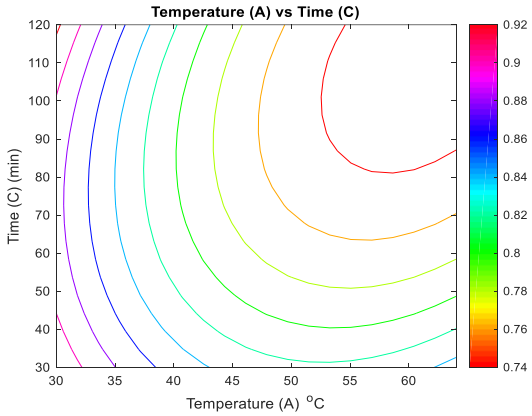

Figure 64 – Sunflower Oil Contour (A) vs (C)

With reference to Table 41, it can be seen that the interaction between temperature and time is statistically insignificant as the F-Value of 3.01 and P-Value of 0.109 are among the lowest of the interaction between parameters. Furthermore, since the P-Value is greater than the 95 % confidence interval used in this work, the interaction between temperature and time is regarded as statistically insignificant.

However, as shown earlier, the removal of insignificant interactions from the full quadratic model has negative effects on the coefficient of determination. As such, if all the insignificant interactions are removed from the ANOVA in Table 41, the resulting R^2 value would be 93.06 % which is a decrease in the models ability to predict the variance of the data. Furthermore, 6.94 % of the variance of the data would not be explained by the regression model.

With reference to Figure 63, an increase in biodiesel yield can be seen at low reaction times and high reaction temperatures which may be attributed to the mass transfer limitations imposed at low reaction temperatures due to high kinematic viscosity. However, as temperature increases, the overall viscosity of the reaction mixture decreases which reduces the mass transfer limitations and results in an increase in yield. However, for a reaction time of 120 $mins$ an increase in yield is expected with an increase in temperature. However, no such increase in yield is observed which may be attributed to an insufficient catalyst loading of 1 $wt\%$ which is necessary to sustain the forward reaction at prolonged reaction times.

7.5.3. The Effect of Temperature & Alcohol/Oil Molar Ratio on Yield

The 3-D response surface for the interaction between temperature and alcohol/oil molar ratio is shown in Figure 65 and the contour plot between temperature and alcohol/oil molar ratio is shown in Figure 66 whilst the catalyst loading and reaction time were set at 1 $wt\%$ and 75 $mins$, respectively, in the regression equation. A maximum yield of approximately 99 % is found to occur at a reaction temperature and alcohol/oil molar ratio of 64℃ and 15: 1, respectively. These conditions were found to be within the Box-Behnken experimental design and a yield of 97 % was achieved experimentally at these conditions. It can therefore be said that the high yield of 99 % is as a result of over-prediction by the regression equation.

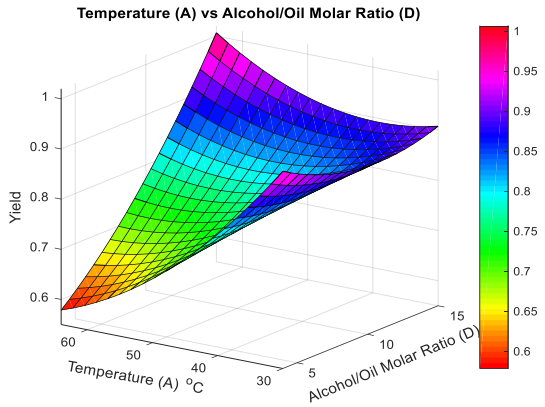

Figure 65 – Sunflower Oil Response Surface (A) vs (D)

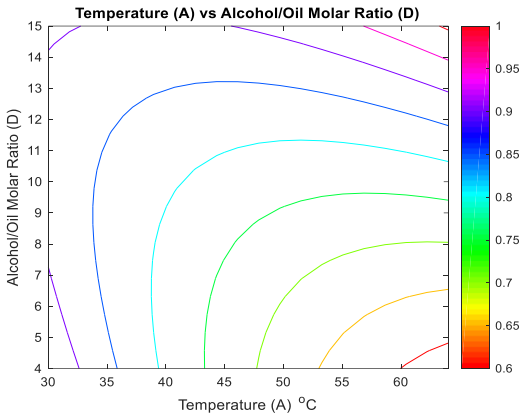

Figure 66 – Sunflower Oil Contour (A) vs (D)

The interaction between temperature and alcohol/oil molar ratio is ranked as the most influential interaction over the yield according to the ANOVA presented in Table 41. The high F-Value of 41.58 and low P-Value of less than 0.0001 indicate that the interaction is statistically significant and the results did not occur by chance as the probability of that happening is negligible. Furthermore, according to the linear model presented in the full quadratic model, temperature and alcohol/oil molar ratio have the largest effect on the yield, therefore, the interaction between the two parameters should have a large effect on the yield.

Similar results to this work were found by Kostić et al. (2016) in the case of sunflower transesterification using methanol and calcium oxide derived from palm kernel biochar. In their work, biodiesel yield was found to increase with an increase in alcohol/oil molar ratio and temperature. The operation temperatures and alcohol/oil molar ratios are similar to this work, however, a catalyst loading of 3 $wt\%$ and reaction time of 4 hrs was used to generate the response surface. They conclude that a rapid increase in yield occurs at higher temperatures and that this increase is higher than that observed by increasing the alcohol/oil molar ratio, as such, similar conclusions are evident in this work, as seen by the response surface in Figure 65.

However, according to the findings of Todorović et al. (2019) who conducted sunflower transesterification in the presence of calcium oxide and methanol using biodiesel as a cosolvent, at lower temperatures and alcohol/oil molar ratios, the yield should be the lowest. This however, is not the case in this work, as the yield is observed to increase when the aforementioned conditions are imposed. This difference may be as a result of the biodiesel cosolvent employed in their work or an increase in water content present at low temperatures and alcohol/oil molar ratios due to esterification or partial hydrolysis of FAMEs to form free fatty acids. As mentioned earlier, the increased water content in the reaction vessel, increases the overall solubility of the catalyst in the reacting species and hence increases the reaction rate (Kouzu, et al., 2009).

7.5.4. The Effect of Catalyst Loading & Time on Yield

The 3-D response surface for the interaction between catalyst loading and time is shown in Figure 67 and the contour plot between catalyst loading and time is shown in Figure 68 whilst the reaction temperature and alcohol/oil molar ratio were set at $47℃$ and $9.5:1$, respectively, in the regression equation. The maximum yield of $92\ \%$ is seen to occur at a catalyst loading of $0.5\ wt\%$ and reaction time of $120\ mins$ whilst the minimum yield of $76\ \%$ occurs at a catalyst loading range of $1\ wt\%$ to $1.4\ wt\%$ and time range of $80\ mins$ to $120\ mins$.

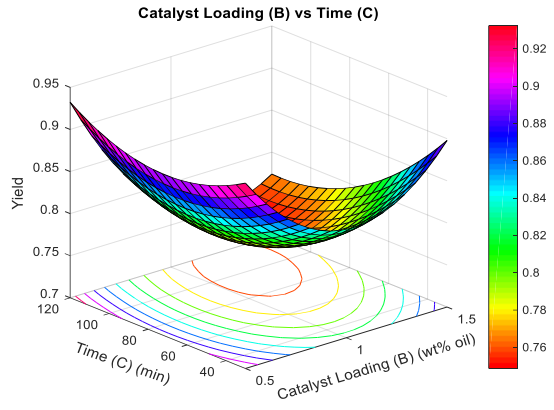

Figure 67 – Sunflower Oil Response Surface (B) vs (C)

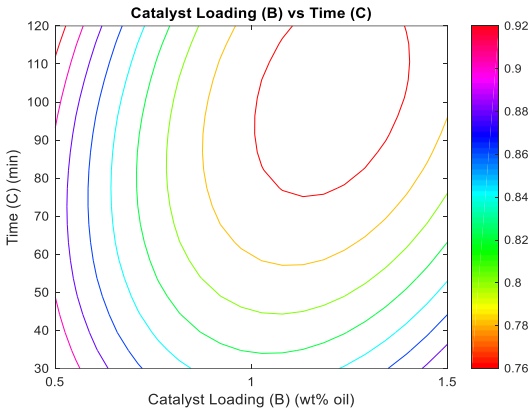

Figure 68 – Sunflower Oil Contour (B) vs (C)

As evident by Table 41, the linear effect of catalyst loading is statistically significant whilst the reaction time is shown to be statistically insignificant in the full quadratic model. However, the result of the two parameters are shown to be statistically insignificant or slightly significant because of the P-Value of 0.083. This value is slightly below the $95\ \%$ confidence interval employed in this work, therefore, it may be regarded as slightly significant. This result is to be expected as the high P-Value of time in the linear model outweighs the low P-Value of catalyst loading in the linear model.

Slightly similar results were reported by El-Gendy et al. (2014) in the case of transesterification of sunflower oil and water cooking sunflower oil in the presence of calcium oxide and methanol. In their work, the yield of biodiesel was found to increase initially with time and then decrease. This effect is seen on the time axis of the response surface, however, a much more pronounced effect was observed in their work with may be attributed to longer reaction times of $3\ hrs$. In addition, their response surface only started at a reaction time of $1\ hr$.

Furthermore, they noted a slight decrease in biodiesel yield with an increase in catalyst loading, however, in this work, a much more noticeable effect may be seen. This may be attributed to insufficient catalyst at lower catalyst loadings which result in side reactions and an increase in water production. However, as catalyst loading increased past $1\ wt\%$ an increase in yield is observed which may be as a result of the increased solubility between the catalyst and reacting species. Therefore, the more

noticeable effect in this work may be as a result of water addition at the start of the reaction, which is a factor that is not explored in their work.

The decrease in yield at the upper catalyst limit with an increase in reaction time may be due to excess catalyst in the reaction system which promotes the occurrence of side reactions, as such the yield of biodiesel produced decreases as the catalyst is consumed by side reactions, i.e. saponification.

7.5.5. The Effect of Catalyst Loading & Alcohol/Oil Molar Ratio on Yield

The 3-D response surface for the interaction between catalyst loading and alcohol/oil molar ratio is shown in Figure 69 and the contour plot between catalyst loading and alcohol/oil molar ratio is shown in Figure 70 whilst the reaction temperature and time were set at 47℃ and 75 $mins$, respectively, in the regression equation. Over-prediction by the regression model may be seen to occur at a catalyst loading of 1.5 $wt\%$ and alcohol/oil molar ratio of 15: 1, resulting in a maximum yield of 100 %. Fortunately, these conditions fell within the Box-Behnken experimental design and a yield of 97 % was achieved experimentally. The minimum yield of 68 % occurs at a catalyst loading of 1.5 $wt\%$ and alcohol/oil molar ratio of 4: 1.

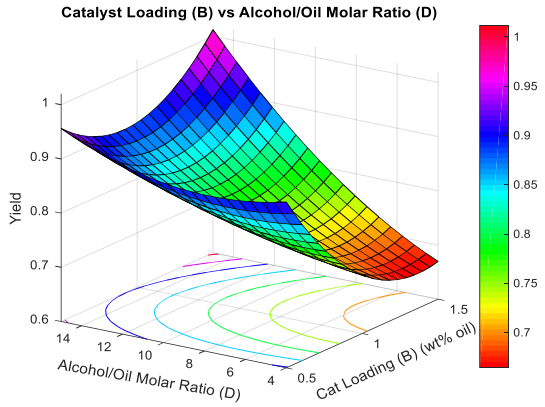

Figure 69 – Sunflower Oil Response Surface (B) vs (D)

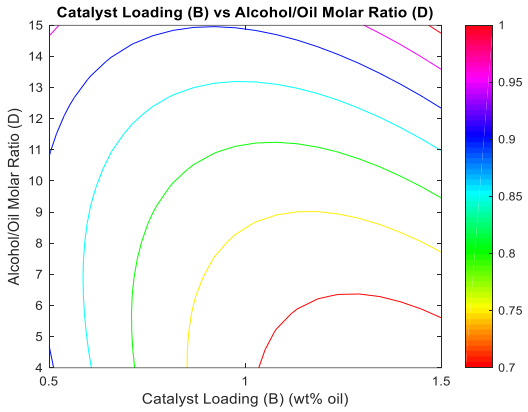

Figure 70 – Sunflower Oil Contour (B) vs (D)

The interaction between catalyst loading and alcohol/oil molar ratio has the second largest effect among the interactions of the parameters according to Table 41. The F-Value and P-Value of 16.57 and 0.002 signify that the interaction is statistically significant, and the results did not occur by chance.

With reference to Figure 69, the yield of biodiesel is found to increase with increasing alcohol/oil molar ratios at both catalyst loading limits. This result is expected as it is in accordance with the ANOVA. In addition, increasing the amount of methanol in the reaction vessel ensures that complete coverage of the catalyst surface is achieved, which is necessary for the formation of the methoxide anions necessary for the transesterification reaction (Esipovich, et al., 2014). Furthermore, it is known that excess methanol is required to drive the forward reaction to equilibrium, as such, higher methanol

concentrations in the reaction vessel will result in higher reaction rates, thus resulting in higher yields produced.

Similar results were reported by El-Gendy et al. (2014) in the case of transesterification of sunflower oil and waste cooking sunflower oil. In their work, a decrease in yield was noticed with an increase in catalyst loading, as seen in this work. This may be due to possible side reactions that result in a reduction in yield. However, they reported that yield increased with increasing alcohol/oil molar ratio up to 7.5: 1, after which a reduction in yield was observed. No such conclusion may be drawn in this work but a moderate change in yield is observed with increasing alcohol/oil molar ratio at the lower catalyst limit.

7.5.6. The Effect of Time & Alcohol/Oil Molar Ratio on Yield

The 3-D response surface for the interaction between reaction time and alcohol/oil molar ratio is shown in Figure 71 and the contour plot between reaction time and alcohol/oil molar ratio is shown in Figure 72 whilst the reaction temperature and catalyst loading were set at 47℃ and 1 $wt\%$, respectively, in the regression equation. The maximum yield of approximately 96 % can be seen to occur at a time of 120 $mins$ and alcohol/oil molar ratio of 15: 1 whereas the minimum yield of 66 % occurs at a time of 120 $mins$ and alcohol/oil molar ratio of 4: 1.

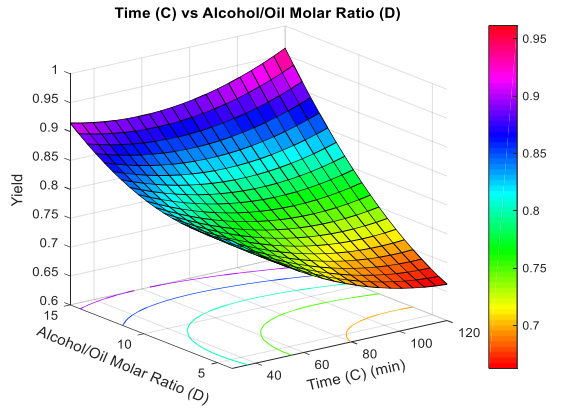

Figure 71 – Sunflower Oil Response Surface (C) vs (D)

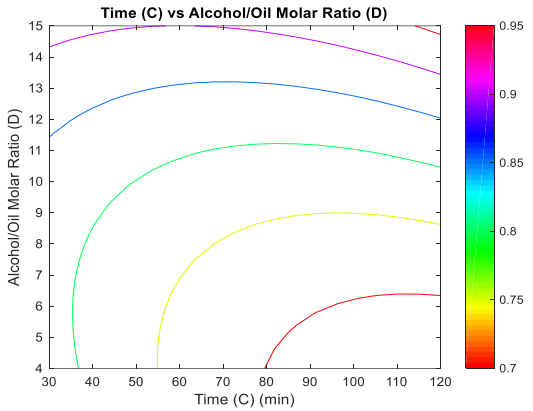

Figure 72 – Sunflower Oil Contour (C) vs (D)

With reference to Table 41, it can be seen that the interaction between time and alcohol/oil molar ratio is statistically significant with a P-Value of 0.014, which is below the 95 % confidence interval employed in this work. Furthermore, the F-Value of 8.17 makes the interaction the third most significant among the interaction between the other parameters. It is important to note that all interactions involving alcohol/oil molar ratio were statistically significant, whereas other interactions were slightly or not significant.

Similar results to this work were noted by Avramovic et al. (2015) in the case of sunflower oil transesterification in the presence of calcium oxide and ethanol. In their work, an increase in yield was observed as alcohol/oil molar ratio increased at lower reaction times. They however, conclude that

higher reaction times of $480\,mins$ resulted in high yields despite the low alcohol/oil molar ratios employed. In this work, the opposite was shown to be true.

Considering the minimum yield of 66 % achieved at the lower limit of alcohol/oil molar ratio and upper limit of time. It may be valid to assume that insufficient methanol in the reaction vessel resulted in a low reaction rate which struggled to drive the forward reaction. This assumption is shown to be appropriate as at the upper limit of time and alcohol/oil molar ratio, a yield of 96 % is achieved. Therefore, it can be said that longer reaction times and higher alcohol/oil molar ratios promote the forward reaction and result in high yields of biodiesel.

The following table illustrates the actual yield and the predicted yield from the regression equation associated with the coded units; A, B, C and D which represent temperature, catalyst loading, time and alcohol/oil molar ratio, respectively.

Table 44 – Box-Behnken Design Matrix for Sunflower Oil Transesterification in Coded Units

Run Order	A	B	C	D	Actual Yield	Predicted Yield
1	47	1.5	30	9.5	0.87	0.90
2	47	1	30	15	0.93	0.91
3	47	1.5	120	9.5	0.80	0.77
4	47	1	75	9.5	0.75	0.77
5	47	0.5	75	4	0.93	0.91
6	64	1	120	9.5	0.73	0.73
7	47	1	75	9.5	0.78	0.77
8	47	1.5	75	15	0.97	1.01
9	30	1	30	9.5	0.93	0.92
10	47	1.5	75	4	0.65	0.67
11	47	1	120	15	0.92	0.96
12	47	0.5	120	9.5	0.95	0.93
13	64	0.5	75	9.5	0.87	0.87
14	64	1	75	15	0.97	1.01
15	47	1	120	4	0.64	0.66
16	47	0.5	30	9.5	0.89	0.92
17	47	1	30	4	0.85	0.82
18	30	0.5	75	9.5	0.97	1.02
19	64	1	75	4	0.55	0.58
20	64	1	30	9.5	0.85	0.85
21	47	0.5	75	15	0.96	0.96
22	30	1	75	15	0.94	0.91
23	64	1.5	75	9.5	0.84	0.80
24	47	1	75	9.5	0.77	0.77
25	30	1	75	4	0.96	0.94
26	30	1	120	9.5	0.93	0.92
27	30	1.5	75	9.5	0.90	0.91

Figure 73 shows the actual yield plotted against the predicted yield obtained from the regression equation. As seen below, a linear regression equation can be fitted to the data set and the regression coefficient of determination (R^2) is 0.9551 which indicates a very strong relationship between the actual experimental data and the predicted data from the regression equation. Therefore, the use of the full quadratic model is valid for optimisation where interpolation between the different parameters can occur to maximise the yield.

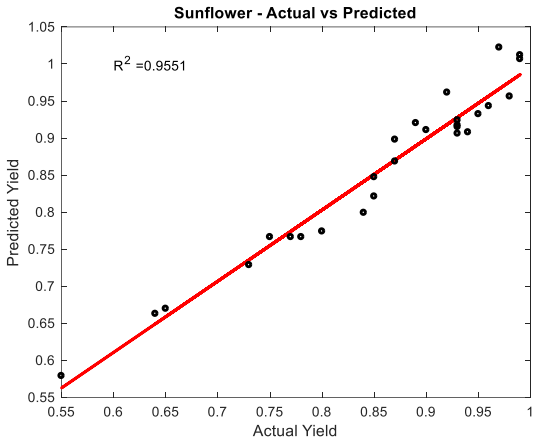

Figure 73 – Sunflower Oil Predicted Yield vs Actual Yield

The optimisation of the sunflower oil transesterification Box-Behnken Design using a full quadratic model was conducted on *Minitab*™ where all the parameters where constrained to their respective domains as to avoid maximisation of the response variable beyond 100 %. However, further restriction was applied within the respective domains to prevent the prediction of yields higher than 100 %. As mentioned earlier, low temperature optimisation was possible and higher reaction times and alcohol/oil molar ratios need to be applied to maximise the yield. Three model validation experiments were conducted and the average yield of 98 % is presented in the table below. The results of the optimisation are deemed suitable as saponification did not occur and the difference between the predicted and actual yields are 1 %.

Table 45 – Optimum Conditions for Sunflower Oil Transesterification – Yield Maximisation

Parameter	Optimum Value
Temperature (A)	35 ℃
Catalyst Loading (B)	1.38 $(wt\%\ oil)$
Time (C)	115 min
Alcohol/Oil Molar Ratio (D)	14.44
Yield (Predicted)	0.99
Yield (Actual)	0.98

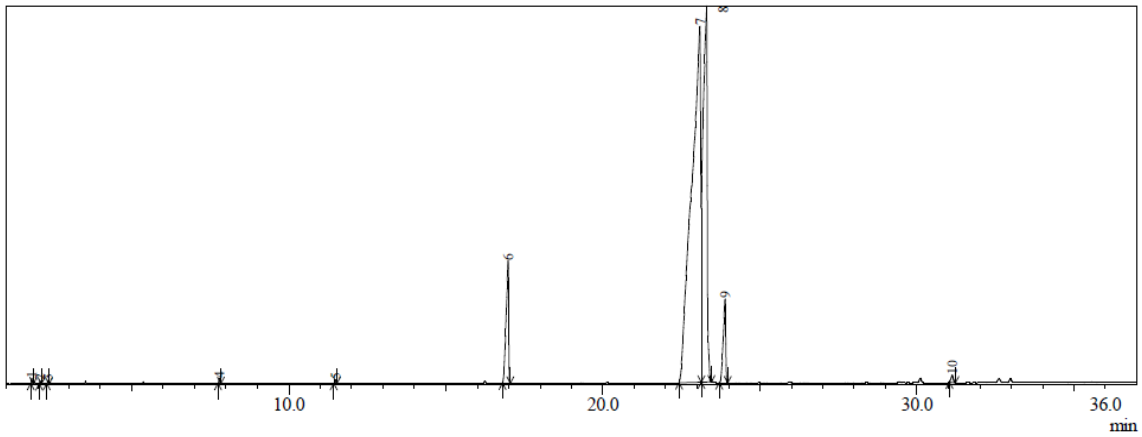

Figure 74 – Sunflower Oil Biodiesel (Optimal Conditions) Chromatogram

Table 46 – Sunflower Oil Biodiesel (Optimal Conditions) GCMS

Peak Number	Retention Time (min)	Area (%)	Name
1	1.816	0.08	Octanoic acid, methyl ester
2	2.082	0.04	Decanoic acid, methyl ester
3	2.325	0.05	Dodecanoic acid, methyl ester
4	7.791	0.1	Methyl tetradecanoate
5	11.481	0.09	Pentadecanoic acid, methyl ester
6	16.983	5.76	Hexadecenoic acid, methyl ester
7	23.091	60.17	9,12-Octadecadienoic acid (Z,Z)-, methyl ester
8	23.302	29.54	9-Octadecenoic acid, methyl ester
9	23.889	3.88	Methyl stearate
10	31.121	0.3	9,12-Octadecadienoic acid, methyl ester

7.6. Summary

Sunflower oil transesterification was conducted in the presence of calcium oxide and methanol with the addition of 0.2 $wt\%$ of oil of water. Box-Behnken response surface methodology was used to design and analyse the experimental results. A total of 27 experiments were conducted inclusive of 3 replicates which are necessary for the determination of the regression coefficients by *Minitab™*. Statistical analysis in the form of an ANOVA revealed that alcohol/oil molar ratio was the most important parameter according to the full quadratic model chosen. Reaction temperature, catalyst loading and time were ranked second, third and fourth, respectively, in terms of influence on yield according to the linear part of the full quadratic model. All interactions with the alcohol/oil molar ratio parameter were shown to be statistically significant. In this section, over-prediction by the regression model was particularly significant which resulted in the restriction of the respective domains of all parameters. The optimisation revealed a maximum predicted yield of 99 % which is in accordance with the factors discussed earlier. The actual yield attained at the optimal conditions was 98 % which proves that the model and optimisation is valid. This yield is in accordance with the literature (Veljković, et al., 2009).

Chapter 8 – Physical Properties & Blending

8.1. Introduction

With the production of biodiesel, comes the need to determine if the product is suitable for use in normal engines without modification. This is achieved via physical property testing which is in accordance with fuel standards. In this work, however, more important physical properties such as density, viscosity, acid value, flash point, pour point and heat of combustion were evaluated. The samples tested are inclusive of the base castor oil, esterified castor oil, castor oil transesterification (Biodiesel), base sunflower oil, sunflower oil transesterification (Biodiesel) and blends of both the biodiesel samples with kerosene, i.e. 10 % biodiesel and 90 % kerosene and lastly 20 % biodiesel and 80 % kerosene.

8.1.1. Density

The density of the samples was determined via the use of a measuring cylinder and a hydrometer. The measuring cylinder was filled with the sample and the hydrometer was spun and dropped into the measuring cylinder. The reading, taken from the top of the sample surface, on the hydrometer corresponds to the specific gravity of the sample. After which, the specific gravity of the sample was converted into the density of the sample by taking a reference density of 1000 kg/m^3 of water.

Table 47 – Density Measurements

Density (kg/m^3)	Test 1	Test 2	Test 3	Average
Castor oil at 15℃	954	955	956	955
Esterified castor oil at 15℃	950	946	948	948
Castor oil biodiesel at 15℃	912	913	914	913
Sunflower oil at 15℃	912	919	916	916
Sunflower oil biodiesel at 15℃	890	895	892	892
Blends with Kerosene				
Castor oil biodiesel 10 %: 90% at 15℃	816	812	817	815
Castor oil biodiesel 20 %: 80% at 15℃	834	832	826	830
Sunflower oil biodiesel 10 %: 90% at 15℃	814	815	809	812
Sunflower oil biodiesel 20 %: 80% at 15℃	813	815	818	815

As seen from the above table, the density of castor oil biodiesel is slightly above the limit of 900 (kg/m^3) as specified by ASTM D941, whereas the densities of the other fuels are within range. The density of the jet fuel samples are within range because the density range for jet fuel is 775 – 840 (kg/m^3) according to ASTM D1655.

8.1.2. Kinematic Viscosity

The absolute or dynamic viscosity of the samples were determined using a viscometer equipped with a jacketed sampler capable of heating the samples to a temperature of 40℃ using a hot water bath with temperature control. A general spindle size of S21 was selected as this gave the most accurate results

with were in accordance with literature. A small sample was loaded into the jacketed vessel and left for a period of $30\ mins$ to reach the required temperature, after which the spindle was lowered into the vessel and turned on at a speed of $60\ rpm$. The absolute or dynamic viscosity in units of centipoise was recorded and the kinematic viscosity of the samples were determined by dividing the absolute or dynamic viscosity by the density of the respective sample.

Table 48 – Kinematic Viscosity Measurements

Kinematic Viscosity (mm^2/s)	Test 1	Test 2	Test 3	Average
Castor oil at 25℃	265	254	262	260
Esterified castor oil at 40℃	90	87	79	85
Castor oil biodiesel at 40℃	10	8.5	9.5	9.3
Sunflower oil at 25℃	35	29	33	32
Sunflower oil biodiesel at 40℃	3.1	2.6	2.8	2.8
Blends with Kerosene				
Castor oil biodiesel 10 %: 90% at 20℃	2	1.6	1.7	1.8
Castor oil biodiesel 20 %: 80% at 20℃	1	1.3	1.3	1.2
Sunflower oil biodiesel 10 %: 90% at 20℃	1.3	1.2	1.2	1.2
Sunflower oil biodiesel 20 %: 80% at 20℃	1.2	1.2	1.2	1.2

As seen from the above table, the kinematic viscosity of castor oil biodiesel is slightly above the limit of $6\ mm^2/s$ as specified by ASTM D445 standards, furthermore, it can be seen that sunflower oil biodiesel is well within the range. The blends of jet fuel are also within the range because the maximum allowed kinematic viscosity is $8\ mm^2/s$ at a temperature of 20℃, as specified by ASTM D1665.

8.1.3. Acid Value

The acid value of the samples were determined by titration against a $0.1\ M$ solution of KOH. A sample mass of $2\ g$ was used for base castor oil because the acid value was expected to be high whereas a sample mass of $20\ g$ was used for sunflower oil because the acid value was expected to be low. Titration solvent in the form of toluene:propan-2-ol:water in a ratio of $100:99:1$ was added in a volume of $100\ ml$ to the conical flask along with approximately 5 drops of phenolphthalein indicator and titrated. Endpoint was reached when the solution turned pale pink with a persistent colour. The volume difference was recorded, and the acid value was calculated according to the formula shown in Appendix A – Sample Calculations.

Table 49 – Acid Value Measurements

Acid Value ($mgKOH/g$)	Test 1	Test 2	Test 3	Average
Castor oil	25.892	22.469	23.248	23.872
Esterified castor oil	0.719	0.714	0.711	0.715
Castor oil biodiesel	0.573	0.532	0.565	0.557
Sunflower oil	0.375	0.224	0.211	0.265
Sunflower oil biodiesel	0.214	0.208	0.212	0.211

Blends with Kerosene				
Castor oil biodiesel 10 %: 90%	0.523	0.553	0.560	0.545
Castor oil biodiesel 20 %: 80%	0.537	0.545	0.572	0.551
Sunflower oil biodiesel 10 %: 90%	0.207	0.213	0.205	0.208
Sunflower oil biodiesel 20 %: 80%	0.209	0.214	0.213	0.212

It can be seen by the table above that castor oil biodiesel is slightly above the limit of $0.5\ mgKOH/g$ as specified by ASTM D974 and sunflower oil biodiesel falls below this limit. In addition, the jet fuel maximum allowed acid value is $0.015\ mgKOH/g$ which means that all of the samples tested are above this limit. Further processing may be required to reduce the acid content of the blended samples.

8.1.4. Flash Point (Closed Cup)

A flash point apparatus was used to determine the flash point of the samples in question. Sufficient fuel was added to the cup and closed. Hot water was added to the apparatus for further heating inside the apparatus. A thermometer was used to record the sample temperature. At 1℃ intervals, the lid was opened and exposed to an ignition source and the lowest temperature was recorded when the fuel vapours flashed above the fuel source.

Table 50 – Flash Point Measurements

Flash Point (℃)	Test 1	Test 2	Test 3	Average
Castor oil	–	–	–	–
Esterified castor oil	–	–	–	–
Castor oil biodiesel	156	161	159	159
Sunflower oil	–	–	–	–
Sunflower oil biodiesel	105	95	97	99
Blends with Kerosene				
Castor oil biodiesel 10 %: 90%	58	63	59	60
Castor oil biodiesel 20 %: 80%	72	65	67	68
Sunflower oil biodiesel 10 %: 90%	55	59	58	57
Sunflower oil biodiesel 20 %: 80%	59	65	63	62

As shown in the table above, both castor oil biodiesel and sunflower oil biodiesel are above the minimum flash point temperature range of 93℃ and below the limit of 170℃ as specified by ASTM D93. However, only the minimum flash point temperature limit is specified according to ASTM D1655 for jet fuel and this limit is 38℃, of which all samples tested are above the minimum limit for jet fuel.

8.1.5. Pour Point

The pour point of the samples were determined by placing a sufficient amount of the sample in a beaker which was surrounded by dry ice. A thermometer was used to record the lowest temperature achieved at which the mixture was fluid enough to be poured.

Table 51 – Pour Point Measurements

Pour Point (℃)	Test 1	Test 2	Test 3	Average
Castor oil	–	–	–	–
Esterified castor oil	–	–	–	–
Castor oil biodiesel	10	8	6	8
Sunflower oil	–	–	–	–
Sunflower oil biodiesel	0	-1	-3	-1
Blends with Kerosene				
Castor oil biodiesel 10 %: 90%	–	–	–	–
Castor oil biodiesel 20 %: 80%	–	–	–	–
Sunflower oil biodiesel 10 %: 90%	–	–	–	–
Sunflower oil biodiesel 20 %: 80%	–	–	–	–

As seen from the table above, the pour point was determined only for castor oil biodiesel and sunflower oil biodiesel as the reported pour point temperature of $-47℃$ for jet fuel, as seen in ASTM D1655, could not be tested due to temperature restrains. However, both castor oil biodiesel and sunflower oil biodiesel are within the range of $-15℃$ to $10℃$ according to ASTM D6751 for pour point temperatures. The castor oil biodiesel has a larger pour point temperature due to higher kinematic viscosity.

8.1.6. Heat of Combustion

The heat of combustion was determined only for jet fuel where the following formula is applicable (Speight, 2002):

$$Heat\ of\ combustion = 12400 - 2100(SG)^2 = btu/lb$$

Table 52 – Heat of Combustion Results

Heat of Combustion (btu/lb)	Test 1	Test 2	Test 3	Average
Blends with Kerosene				
Castor oil biodiesel 10 %: 90% at 15℃	11002	11015	10998	11005
Castor oil biodiesel 20 %: 80% at 15℃	10939	10946	10967	10953
Sunflower oil biodiesel 10 %: 90% at 15℃	11009	11005	11026	11015
Sunflower oil biodiesel 20 %: 80% at 15℃	11012	11005	10995	11005

8.1.7. API Gravity

The API gravity was determined only for jet fuel where the following formula is applicable (Speight, 2002):

$$API\ gravity = \frac{141.5}{SG} - 131.5$$

Table 53 – API Gravity Results

API Gravity	Test 1	Test 2	Test 3	Average
Blends with Kerosene				
Castor oil biodiesel 10 %: 90% at 15℃	42	43	42	42
Castor oil biodiesel 20 %: 80% at 15℃	38	39	40	39
Sunflower oil biodiesel 10 %: 90% at 15℃	42	42	43	43
Sunflower oil biodiesel 20 %: 80% at 15℃	43	42	41	42

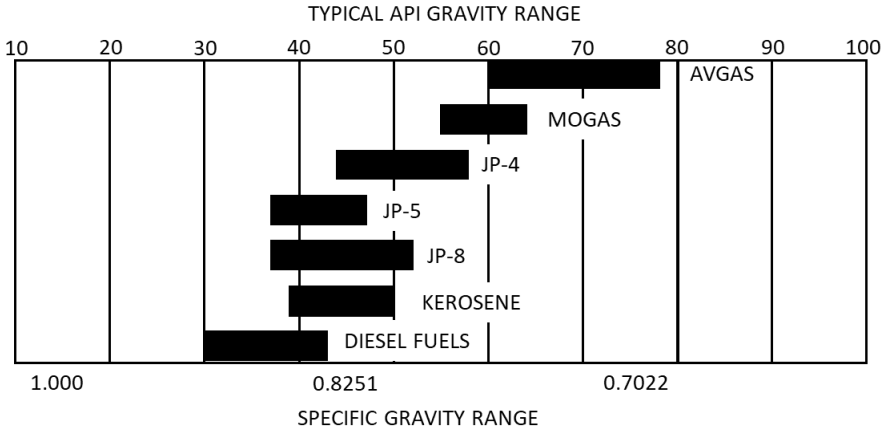

Figure 75 – Density Range for Jet Fuel (Kaiser, et al., 2019)

From the figure above, it can be seen that jet fuels $JP-5$ and $JP-8$ have been synthesized by blending kerosene with biodiesel obtained from castor and sunflower oils. However, with reference to the heat of combustion, jet fuel with a lower heat of combustion has been produced as the recommended heat of combustion by Kaiser et al. (2019) is $17280\ btu/lb$.

8.2. Summary

The important physical properties such as density, kinematic viscosity, acid value, flash point, pour point and in the case of blending only, heat of combustion and API gravity have been determined. The density of castor oil biodiesel was slightly above the limit, whereas the densities of all other fuels tested were within range. A similar observation can be made about kinematic viscosity. However, for acid value, only sunflower oil biodiesel was within the limits whereas the flash point and pour point temperatures for all fuels tested were within the limits. Jet fuel, $JP-5$ and $JP-8$, have been synthesized according to the respective API gravities. The heat of combustion of jet fuel produced was lowered than the recommended limit, however, lower blending ratios of castor oil biodiesel and sunflower oil biodiesel produced higher heats of combustion.

Chapter 9 – Conclusion & Recommendations

Castor oil and sunflower oil were used in the production of bio-fuel, viz, biodiesel and jet fuel via heterogeneous alkaline catalyst. The high acid value of castor oil of approximately 12 % free fatty acids (oleic acid) meant that alkaline catalyst would be ineffective in the conversion of triglycerides present in the oil to biodiesel. Hence, a two-step process comprising acid-catalysed esterification and base-catalysed transesterification employed. The acid catalyst employed was sulphuric acid due to its wide availability and low cost. The heterogenous base catalyst employed was calcium oxide for similar reasons, however, calcium oxide readily deactivates in the presence of atmospheric conditions and calcination at a temperature of 600℃ for 3 hrs was necessary.

The objectives of this study was to investigate and optimise the parameters that effect the yield of biodiesel produced, viz, reaction temperature, catalyst loading, time and alcohol/oil molar ratio. This is achieved in *Minitab*™ where the Box-Behnken response surface methodology was employed to design the 27 experiments necessary to determine a suitable regression model. The type of regression model chosen was the full quadratic model as it resulted in the highest coefficient of determination (R^2) value among the other models tested. Statistical analysis in form of an ANOVA was conducted to evaluate the effects and interaction between the parameters and the response variable. The regression equation was then used to generate the plots showing the individual effects and interactions between two variables and the resulting effect on the response variable.

With reference to the esterification process, the objective was the minimisation of the free fatty acids present in castor oil. The optimisation revealed that a minimal value of 0.72 % was possible, however, a value of 0.715 % was obtained experimentally. A large amount of esterified castor oil was produced at those conditions and used in the transesterification of castor oil. A total of 90 experiments were conducted inclusive of replicates and model validation. With reference to castor oil transesterification, a possible yield of 98.6 % was predicted but a yield of 97.2 % was achieved experimentally. Finally, a maximum yield of 99 % was predicted for sunflower oil transesterification but a yield of 98 % was achieved experimentally. The coefficient of determination for castor oil esterification, castor oil transesterification and sunflower oil transesterification was 99.21 %, 95.83 % and 95.60 %, respectively. In all three cases, however, restriction of the parameter domains was necessary, especially in the case of sunflower oil transesterification, to limit the optimisation from producing conditions that resulted in the free fatty acid content being zero and yields produced over 100 %. Catalyst reusability was investigated independently and found to be significant in the sense that after the reaction, the catalyst was unable to be reused without calcination.

Physical property testing was conducted on the biodiesels produced. In addition, the resulting fuels were mixed with kerosene in 10 % and 20 % ratios to produce jet fuel. The density of biodiesel produced

from castor oil was slightly over the specified limit of 900 kg/m^3, whereas all other densities were within range. Similar conclusions are drawn in the case of kinematic viscosity and acid value. However, in the case of acid value, only biodiesel produced from sunflower oil met the required specifications. Biodiesel produced from castor oil resulted in higher flash and pour point temperatures as compared to that of sunflower oil which may be attributed to the high kinematic viscosity of castor oil, even after esterification.

The objectives of this work were met in the sense that the parameters influencing the yield of biodiesel production were investigated. The resulting process was optimised and there was a strong relationship between the optimisation and experimental values. Finally, physical property testing of the biodiesel and blending of biodiesel with kerosene for the production of jet fuel was conducted. Furthermore, castor oil biodiesel did not meet most of the standards required by ASTM D6751, hence it is not recommended for biodiesel production whereas sunflower oil is suitable for biodiesel production. The heterogeneous nature of calcium oxide made it easy to work with and separate from the reaction mixture by centrifugation. However, further testing and refinement is required in the case of biodiesel produced from castor oil. The main parameters, density and viscosity, of the produced jet fuel were within specification however further testing is required before use in a jet engine. The heat of combustion of jet fuel produced was lowered than the recommended limit, however, lower blending ratios of castor oil biodiesel and sunflower oil biodiesel produced higher heats of combustion. It is therefore a viable assumption that biodiesel produced from sunflower oil may serve as a replacement for petro-diesel in the use of normal diesel engines without modification.

References

Agra, I. & Warnijati, S., 1996. Two steps ethanolysis of castor oil using sulphuric acid as catalyst to produce motor oil. *Renewable energy,* 9(1-4), pp. 1025-1028.

Ambat, I., Srivastava, V. & Sillanpää, M., 2018. Recent advancement in biodiesel production methodologies using various feedstock: A review. *Renewable and Sustainable Energy Reviews,* Volume 90, pp. 356-369.

Anastopoulos, G., Dodos, G., Kalligeros, S. & Zannikos, F., 2013. Methanolysis of sunflower oil and used frying oil using LiNO3/CaO as a solid base catalyst. *International Journal of Ambient Energy,* 34(2), pp. 73-82.

Andreani, L. & Rocha, J., 2012. Use of ionic liquids in biodiesel production: a review. *Brazilian Journal of Chemical Engineering,* 29(1), pp. 1-13.

Anguebes-Franseschi, F. et al., 2016. Optimization of Biodiesel Production from African Crude Palm Oil (Elaeis guineensis Jacq) with High Concentration of Free Fatty Acids by a Two-Step Transesterification Process. *Open Journal of Ecology,* Volume 6, pp. 13-21.

Aransiola, E. et al., 2014. A review of current technology for biodiesel production: State of the art. *Biomass and bioenergy,* Volume 61, pp. 276-297.

ASTM-D974-12, 2012. *Standard Test Method for Acid and Base Number by Color-Indicator Titration,* ASTM International, West Conshohocken: PA.

Atadashi, I., Aroua, M. & Aziz, A., 2010. High quality biodiesel and its diesel engine application: a review. *Renewable and sustainable energy reviews,* 14(7), pp. 1999-2008.

Avramović, J. et al., 2015. Optimization of sunflower oil ethanolysis catalyzed by calcium oxide: RSM versus ANN-GA. *Energy Conversion and Management,* Volume 105, pp. 1149-1156.

Ayetor, G. K., Sunnu, A. & Parbey, J., 2015. Effect of biodiesel production parameters on viscosity and yield of methyl esters: Jatropha curcas, Elaeis guineensis and Cocos nucifera. *Alexandria Engineering Journal,* 54(4), pp. 1285-1290.

Azócar, L. et al., 2007. *Biodiesel production from Rapeseed oil with waste frying oils.* In ISWA World Congress, Amesterdam.

Banani, R., Youssef, S., Bezzarga, M. & Abderrabba, M., 2015. Waste frying oil with high levels of free fatty acids as one of the prominent sources of biodiesel production. *J. Mater. Environ. Sci,* 6(4), pp. 1178-1185.

Barnwal, B. K. & Sharma, M. P., 2005. Prospects of Biodiesel Production from Vegetable Oils in India. *Renewable and sustainable energy reviews,* 9(4), p. 363–378.

Bet-Moushoul, E. et al., 2016. Application of CaO-based/Au nanoparticles as heterogeneous nanocatalysts in biodiesel production. *Fuel,* Volume 164, pp. 119-127.

Bharti, P., Singh, B. & Dey, R., 2019. Process optimization of biodiesel production catalyzed by CaO nanocatalyst using response surface methodology. *Journal of Nanostructure in Chemistry,* pp. 1-12.

Bilgin, A., Durgun, O. & Sahin, Z., 2002. The effects of diesel-ethanol blends on diesel engine performance. *Energy sources,* 24(5), pp. 431-440.

Bojan, S., Chelladurai, S. & Durairaj, S., 2011. Response surface methodology for optimization of biodiesel production from high FFA Jatropha curcas oil. *International journal of green energy,* 8(6), pp. 607-617.

Borah, M. et al., 2019. Transesterification of waste cooking oil for biodiesel production catalyzed by Zn substituted waste egg shell derived CaO nanocatalyst. *Fuel,* Volume 242, pp. 345-354.

Boz, N., Degirmenbasi, N. & Kalyon, D., 2015. Esterification and transesterification of waste cooking oil over Amberlyst 15 and modified Amberlyst 15 catalysts. *Applied Catalysis B: Environmental,* Volume 165, pp. 723-730.

Canakci, M. & Sanli, H., 2008. Biodiesel production from various feedstocks and their effects on the fuel properties. *Journal of industrial microbiology & biotechnology,* 35(5), pp. 431-441.

Canakci, M. & Sanli, H., 2008. Biodiesel production from various feedstocks and their effects on the fuel properties. *ournal of industrial microbiology & biotechnology,* 35(5), pp. 431-441.

Cao, P., Tremblay, A. & Dubé, M., 2009. Kinetics of canola oil transesterification in a membrane reactor. *Industrial & Engineering Chemistry Research,* 48(5), pp. 2533-2541.

Chaudhary, P., Verma, A., Kumar, S. & Gupta, V., 2018. Experimental design and optimization of castor oil transesterification process by response surface methodology. *Biofules,* 9(1), pp. 7-17.

Cheng, J. et al., 2013. Using wet microalgae for direct biodiesel production via microwave irradiation. *Bioresource technology,* Volume 131, pp. 531-535.

Chen, K., Lin, Y., Hsu, K. & Wang, H., 2012. Improving biodiesel yields from waste cooking oil by using sodium methoxide and a microwave heating system. *Energy,* 38(1), pp. 151-156.

Chen, K., Lin, Y., Hsu, K. & Wang, H., 2012. Improving biodiesel yields from waste cooking oil by using sodium methoxide and a microwave heating system. *Energy,* 38(1), pp. 151-156.

Chen, Y., Chang, C., Chang, M. & Chang, C., 2011. Biodiesel production from Tung oil and blended oil via ultrasonic transesterification process. *Journal of the Taiwan Institute of Chemical Engineers,* 42(4), pp. 640-644.

Chiaramonti, D. et al., 2003. Development of emulsions from biomass pyrolysis liquid and diesel and their use in engines—Part 1: emulsion production. *Biomass and bioenergy,* 25(1), pp. 58-99.

Choi, C. & Reitz, R., 1999. A numerical analysis of the emissions characteristics of biodiesel blended fuels. *Journal of engineering for gas turbines and power,* 121(1), pp. 31-37.

Choi, C. & Reitz, R., 1999. A numerical analysis of the emissions characteristics of biodiesel blended fuels. *Journal of engineering for gas turbines and power,* 121(1), pp. 31-37.

Chumuang, N. & Punsuvon, V., 2017. Response surface methodology for biodiesel production using calcium methoxide catalyst assisted with tetrahydrofuran as cosolvent. *Journal of Chemistry.*

Colosi, L., Resurreccion, E. & Zhang, Y., 2015. Assessing the energy and environmental performance of algae-mediated tertiary treatment of estrogenic compounds. *Environmental Science: Processes & Impacts,* 17(2), pp. 421-428.

da Silva Castro, L. et al., 2019. Biodiesel production from cotton oil using heterogeneous CaO catalysts from eggshells prepared at different calcination temperatures. *Green Processing and Synthesis,* 8(1), pp. 235-244.

Deb, A. et al., 2017. Prospect of castor oil biodiesel in Bangladesh: Process development and optimization study. *International journal of green energy,* 14(12), pp. 1063-1072.

Demirbas, A., 2008. Biodiesel from triglycerides via transesterification. *Biodiesel: A Realistic Fuel Alternative for Diesel Engines,* pp. 121-140.

Deshpande, D., Urunkar, Y. & Thakare, P., 2012. Production of Biodiesel from Castor Oil using acid and Base catalysts. *Research Journal of Chemical Sciences,* 2(8), pp. 51-56.

Dhawane, S., Karmakar, B., Ghosh, S. & Halder, G., 2018. Parametric optimisation of biodiesel synthesis from waste cooking oil via Taguchi approach. *Journal of environmental chemical engineering,* 6(4), pp. 3971-3980.

Dorado, M., Ballesteros, E., Mittelbach, M. & López, F., 2004. Kinetic parameters affecting the alkali-catalyzed transesterification process of used olive oil. *Energy & Fuels,* 18(5), pp. 1457-1462.

El Sherbiny, S., Refaat, A. & El Sheltawy, S., 2010. Production of biodiesel using the microwave technique. *Journal of Advanced Research,* 1(4), pp. 309-314.

El Sherbiny, S., Refaat, A. & El Sheltawy, S., 2010. Production of biodiesel using the microwave technique. *Journal of Advanced Research,* 1(4), pp. 309-314.

El-Gendy, N., Abu Amr, S. & Aziz, H., 2014. The optimization of biodiesel production from waste frying sunflower oil using a heterogeneous catalyst. *Energy Sources, Part A: Recovery, Utilization, and Environmental Effects,* 36(15), pp. 1615-1625.

Endalew, A., Kiros, Y. & Zanzi, R., 2011. Heterogeneous catalysis for biodiesel production from Jatropha curcas oil (JCO). *Energy,* 36(5), pp. 2693-2700.

Esipovich, A., Danov, S., Belousov, A. & Rogozhin, A., 2014. Improving methods of CaO transesterification activity. *Journal of Molecular Catalysis A: Chemical,* Volume 395, pp. 225-233.

Fan, X., Chen, F. & Wang, X., 2010. Ultrasound-assisted synthesis of biodiesel from crude cottonseed oil using response surface methodology. *Journal of oleo science,* 59(5), pp. 235-241.

Ferdous, K. et al., 2013. Preparation of Biodiesel from higher FFA containing castor oil. *Ijser*, Volume 4, pp. 401-406.

Fereidooni, L., Hosseini, S. N. & Mehrpooya, M., 2017. *Bentonite, as a natural zeolite enhanced biodiesel production through trans-esterification of waste oil.* The first international congress of specialized research in science, engineering and university technology.

Ferreira, S. et al., 2007. Box-Behnken design: an alternative for the optimization of analytical methods. *Analytica chimica acta*, 597(2), pp. 179-186.

Feyzi, M. & Shahbazi, E., 2015. Catalytic performance and characterization of Cs–Ca/SiO2–TiO2 nanocatalysts for biodiesel production. *Journal of Molecular Catalysis A: Chemical*, Volume 404, pp. 131-138.

Freedman, B. & Pryde, E., 1982. *Fatty esters from vegetable oils for use as a diesel fuel (No. CONF-820860-).* Dept. of Agriculture, Peoria, IL.

Gabriel, R. et al., 2018. Empirical modeling of different viscosity and density behavior of biodiesel from chichá (Sterculiastriata) with diesel versus temperature variation. *Journal of King Saud University-Science.*

Gebremariam, S. & Marchetti, J., 2017. Biodiesel production technologies. *AIMS Energy*, 5(3), pp. 425-457.

Gebremariam, S. N. & Marchetti, J. M., 2017. Biodiesel production technologies: review. *AIMS Energy*, 5(3), pp. 425-457.

Ghazali, W., Mamat, R., Masjuki, H. & Najafi, G., 2015. Effects of biodiesel from different feedstocks on engine performance and emissions: A review. *Renewable and Sustainable Energy Reviews*, Volume 51, pp. 585-602.

Giakoumis, E. & Sarakatsanis, C., 2019. A Comparative Assessment of Biodiesel Cetane Number Predictive Correlations Based on Fatty Acid Composition. *Energies*, 12(3), p. 422.

Goering, C. et al., 1982. Fuel properties of eleven vegetable oils. *Transactions of the ASAE*, 25(6), pp. 1472-1477.

Gole, V. & Gogate, P., 2013. Intensification of synthesis of biodiesel from non-edible oil using sequential combination of microwave and ultrasound. *Fuel Processing Technology*, Volume 106, pp. 62-69.

Goyal, P., Sharma, M. & Jain, S., 2012. Optimization of esterification and transesterification of high FFA Jatropha curcas oil using response surface methodology. *Journal of Petroleum Science Research*, 1(3), pp. 36-43.

Granados, M. et al., 2007. Biodiesel from sunflower oil by using activated calcium oxide. *Applied Catalysis B: Environmental, 73(3-4), pp.317-326.*, 73(3-4), pp. 317-326.

Gryglewicz, S., 1999. Rapeseed oil methyl esters preparation using heterogeneous catalysts. *Bioresource Technology,* 70(3), pp. 249-253.

Guo, W. et al., 2014. *Ionic liquids-catalyzed transesterification of soybean oil under ultrasound irradiation.* In 2013 International Conference on Materials for Renewable Energy and Environment (Vol. 1, pp. 295-297), IEEE.

Gurunathan, B. & Ravi, A., 2015. Biodiesel production from waste cooking oil using copper doped zinc oxide nanocomposite as heterogeneous catalyst. *Bioresource technology,* Volume 188, pp. 124-127.

Halder, S., Dhawane, S., Kumar, T. & Halder, G., 2015. Acid-catalyzed esterification of castor (Ricinus communis) oil: optimization through a central composite design approach. *Biofuels,* 6(3-4), pp. 191-201.

Harwood, H., 1984. Oleochemicals as a fuel: Mechanical and economic feasibility. *Journal of the American Oil Chemists' Society,* 61(2), pp. 315-324.

Hashmi, S. et al., 2016. Biodiesel production by using CaO-Al2O3 Nano catalyst. *International Journal of Engineering Research & Science,* 2(3), pp. 43-49.

Hayyan, A. et al., 2011. Reduction of high content of free fatty acid in sludge palm oil via acid catalyst for biodiesel production. *Fuel Processing* , 92(5), pp. 920-924.

Hingu, S., Gogate, P. & Rathod, V., 2010. Synthesis of biodiesel from waste cooking oil using sonochemical reactors. *Ultrasonics sonochemistry,* 17(5), pp. 827-832.

Hoekman, S. et al., 2012. Review of biodiesel composition, properties, and specifications. *Renewable and sustainable energy reviews,* 16(1), pp. 143-169.

Hossain, A. & Boyce, A., 2009. Biodiesel production from waste sunflower cooking oil as an environmental recycling process and renewable energy. *Bulgarian Journal of Agricultural Science,* 15(4), pp. 312-317.

Huaping, Z. et al., 2006. Preparation of biodiesel catalyzed by solid super base of calcium oxide and its refining process. *Chinese Journal of Catalysis,* 27(5), pp. 391-396.

Hu, S., Guan, Y., Wang, Y. & Han, H., 2011. Nano-magnetic catalyst KF/CaO–Fe3O4 for biodiesel production. *Applied Energy,* 88(8), pp. 2685-2690.

Istadi, I., Prasetyo, S. & Nugroho, T., 2015. Characterization of K2O/CaO-ZnO catalyst for transesterification of soybean oil to biodiesel. *Procedia Environmental Sciences,* Volume 23, pp. 394-399.

Jain, S. & Sharma, M., 2010. Prospects of biodiesel from Jatropha in India: a review. *Renewable and Sustainable Energy Reviews,* 14(2), pp. 763-771.

Ji, J. et al., 2006. Preparation of biodiesel with the help of ultrasonic and hydrodynamic cavitation. *Ultrasonics,* Volume 44, pp. e411-e414.

Kaiser, M., de Klerk, A., Gary, J. & Handwerk, G., 2019. *Petroleum Refining: Technology, Economics, and Markets.* s.l.:CRC Press.

Kapilan, N. & Baykov, B., 2014. A Review On New Methods Used For The Production Of Biodiesel. *Petroleum & Coal,* 56(1), pp. 62-73.

Karmakar, A., Karmakar, S. & Mukherjee, S., 2010. Properties of various plants and animals feedstocks for biodiesel production. *Bioresource technology,* 101(19), pp. 7201-7210.

Karmakar, B., Dhawane, S. & Halder, G., 2018. Optimization of biodiesel production from castor oil by Taguchi design. *Journal of Environmental Chemical Engineering,* 6(2), pp. 2684-2695.

Kaur, M. & Ali, A., 2011. Lithium ion impregnated calcium oxide as nano catalyst for the biodiesel production from karanja and jatropha oils. *Renewable Energy,* 36(11), pp. 2866-2871.

Kaur, N. & Ali, A., 2013. Lithium ions-supported magnesium oxide as nano-sized solid catalyst for biodiesel preparation from mutton fat. *Energy Sources, Part A: Recovery, Utilization, and Environmental Effects,* 35(2), pp. 184-192.

Khan, M., Yusup, S. & Ahmad, M., 2010. Acid esterification of a high free fatty acid crude palm oil and crude rubber seed oil blend: Optimization and parametric analysis. *Biomass and bioenergy ,* 34(12), pp. 1751-1756.

Khemthong, P. L. C. N. W. C. P. T. P. V.-E. N. & Faungnawakij, K., 2012. Industrial eggshell wastes as the heterogeneous catalysts for microwave-assisted biodiesel production. *Catalysis Today,* 190(1), p. 11.

Khemthong, P. et al., 2012. Industrial eggshell wastes as the heterogeneous catalysts for microwave-assisted biodiesel production. *Catalysis Today,* 190(1), pp. 112-116.

Kiss, F. et al., 2014. Supercritical transesterification: impact of different types of alcohol on biodiesel yield and LCA results. *The Journal of Supercritical Fluids,* Volume 86, pp. 23-32.

Kostić, M. et al., 2016. Optimization and kinetics of sunflower oil methanolysis catalyzed by calcium oxide-based catalyst derived from palm kernel shell biochar. *Fuel,* Volume 163, pp. 304-313.

Kouzu, M., Yamanaka, S., Hidaka, J. & Tsunomori, M., 2009. Heterogeneous catalysis of calcium oxide used for transesterification of soybean oil with refluxing methanol. *Applied Catalysis A: General,* 355(1-2), pp. 94-99.

Kumar, D., Kumar, G. & Singh, C., 2010. Fast, easy ethanolysis of coconut oil for biodiesel production assisted by ultrasonication. *Ultrasonics Sonochemistry,* 17(3), pp. 555-559.

Kumar, G., Kumar, D., Johari, R. & Singh, C., 2011. Enzymatic transesterification of Jatropha curcas oil assisted by ultrasonication. *Ultrasonics sonochemistry,* 18(5), pp. 923-927.

Kumar, R., Kumar, G. & Chandrashekar, N., 2011. Microwave assisted alkali-catalyzed transesterification of Pongamia pinnata seed oil for biodiesel production. *Bioresource technology*, 102(11), pp. 6617-6620.

Kundu, A., Mukherjee, A., Halder, G. & Datta, D., 2016. A Kinetic Study on Acid Catalyzed Esterification of Free Fatty Acids in Ricinus Communis Oil for the Production of Biodiesel. *Int. J. Res. Eng. Technol,* Volume 5, pp. 31-44.

Kusdiana, D. & Saka, S., 2004. Effects of water on biodiesel fuel production by supercritical methanol treatment. *Bioresource technology,* 91(3), p. 289–295.

Lamba, N., Gupta, R., Modak, J. & Madras, G., 2019. ZnO catalyzed transesterification of Madhuca indica oil in supercritical methanol. *Fuel,* Volume 242, pp. 323-333.

Lee, S., Tanaka, D., Kusaka, J. & Daisho, Y., 2002. Effects of diesel fuel characteristics on spray and combustion in a diesel engine. *JSAE review,* 23(4), pp. 407-414.

Lertsathapornsuk, V., Pairintra, R., Aryusuk, K. & Krisnangkura, K., 2008. Microwave assisted in continuous biodiesel production from waste frying palm oil and its performance in a 100 kW diesel generator. *Fuel Processing Technology,* 89(12), pp. 1330-1336.

Lertsathapornsuk, V., Pairintra, R., Aryusuk, K. & Krisnangkura, K., 2008. Microwave assisted in continuous biodiesel production from waste frying palm oil and its performance in a 100 kW diesel generator. *Fuel Processing Technology,* 89(12), pp. 1330-1336.

Leung, D. & Guo, Y., 2006. Transesterification of neat and used frying oil: optimization for biodiesel production. *Fuel processing technology,* 87(10), pp. 883-890.

Leung, D. & Guo, Y., 2006. Transesterification of neat and used frying oil: optimization for biodiesel production. *Fuel processing technology,* 87(10), pp. 883-890.

Leung, D., Wu, X. & Leung, M., 2010. A review on biodiesel production using catalyzed transesterification. *Applied energy,* 87(4), pp. 1083-1095.

Lin, L., Liu, K., Wang, R. & Yu, M., 2017. Acid ionic liquid [HMIM]HSO4 as catalyst for the production of biodiesel from microalgae. *Petroleum and Coal,* 59(6), pp. 877-883.

Liu, H., Su, L., Shao, Y. & Zou, L., 2012. Biodiesel production catalyzed by cinder supported CaO/KF particle catalyst. *Fuel,* Volume 97, pp. 651-657.

Liu, X. et al., 2008. Transesterification of soybean oil to biodiesel using CaO as a solid base catalyst. *Fuel,* 87(2), pp. 216-221.

Li, Y. & Khanal, S., 2016. *Bioenergy: principles and applications.* s.l.:John Wiley & Sons.

Lukić, I. et al., 2013. Kinetics of sunflower and used vegetable oil methanolysis catalyzed by CaO· ZnO. *Fuel,* Volume 133, pp. 367-378.

Maawa, W., Rizalman, M., Yusri, I. & Febrina, R., 2019. *Effect of Emulsified Palm Oil Biodiesel-Diesel Blends to the Combustion Characteristics of Compression Ignition Engine.* In IOP Conference Series: Materials Science and Engineering (Vol. 469, No. 1, p. 012080), IOP Publishing.

Ma, F. & Hanna, M., 1999. Biodiesel production: a review. *Bioresource technology*, 70(1), pp. 1-15.
Mahdavi, M., Abedini, E. & Hosein Darabi, A., 2015. Biodiesel synthesis from oleic acid by nano-catalyst (ZrO2/Al2O3) under high voltage conditions. *RSC Advances*, 5(68), pp. 55027-55032.

Malani, R. et al., 2019. Ultrasound–assisted biodiesel production using heterogeneous base catalyst and mixed non–edible oils.. *Ultrasonics sonochemistry*, Volume 52, pp. 232-243..

Malpani, M., Varma, A. & Mondal, P., 2016. Production of bio-oil from algal biomass and its upgradation to biodiesel using CaO-based heterogeneous catalysts. *International journal of green energy*, 13(10), pp. 969-976.

Marinković, D. et al., 2016. Calcium oxide as a promising heterogeneous catalyst for biodiesel production: current state and perspectives. *Renewable and Sustainable Energy Reviews*, Volume 56, pp. 1387-1408.

Marulanda, V., 2012. Biodiesel production by supercritical methanol transesterification: process simulation and potential environmental impact assessment. *Journal of Cleaner Production*, Volume 33, pp. 109-116.

Marwaha, A., Dhir, A., Mahla, S. & Mohapatra, S., 2018. An overview of solid base heterogeneous catalysts for biodiesel production. *Catalysis Reviews*, 60(4), pp. 594-628.

Miao, X., Li, R. & Yao, H., 2009. Effective acid-catalyzed transesterification for biodiesel production. *Energy Conversion and Management*, 50(10), pp. 2680-2684.

Miladinović, M. et al., 2014. A kinetic study of quicklime-catalyzed sunflower oil methanolysis. *Chemical Engineering Research and Design*, 92(9), pp. 1740-1752.

Muhammad, C. et al., 2019. Assessment of Low Temperature Refining Process of Castor Seed Oil for Biodiesel Production. *American Journal of Chemical and Biochemical Engineering*, 3(1), pp. 1-6.

Muhammad, C. et al., 2019. Assessment of Low Temperature Refining Process of Castor Seed Oil for Biodiesel Production. *American Journal of Chemical and Biochemical Engineering*, 3(1), pp. 1-6.

Mujeeb, M., Vedamurthy, A. & Shivasharana, C., 2016. Current strategies and prospects of biodiesel production: A review. *Applied Scientific Research*, 7(1), pp. 120-133.

N.i, B. et al., 2018. Application of ANNs, ANFIS and RSM to estimating and optimizing the parameters that affect the yield and cost of biodiesel production. *Engineering Applications of Computational Fluid Mechanics*, 12(1), pp. 611-624.

Najafi, B. et al., 2018. Application of ANNs, ANFIS and RSM to estimating and optimizing the parameters that affect the yield and cost of biodiesel production. *Engineering Applications of Computational Fluid Mechanics*, 12(1), pp. 611-624.

Nayak, S., Bhasin, C. & Nayak, M., 2019. A review on microwave-assisted transesterification processes using various catalytic and non-catalytic systems. *Renewable Energy*.

Niehaus, R., Goering, C., Savage, L. & Sorenson, S., 1986. Cracked soybean oil as a fuel for a diesel engine. *Transactions of the ASAE*, 29(3), pp. 683-689.

Okitsu, K. et al., 2010. Ultrasound-assisted production of biodiesel fuel from vegetable oils in a small scale circulation process. *Bioresource Technology*, 101(2), pp. 639-645.

Omari, A., Mgani, Q. & Mubofu, E., 2015. Fatty acid profile and physico-chemical parameters of castor oils in Tanzania. *Green and Sustainable Chemistry*, 5(4), pp. 154-163.

Pairiawi, W., 2010. Biodiesel production from Jatropha curcas: A review. *Sci Res Essays 5: 1796–1808.* Parawira, W., 2010. Biodiesel production from Jatropha curcas: A review. *Scientific Research and Essays*, 5(14), pp. 1796-1808.

Parawira, W., 2010. Biodiesel production from Jatropha curcas: A review. *Scientific Research and Essays*, 5(14), pp. 1796-1808.

Park, J., Wang, Z., Kim, D. & Lee, J., 2010. Effects of water on the esterification of free fatty acids by acid catalysts. *Renewable Energy*, 35(3), pp. 614-618.

Pioch, D. et al., 1993. Synthesis of biofuels by catalytic cracking of vegetable oils of tropical origin. *Oilseeds*, 48(6), pp. 289-292.

Plaza, M., Herrero, M., Cifuentes, A. & Ibanez, E., 2009. Innovative natural functional ingredients from microalgae. *Journal of agricultural and food chemistry*, 57(16), pp. 7159-7170.

Pradhan, S., Madankar, C., Mohanty, P. & Naik, S., 2012. Optimization of reactive extraction of castor seed to produce biodiesel using response surface methodology. *Fuel*, Volume 97, pp. 848-855.

Pratas, M. et al., 2011. Biodiesel density: experimental measurements and prediction models. *Energy & Fuels*, 25(5), pp. 2333-2340.

Qiu, F. et al., 2011. Heterogeneous solid base nanocatalyst: preparation, characterization and application in biodiesel production. *Bioresource technology*, 102(5), pp. 4150-4156.

Ranganathan, S., Narasimhan, S. & Muthukumar, K., 2008. An overview of enzymatic production of biodiesel. *Bioresource technology*, 99(10), pp. 3975-3981.

Ranganathan, S., Narasimhan, S. & Muthukumar, K., 2008. An overview of enzymatic production of biodiesel. *Bioresource Technol*, Volume 99, p. 3975– 3981.

Razavi, R. et al., 2019. An insight into the estimation of fatty acid methyl ester based biodiesel properties using a LSSVM model. *Fuel*, Volume 243, pp. 133-141.

Reddy, P., 2015. A critical review of ionic liquids for the pretreatment of lignocellulosic biomass. *South African Journal of Science,* Volume 111.

Refaat, A., 2011. Biodiesel production using solid metal oxide catalysts. *International Journal of Environmental Science & Technology,* 8(1), pp. 203-221.

Roman, F. et al., 2019. Optimization and kinetic study of biodiesel production through esterification of oleic acid applying ionic liquids as catalysts. *Fuel,* Volume 239, pp. 1231-1239.

Ruhul, A. et al., 2015. State of the art of biodiesel production processes: a review of the heterogeneous catalyst. *RSC Advances,* 5(122), pp. 101023-101044.

Salimi, Z. & Hosseini, S., 2019. Study and optimization of conditions of biodiesel production from edible oils using ZnO/BiFeO3 nano magnetic catalyst. *Fuel,* Volume 239, pp. 1204-1212.

Samuel, O., Amosun, S. & Boye, T., 2015. Optimal transesterification duration for biodiesel produced from Nigerian waste frying oil. *Br. J. Renewable Energy,* Volume 1, pp. 16-19.

Sanli, H. & Canakci, M., 2008. Effects of different alcohol and catalyst usage on biodiesel production from different vegetable oils. *Energy & Fuels,* 22(4), pp. 2713-2719.

Saxena, V., Sharma, S. & Pandey, L., 2019. Fe (III) doped ZnO nano-assembly as a potential heterogeneous nano-catalyst for the production of biodiesel. *Material Letters,* Volume 237, pp. 232-235.

Schwab, A., Bagby, M. & Freedman, B., 1987. Preparation and properties of diesel fuels from vegetable oils. *Fuel,* 66(10), pp. 1372-1378.

Schwab, A. et al., 1988. Diesel fuel from thermal decomposition of soybean oil. *Journal of the American Oil Chemists' Society,* 65(11), pp. 1781-1786.

Seffati, K., Honarvar, B., Esmaeili, H. & Esfandiari, N., 2019. Enhanced biodiesel production from chicken fat using CaO/CuFe2O4 nanocatalyst and its combination with diesel to improve fuel properties. *Fuel,* Volume 235, pp. 1238-1244.

Shahid, E. & Jamal, Y., 2011. Production of biodiesel: a technical review. *Renewable and Sustainable Energy Reviews,* 15(9), pp. 4732-4745.

Sheehan, J., Dunahay, T., Benemann, J. & Roessler, P., 1998. *Look back at the US department of energy's aquatic species program: biodiesel from algae,* Golden, CO.(US): National Renewable Energy Lab.

Sheet, E., 2018. Effect of preheating waste cooking oil on biodiesel production and properties. *Energy Sources, Part A: Recovery, Utilization, and Environmental Effects,* 40(2), pp. 207-213.

Shi, W. et al., 2013. Biodiesel production from waste chicken fat with low free fatty acids by an integrated catalytic process of composite membrane and sodium methoxide. *Bioresource technology,* Volume 139, pp. 316-322.

Singh, S. & Singh, D., 2010. Biodiesel production through the use of different sources and characterization of oils and their esters as the substitute of diesel: a review. *Renewable and sustainable energy reviews,* 14(1), pp. 200-216.

Sivaramakrishnan, K. & Ravikumar, P., 2012. Determination of cetane number of biodiesel and its influence on physical properties. *ARPN journal of engineering and applied sciences,* 7(2), pp. 205-211.

Son, S. & Kusakabe, K., 2011. Transesterification of sunflower oil in a countercurrent trickle-bed reactor packed with a CaO catalyst. *Chemical Engineering and Processing: Process Intensification,* 50(7), pp. 650-654.

Son, S., Kusakabe, K. & Guan, G., 2010. Biodiesel synthesis and properties from sunflower and waste cooking oils using CaO catalyst under reflux conditions. *Journal of Applied Sciences(Faisalabad),* 10(24), pp. 3191-3198.

Soriano Jr, N., Venditti, R. & Argyropoulos, D., 2009. Biodiesel synthesis via homogeneous Lewis acid-catalyzed transesterification. *Fuel,* 88(3), pp. 560-565.

Sousa, L., Lucena, I. & Fernandes, F., 2010. Transesterification of castor oil: Effect of the acid value and neutralization of the oil with glycerol. *Fuel Processing Technology,* 91(2), pp. 194-196.

Speight, J., 2002. *Chemical and process design handbook.* s.l.:The McGraw-Hill Companies.

Srikanth, H., Venkatesh, J. & Godiganur, S., 2018. Box-Behnken response surface methodology for optimization of process parameters for dairy washed milk scum biodiesel production. *Biofuels,* pp. 1-11.

Srivastava, A. & Prasad, R., 2000. Triglycerides-based diesel fuels. *Renewable and sustainable energy reviews,* 4(2), pp. 111-133.

Tan, Y., Abdullah, M. & Nolasco Hipolito, C., 2016. Comparison of biodiesel production between homogeneous and heterogeneous base catalysts. *In Applied Mechanics and Materials,* Volume 833, pp. 71-77.

Tchameni, A., Zhao, L., Nagre, R. & Chao, M., 2015. Biodiesel production from high acid value waste vegetable oil using homogeneous catalyst. *Petroleum & Coal,* 57(4), pp. 336-345.

Tchameni, A., Zhao, L., Nagre, R. & Chao, M., 2015. Biodiesel production from high acid waste vegetable oil using homogeneous catalyst. *Petroleum & Coal,* 57(4), pp. 336-345.

Teo, S., Islam, A. & Taufiq-Yap, Y., 2016. Algae derived biodiesel using nanocatalytic transesterification process. *Chemical engineering research and design,* Volume 111, pp. 362-370.

Thangaraj, B. & Piraman, S., 2016. Heteropoly acid coated ZnO nanocatalyst for Madhuca indica biodiesel synthesis. *Biofuels,* 7(1), pp. 13-20.

Thanh, L., Okitsu, K., Boi, L. & Maeda, Y., 2012. Catalytic technologies for biodiesel fuel production and utilization of glycerol: a review. *Catalysts,* 2(1), pp. 191-222.

Todorović, Z. et al., 2019. Optimization of CaO-catalyzed sunflower oil methanolysis with crude biodiesel as a cosolvent. *Fuel,* Volume 237, pp. 903-910.

Tubino, M. & Aricetti, J., 2011. A green method for determination of acid number of biodiesel. *Journal of the Brazilian Chemical Society,* 22(6), pp. 1073-1081.

Van Gerpen, J. et al., 2004. Biodiesel production technology. *National Renewable Energy Laboratory,* pp. Paper contract No. DE-AC36-99-GO10337.

Van Kasteren, J. & Nisworo, A., 2007. A process model to estimate the cost of industrial scale biodiesel production from waste cooking oil by supercritical transesterification. *Resources, Conservation and Recycling,* 50(4), pp. 442-458.

Veličković, A., Avramović, J., Stamenković, O. & Veljković, V., 2016. Kinetics of the sunflower oil ethanolysis using CaO as catalyst. *Chemical Industry and Chemical Engineering Quarterly,* 22(4), pp. 409-418.

Veljković, V. et al., 2009. Kinetics of sunflower oil methanolysis catalyzed by calcium oxide. *Fuel,* 88(9), pp. 1554-1562.

Vujicic, D. et al., 2010. Kinetics of biodiesel synthesis from sunflower oil over CaO heterogeneous catalyst. *Fuel,* 89(8), pp. 2054-2061.

Wali, W. et al., 2013. Real time monitoring and intelligent control for novel advanced microwave biodiesel reactor. *Measurement,* 46(1), pp. 823-839.

Warra, A., 2015. Physico-chemical and GC/MS analysis of castor bean (Ricinus communis L.) seed oil. *Chem Mater Res,* Volume 7, pp. 56-61.

Wen, L. et al., 2010. Preparation of KF/CaO nanocatalyst and its application in biodiesel production from Chinese tallow seed oil. *Fuel,* 89(9), pp. 2267-2271.

Win, T. & Khine, M., 2017. Synthesis and characterization of CaO and KF doped CaO (KF/CaO) derived from chicken eggshell waste as heterogeneous catalyst in biodiesel production. *American Scientific Research Journal for Engineering, Technology, and Sciences (ASRJETS),* 38(2), pp. 134-151.

Yin, X. et al., 2012. Comparison of four different enhancing methods for preparing biodiesel through transesterification of sunflower oil. *Applied Energy,* 91(1), pp. 320-325.

Zahan, K. & Kano, M., 2018. Biodiesel production from palm oil, its by-products, and mill effluent: A review. *Energies,* 11(8), p. 2132.

Zhang, S. et al., 2010. Rapid microwave-assisted transesterification of yellow horn oil to biodiesel using a heteropolyacid solid catalyst. *Bioresource technology,* 101(3), pp. 931-936.

Zheng, S., Kates, M., Dubé, M. & McLean, D., 2006. Acid-catalyzed production of biodiesel from waste frying oil. *Biomass and bioenergy,* 30(3), pp. 267-272.

Ziejewski, M., Goettler, H. & Pratt, G., 1986. *February, Paper No. 860301*. In International congress and exposition, Detroit, MI, pp. 24-28.

Ziejewski, M., Kaufman, K., Schwab, A. & Pryde, E., 1984. Diesel engine evaluation of a nonionic sunflower oil-aqueous ethanol microemulsion. *Journal of the American Oil Chemists' Society*, 61(10), pp. 1620-1626.

Appendix A – Sample Calculations

Determination of Molar Mass:

The molar mass of the base oils, castor and sunflower, may be calculated via the following formula (Huaping, et al., 2006):

$$MW_{oil} = \frac{56.1 * 1000 * 3}{SV - AV} \tag{A.1}$$

The application of this formula (Eq. (A.1)) involves the determination of the Saponification Value, SV, and the Acid Value, AV, of the base oils.

The Acid Value, AV, of the base oils were calculated according to the (ASTM-D974-12, 2012) standard. The following formula is applicable:

$$AV = \frac{56.1 * M * (V_t - V_b)}{m} = \frac{mg\ KOH}{g\ oil} \tag{A.2}$$

Where, M, represents the molarity of the potassium hydroxide solution and V_t and V_b represent the volume of potassium hydroxide solution titrated and used for the blank titration. The mass of the sample is shown by m. The procedure outlined by the standard requires the use of $2\ g$ of sample to be used if the expected acid value is high and a mass of $20\ g$ is to be used if the expected acid value is low.

The blank titration is completed by first preparing a titration solvent comprising toluene, propan-2-ol and de-ionised water in a ratio of 100:99:1, respectively. Then, $100\ ml$ of titration solvent and 5 drops of phenolphthalein indicator were mixed and swirled in a conical flask. A $0.1\ M$ KOH solution was prepared by the addition and mixing of $5.61\ g$ of solid potassium hydroxide pellets in $1\ L$ of de-ionised water. The initial reading of the titrant level on the burette was recorded prior to titration and the final reading of the level was recorded when the contents of the conical flask turned pale pink for at least a period of $15\ mins$ under constant swirling. The difference in volume between the final and initial reading was calculated to be $0.2\ cm^3$.

Similarly, the acid value of sunflower oil of sample mass $20\ g$ needed $1.15\ cm^3$ of titrant to reach endpoint:

$$AV_{sunflower} = \frac{56.1 * 0.1 * (1.15 - 0.2)}{20} = 0.265\ \frac{mg\ KOH}{g\ oil}$$

The acid value of castor oil is expected to be high, therefore a sample of mass $2\ g$ was used:

$$AV_{castor} = \frac{56.1 * 0.1 * (8.71 - 0.2)}{2} = 23.872 \ \frac{mg\ KOH}{g\ oil}$$

Additionally, the free fatty acid calculated as a percentage of oleic acid is then computed for sunflower oil and castor oil as follows (ASTM-D974-12, 2012):

$$FFA_{sunflower} = \frac{28.2 * 0.1 * (1.15 - 0.2)}{20} = 0.134\ (\%\ oleic\ acid)$$

And the FFA content of castor oil is determined in a similar way:

$$FFA_{castor} = \frac{28.2 * 0.1 * (8.71 - 0.2)}{2} = 12.0\ (\%\ oleic\ acid)$$

The saponification value, SV, is determined by the procedure outlined in (Muhammad, et al., 2019) where $2\ g$ of the sample and $25\ cm^3$ of $0.1N$ ethanolic KOH was boiled at total reflux under constant stirring. Once the mixture cooled, without gelling or solidifying; approximately 5 drops of phenolphthalein indicator was added and the mixture turned pink or pale pink. Titration against $0.5M$ HCL solution was performed until the pink colour disappeared and the volume of the titrant used was recorded for the actual sample and blank titration. The following formula was then used to determine the saponification value, SV:

$$SV = \frac{56.1 * M * (V_b - V_t)}{m} = \frac{mg\ KOH}{g\ oil} \tag{A.3}$$

Where, M represents the molarity of the HCL solution used as the titrant and the other variables were mentioned earlier. The saponification value for sunflower oil is calculated as follows:

$$SV_{sunflower} = \frac{56.1 * 0.5 * (20 - 6.3)}{2} = 192.14 \ \frac{mg\ KOH}{g\ oil}$$

Similarly, the saponification value for castor oil is calculated:

$$SV_{castor} = \frac{56.1 * 0.5 * (20 - 5.4)}{2} = 204.77 \ \frac{mg\ KOH}{g\ oil}$$

And hence the molar mass of sunflower oil can be calculated via Eq. (A.1):

$$MW_{sunflower} = \frac{56.1 * 1000 * 3}{192.14 - 0.265} = 877.13 \ \frac{g}{gmol}$$

Similarly, the molar mass of castor oil is calculated:

$$MW_{castor} = \frac{56.1 * 1000 * 3}{204.77 - 23.872} = 930.36 \frac{g}{gmol}$$

The calculated values of molar mass for sunflower and castor oil are within 0.11% and 0.36%, respectively, when compared to the literature values.

Esterification:

1. Determination of amount of alcohol and catalyst loading

Firstly, the limits of the alcohol/oil molar ratio and catalyst loading must be set. The limits in the case of esterification using sulphuric acid as a catalyst was set at an alcohol/oil molar ratio of 4:1 to 15:1 and $0.25\ wt(\%)$ to $3.25\ wt(\%)$ of the oil mass for catalyst loading. The following calculation procedure is illustrated for an alcohol/oil molar ratio of 15:1 and $0.25\ wt(\%)$ catalyst loading, but is applicable to all possible combinations thereafter, however, esterification is exclusive to castor oil only.

The volume of oil used was limited to the maximum reaction vessel volume of $500\ ml$, therefore, the volume of oil was selected based on the maximum alcohol/oil molar ratio of 15:1. The volume of oil used in all experiments was $300\ ml$. The following equation is then applicable:

$$m_{castor} = \rho_{oil} * V_{oil} = \frac{955 * 300}{1000} = 286.5\ g$$

Next, the number of moles of oil must be computed:

$$n_{castor} = \frac{m_{castor}}{MW_{castor}} = \frac{286.5}{930.36} = 0.308\ mol$$

Applying an alcohol/oil molar ratio of 15:1

$$n_{alcohol} = n_{castor} * 15 = 0.308 * 15 = 4.619\ mol$$

Next, using the molar mass of the alcohol (methanol), the mass of the alcohol to be weighted can be determined:

$$m_{alcohol} = n_{alcohol} * MW_{alcohol} = 4.619 * 32.04 = 147.99\ g$$

And finally, the catalyst loading can be computed:

$$m_{cat} = m_{castor} * 0.25\% = 286.5 * 0.0025 = 0.716\ g$$

A check of the total volume of the reaction mixture may be performed using the density of the alcohol:

$$V_{total} = V_{castor} + V_{alcohol} = 300 + \frac{147.99 * 1000}{792} = 486.87\ ml$$

2. Determination of amount of base needed to neutralise the acid catalyst

After the esterification reaction, the acid catalyst present in the reaction mixture must be neutralised with the calculated amount of base, to reflect the correct acid value of the esterification reaction. This procedure is outlined below:

The balanced stoichiometric reaction for the acid-base neutralisation reaction is as follows:

$$2KOH + H_2SO_4 \longrightarrow K_2SO_4 + 2H_2O \qquad \text{(A.4)}$$

Since concentrated sulphuric acid was used as the acid catalyst, the purity of the catalyst must be accounted for in determining how much base is necessary for the neutralisation reaction. The purity of sulphuric acid was 98 % by mass. Consider $100\ g$ of sulphuric acid:

$$V_{100\ g} = \frac{m_{100\ g}}{\rho_{H_2SO_4}} = \frac{100}{1.827} = 54.73\ ml$$

Therefore, the number of grams in $1000\ ml$ with a purity of 98 %:

$$m_{1000\ ml} = \frac{purity_{100\ g}}{V_{100\ g}} * 1000 = \frac{98}{54.73} * 1000 = 1790.61\ g$$

Next, the number of moles must be computed to determine the molarity of the acid:

$$n_{1000\ ml} = \frac{m_{1000\ ml}}{MW_{H_2SO_4}} = \frac{1790.61}{98.08} = 18.26\ mol$$

The molarity of the acid is determined via the following equation:

$$M = \frac{n_{1000\ ml}}{1\ L} = \frac{18.26}{1} = 18.26\ \frac{mol}{L}$$

Once the molarity of the catalyst is determined, the amount of catalyst on a mass basis that has been added to the reaction mixture must be computed. The following calculation procedure is illustrated for $0.25\ wt(\%)$ catalyst loading, but is applicable to all possible combinations thereafter:

$$m_{cat} = m_{castor} * 0.25\% = 286.5 * 0.0025 = 0.716\ g$$

The volume of catalyst added is calculated using the density of the catalyst:

$$V = \frac{m_{0.716\ g}}{\rho_{H_2SO_4}} = \frac{0.716}{1.827} = 0.39\ ml$$

Therefore, using simple algebra:

$$\frac{0.39\ ml}{1} * \frac{18.26\ mol}{1000\ ml} = 7.12 * 10^{-3}\ mol\ H_2SO_4$$

And accounting for the stoichiometry of the reaction:

$$\frac{7.16 * 10^{-3}\ mol\ H_2SO_4}{1} * \frac{2\ mol\ KOH}{1\ mol\ H_2SO_4} * \frac{56.1\ g}{1\ mol\ KOH} = 0.8\ g$$

Hence, $0.8\ g$ of KOH is necessary to neutralise the amount of acid catalyst added to the reaction mixture. However, it may be useful to first prepare a potassium hydroxide solution and then calculate the volume of that solution that is necessary to facilitate the neutralisation reaction, as solid potassium hydroxide pellets may not dissolve quickly in the reaction mixture. The volume of KOH solution is calculated by first preparing a strong basic solution corresponding to the high acidic solution. In the case of this work, since the molarity of the acid was $18.26\ M$, a KOH solution of $1\ M$ was prepared by the addition of $56.1\ g$ of KOH pellets to $1\ L$ of de-ionised water.

Therefore, the volume of $1\ M$ KOH solution that must be added:

$$V = \frac{m}{MW * M} = \frac{0.8\ g * 1000\ ml}{56.1\ g \cdot mol^{-1} * 1\ mol} = 14.26\ ml\ KOH$$

3. Determination of acid value for esterification experiments

After neutralisation of the acid catalyst, the resulting mixture is transferred to a separation funnel for overnight settling, followed by hot tap water washing to remove glycerol, soap and potassium salts and other impurities. After water washing several times, a sample of $2\ g$ is weighted and added to a conical flask containing $100\ ml$ titration solvent and 5 drops of phenolphthalein indicator. A similar procedure is then followed as outlined before.

The following calculation is for the following conditions; reaction temperature, catalyst loading, time and alcohol/oil molar ratio of 47℃, $0.25\ wt(\%)$, $30\ mins$ and 9.5: 1, respectively, but is applicable to all possible combinations thereafter:

$$AV_{esterification} = \frac{56.1 * 0.1 * (1.51 - 0.2)}{2} = 3.67\ \frac{mg\ KOH}{g\ oil}$$

The free fatty acid calculated as a percentage of oleic acid is then computed (ASTM-D974-12, 2012):

$$FFA_{esterification} = \frac{28.2 * 0.1 * (1.51 - 0.2)}{2} = 1.85\ (\%\ oleic\ acid)$$

Transesterification:

1. Determination of amount of alcohol and catalyst loading

This procedure is very similar to the previous procedure with the only a difference in the limits of catalyst loading. The catalyst loading limits in the case of transesterification using calcinated calcium oxide as a catalyst was set at $0.5\ wt(\%)$ to $1.5\ wt(\%)$ of the oil mass. The following calculation procedure is illustrated for sunflower oil with an alcohol/oil molar ratio of 15:1 and $0.5\ wt(\%)$ catalyst loading, but is applicable to all possible combinations thereafter:

The volume of oil used was limited to the maximum reaction vessel volume of $500\ ml$, therefore, the volume of oil was selected based on the maximum alcohol/oil molar ratio of 15:1. The volume of oil used in all experiments was $300\ ml$. The following equation is then applicable:

$$m_{sunflower} = \rho_{oil} * V_{oil} = \frac{916 * 300}{1000} = 274.8\ g$$

Next, the number of moles of oil must be computed:

$$n_{sunflower} = \frac{m_{sunflower}}{MW_{sunflower}} = \frac{274.8}{877.13} = 0.313\ mol$$

Applying an alcohol/oil molar ratio of 15:1

$$n_{alcohol} = n_{sunflower} * 15 = 0.313 * 15 = 4.699\ mol$$

Next, using the molar mass of the alcohol (methanol), the mass of the alcohol to be weighted can be determined:

$$m_{alcohol} = n_{alcohol} * MW_{alcohol} = 4.699 * 32.04 = 150.569\ g$$

And finally, the catalyst loading can be computed:

$$m_{cat} = m_{sunflower} * 0.5\% = 274.8 * 0.005 = 1.374\ g$$

A check of the total volume of the reaction mixture may be performed using the density of the alcohol:

$$V_{total} = V_{sunflower} + V_{alcohol} = 300 + \frac{150.569 * 1000}{792} = 490.11\ ml$$

Similarly, the amount of alcohol and catalyst loading can be calculated for castor oil in the case of transesterification.

2. Determination of amount of acid needed to neutralise the base catalyst

After the transesterification reaction, the base catalyst present in the reaction mixture must be neutralised with the calculated amount of acid, to stop the reaction. Sulphuric acid was used as the neutralising agent.

The balanced stoichiometric reaction for the acid-base neutralisation reaction is as follows:

$$CaO + H_2SO_4 \longrightarrow CaSO_4 + H_2O \tag{A.5}$$

Analytical grade calcium oxide was first calcinated, then used in the transesterification reaction, therefore, the purity was assumed to be greater than 99 % by mass. Consider $100\ g$ of calcium oxide:

$$V_{100\ g} = \frac{m_{100\ g}}{\rho_{CaO}} = \frac{100}{3.34} = 29.94\ ml$$

Therefore, the number of grams in $1000\ ml$ with a purity of 99 %:

$$m_{1000\ ml} = \frac{purity_{100\ g}}{V_{100\ g}} * 1000 = \frac{99}{29.94} * 1000 = 3306.6\ g$$

Next, the number of moles must be computed to determine the molarity of the base:

$$n_{1000\ ml} = \frac{m_{1000\ ml}}{MW_{CaO}} = \frac{3306.6}{56.08} = 58.962\ mol$$

The molarity of the base is determined via the following equation:

$$M = \frac{n_{1000\ ml}}{1\ L} = \frac{58.962}{1} = 58.962\ \frac{mol}{L}$$

Once the molarity of the catalyst is determined, the amount of catalyst on a mass basis that has been added to the reaction mixture must be computed. The following calculation procedure is illustrated for $0.5\ wt(\%)$ catalyst loading, but is applicable to all possible combinations thereafter:

$$m_{cat} = m_{sunflower} * 0.5\% = 274.8 * 0.005 = 1.374\ g$$

The volume of catalyst added is calculated using the density of the catalyst:

$$V = \frac{m_{1.374\,g}}{\rho_{CaO}} = \frac{1.374}{3.34} = 0.411\,ml$$

Therefore, using simple algebra:

$$\frac{0.411\,ml}{1} * \frac{58.962\,mol}{1000\,ml} = 2.43 * 10^{-2}\,mol\,CaO$$

And accounting for the stoichiometry of the reaction:

$$\frac{2.43 * 10^{-2}\,mol\,CaO}{1} * \frac{1\,mol\,H_2SO_4}{1\,mol\,CaO} * \frac{98.08\,g}{1\,mol\,H_2SO_4} = 2.38\,g$$

In the case of this work, a sulphuric acid solution of $1\,M$ was prepared by the addition of $98.08\,g$ of sulphuric acid to $1\,L$ of de-ionised water.

Therefore, the volume of $1\,M\ H_2SO_4$ solution that must be added:

$$V = \frac{m}{MW * M} = \frac{2.38\,g * 1000\,ml}{98.08\,g \cdot mol^{-1} * 1\,mol} = 24.256\,ml\,H_2SO_4$$

3. Determination of yield

As mentioned in the experimental methodology, the yield is calculated as follows:

$$Yield = \frac{mass\ of\ biodiesel}{mass\ of\ oil/esterified\ oil} \tag{A.6}$$

The following is an example of yield calculation for sunflower oil in the case of transesterification with reaction conditions; temperature, catalyst loading, time, alcohol/oil molar ratio of 47℃, $1.5\,wt\%$, $30\,mins$ and $9.5:1$, respectively, which resulted in $240.2\,g$ of biodiesel:

$$Yield = \frac{mass\ of\ biodiesel}{mass\ of\ oil/esterified\ oil} = \frac{240.2}{274.8} = 0.87 * 100 = 87\ \%$$